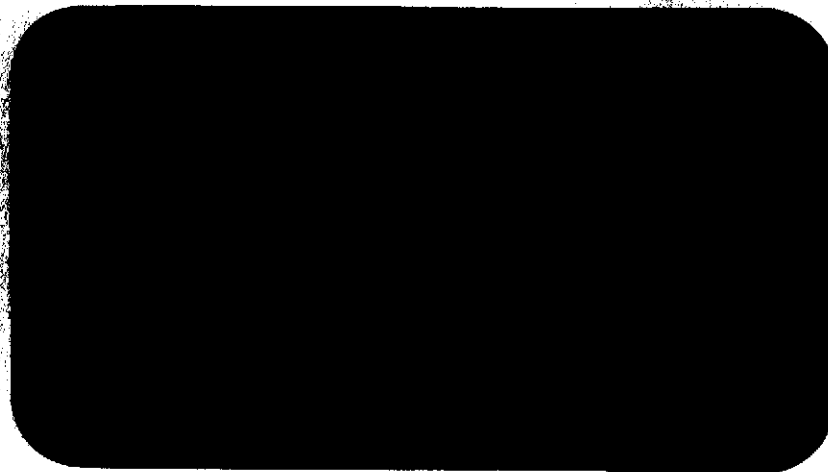iiTRi

Advanced concepts are being used by IIT Research Institute to solve research, development, and design problems for industry and government through contract research. Our services encompass virtually all of the physical and biological sciences. Principal areas are: chemistry, computer sciences, electronics, engineering mechanics, life sciences, mechanics of materials, medical engineering, metals, and management and social science research.

The interdisciplinary approach at IITRI brings the latest technology to bear upon the problem-solving process.

Principal office:
  10 West 35th Street
  Chicago, Illinois 60616

Contract No. NAS8-26791
Report No. IITRI-C6233-44
(Triannual Report)

DEVELOPMENT OF SPACE STABLE THERMAL
CONTROL COATINGS FOR USE ON LARGE
SPACE VEHICLES

National Aeronautics and Space
   Administration
George C. Marshall Space Flight Center
Huntsville, Alabama   35812

Prepared by

J.E. Gilligan and Y, Harada

of

IIT Research Institute
Technology Center
Chicago, Illinois 60616

May 1 through August 31, 1974

Funded under Codes: 124-09-31-0000-33-1-004-080-2510
                      114-03-51-0000-33-2-004-080-2510
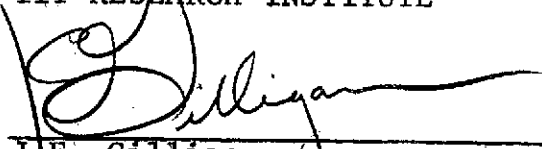
October, 1974

FOREWORD

This is Report No. IITRI-C6233-44 (Triannual Report) of IITRI Project C6233, Contract No. NAS8-26791, entitled "Development of Space Stable Thermal Control Coatings for Use on Large Space Vehicles". This report covers the period from May 1 through August 31, 1974.

Major contributors to the program during this period include: Mr. J.E. Gilligan, Project Leader; Mr. Y. Harada and Mr. W. Logan, pigment manufacturing and related studies; Mr. F.O. Rogers, paint preparation; Messrs A. Lackland and J. E. Brzuskiewicz, Irradiation experiments and reflectance measurements; T.Yamauchi and C. Giori, Binder Modification; V. Adamaitis, Data Analysis and organization, and Dr. A.M. Stake, general consultation and administrative management.

The work reported herein was performed under the technical direction of the Space Sciences Laboratory of the George C. Marshall Space Flight Center; Mr. Daniel W. Gates acted as the Project Manager.

This contract was funded under Codes 124-09-31-0000-33-1-004-080-2510 and 114-03-51-0000-33-2-004-080-2510.

Respectfully submitted,
IIT RESEARCH INSTITUTE

J.E. Gilligan
Group Leader-Thermal Control
Polymer Chemistry Research

APPROVED:

A.M. Stake
Manager
Polymer Chemistry Research

JEG:ge

ABSTRACT

The effort toward the development of a large scale manufacturing method for the production of a stable zinc orthotitanate pigment has been continuing. During this period major emphasis has been placed on the evaluation of ultraviolet radiation stability tests of pigments derived from coprecipitated and individually precipitated oxalates. Emphasis was also placed on an investigation of the conditions (time and temperature) leading to high reflectance and high optical stability. Paints were formulated in OI-650 and in OI-650G vehicles from pigments which had been prepared at various temperatures. Analyses of ultraviolet irradiation test data have been made regarding optimum pigment preparation parameters and treatment conditions.

TABLE OF CONTENTS

TABLE OF CONTENTS (Cont'd)

IIT RESEARCH INSTITUTE

LIST OF TABLES

LIST OF FIGURES

LIST OF FIGURES (Cont'd)

LIST OF FIGURES (Cont'd)

LIST OF FIGURES (Cont'd)

DEVELOPMENT OF SPACE STABLE THERMAL
CONTROL COATINGS FOR USE ON LARGE SPACE VEHICLES

1. INTRODUCTION

The research effort in passive spacecraft temperature control has, historically, been concentrated on the development of the class of surfaces known as solar reflectors - that is, surfaces with high reflectance for solar radiation and with high emittance in the thermal (infrared) spectrum. Basically, these surfaces must be stable in the total environment that they will experience. This requirement means that, once an high level of intrinsic stability in these materials is attained in the laboratory, we must make certain that this stability is preserved in a scaled-up process in manufacturing, protected throughout the entire pre-launch environment, and, finally, that this stability obtains in the space environment. Applications on large space vehicles, therefore, present new R&D problems - not simply traditional ones in greater dimensions.

The program consists of four major tasks: pigment manufacturing development, binder development, environmental effects evaluations, and general coatings investigations. The relative emphasis on each of these tasks varies according to the urgency of the problems elucidated in our investigations, and, of course, with the availability of time and funds. Our present efforts have been expended approximately equally on the development of a pigment manufacturing method and on the complementary environmental testing and evaluation activities.

2. PIGMENT MANUFACTURING DEVELOPMENT

Studies have been conducted both in the development of co-precipitated (COP) and of mixed oxalate (MOX) materials as precursors for Zn_2TiO_4. These are discussed in the following sections.

2.1 Coprecipitated Oxalates (COP)

The work with COP materials has consisted of processing of a large batch of Zn_2TiO_4 to be submitted to K.M. Sancier of Stanford Research Institute. In the precipitation procedure, 4 batches of approximately 1150 grams of oxalate precursor material (the limit of the present equipment) were prepared. These were then mixed prior to the 600°C (and subsequent 1200°C) calcination steps to produce a total batch of approximately 2000 grams of Zn_2TiO_4.

Studies were also conducted to determine equipment needs and cost for scaling up to the production of 5 pound Zn_2TiO_4 batches.

2.2 Mixed Oxalates (MOX) Studies

The mixed oxalate studies were conducted to determine if the particle size of the precursor oxalates and the Zn_2TiO_4 obtained from their calcination could be controlled. This investigation was prompted by the observation that COP materials had a tendency toward agglomeration; it was felt that this might be avoided through mixing of the individually precipitated zinc and titanium oxalates.

In these investigations, three sets of experiments were conducted leading to 3 batches designated: MOX, MOX-A, and MOX-B. The MOX studies which were detailed in Ref. 1 show that a finer particle size material was obtained as compared to COP materials,

both in the precursors and the calcined materials (products).
X-ray analyses of all these materials showed that there is
partial conversion of Zn_2TiO_4 at 600°C, and that formation of
Zn_2TiO_4 is complete at 1050°C.

Based on these results, the MOX studies were expanded to
include a number of calcination conditions. Larger batches of
645 grams (MOX-A) and 276 grams (MOX-B) were used in contrast
to the 23 grams for MOX. The MOX-A materials had a $ZnO:TiO_2$
ratio of 1.5:1, whereas the MOX-B and MOX had a ratio of 2.05:1.
The lower ratio for MOX-A resulted from an incorrect calculation
of yield for the mixture.

The heat treatments used for MOX-A and MOX-B were as follows:

MOX-A:	900°C	-	4, 8, and 16 hours
	1050°C	-	1, 2, 4, and 8 hours
	1200°C	-	0.5, 1, and 2 hours
MOX-B:	900°C	-	4 and 16 hours
	1050°C	-	1, 4, and 8 hours
	1200°C	-	0.5 and 2 hours

All samples were first pre-calcined at 600°C to remove volatiles,
prior to the final flash calcinations listed above.

X-ray analyses of MOX-A materials using both the powder
and diffraction pattern techniques showed the presence of Zn_2TiO_4
in all samples. There was no evidence of any other phase such
as $ZnTiO_3$, ZnO, or TiO_2. This appears strange in view of the 1.5
$ZnO:1.0$ TiO_2 ratio used, i.e., a significant amount of free TiO_2
should exist. This anomaly remains under investigation. MOX-B
samples also were similarly analyzed with the same results.

All samples have been examined using SEM techniques (Ref. 2). The results show that MOX-A and MOX-B materials exhibit a particle size similar to that for COP materials (Figure 1 and 2). The earlier MOX material calcined at 1050°C has a significantly smaller average particle size.

In general the pigments prepared from individually precipitated oxalates, and those oxalates also, possess a smaller average particle size than do those prepared in the COP method. This difference in average particle size results from the ball-milling employed to blend the individually precipitated oxalates. COP materials ordinarily are not ball-milled.

As pointed out earlier, the batches of MOX-A and MOX-B pigments were much larger than the original MOX batch. Examination of the mixing procedures shows that the ball charge was about 30% for MOX and 15% for MOX-A and MOX-B. In addition, the ball to powder charge ratio was about 1:1 for MOX whereas it was about 1:4 for the larger batch MOX-A and MOX-B. Thus, the smaller MOX particle size may have resulted from a more rigorous grinding.

Therefore, experiments were conducted in which MOX-A was ball milled as a small charge (25 grams) duplicating the milling conditions for MOX. Preliminary SEM results show that under these conditions, a significant reduction in particle size occurred for MOX-A. A similar comminution effect also occurred when COP material was given this treatment. Experiments are now being conducted to determine if the finer particle size will be maintained upon calcination.

It is apparent from these studies that ball-milling parameters such as ball charge and balls to powder ratio are quite critical to the blending/grinding process. Particle size reduction can be obtained by fairly rigorous milling conditions.
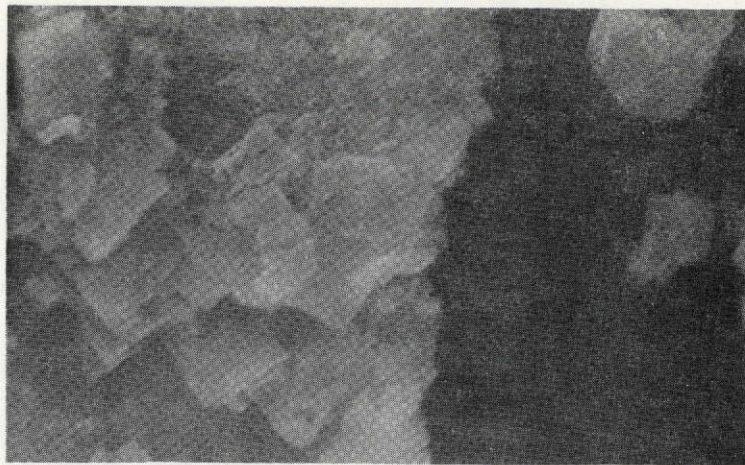
COP
(LH-103)

No. 314   3000X
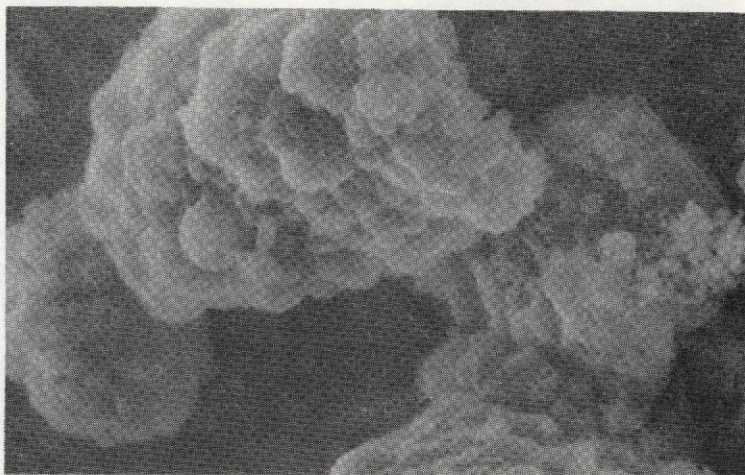
MOXA

No. 473   3000X
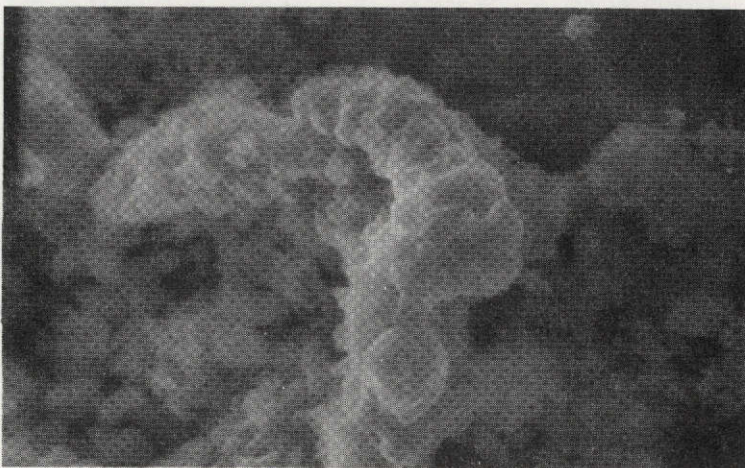
MOXB

No. 486   3000X

Figure 1.   SEM VIEWS OF COP AND MOX MATERIALS
CALCINED AT 600°C.

5   C6233-44

COP
(LH-103)

No. 366   3000X

MOXA

No. 468   3000X
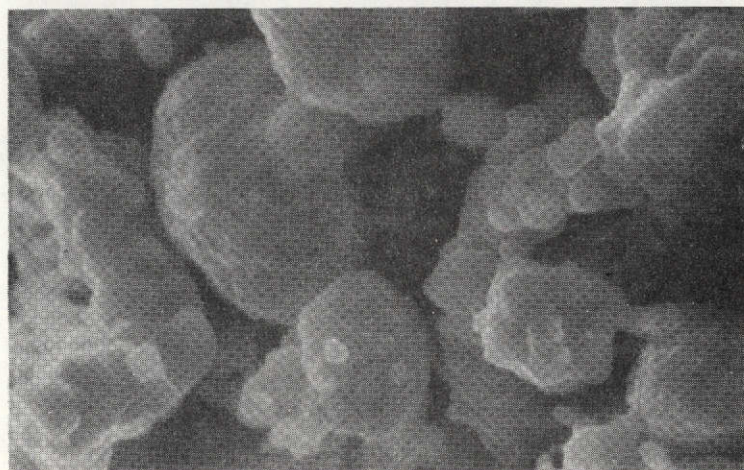
MOXB

No. 490   3000X

Figure 2.   SEM VIEWS OF COP AND MOX MATERIALS
CALCINED AT 1050°C.

C6233-44

However, it is probable that optimum conditions for comminution have not been attained and would require additional study. Furthermore, the effects on reflectance spectra and especially on reflectance stability to ultraviolet-vacuum have yet to be established.

For the present program, the COP materials remain the choice of pigment precursors production method. The COP materials are well characterized in terms of: precipitation process up to 1200 grams of precipitate (550 grams Zn_2TiO_4); calcination at temperatures up to 1400°C; ZnO removal by acid leaching; morphology studies by SEM; and effects of ultraviolet irradiation in vacuum. Importantly, reproducibility in the various COP processes has been established.

MOX materials have received less study. The SEM studies show a lack of reproducibility in the morphology of particles for MOX, MOX-A, and MOX-B. Studies are needed in the areas of precipitation parameters (time, temperature) and of mixing (grinding media, amount, and time) in order to establish the proper conditions for achieving reproducibility. In addition, studies of calcination and recalcination conditions, acid leaching, and encapsulation to maximize reflectance and reflectance stability also would be required. It should be added, however, that a high potential for particle size control has been indicated by these studies.

Table 1 compares the particle sizes as determined from SEM pictures (Ref. 2) of variously prepared materials, including the COP (coprecipitated) materials which have shown good reproducibility in particle size and the MOX materials which have been somewhat inconsistent. In the latter the differences may be attributable in part to the preliminary nature of the work.

Table 1

Average Particle Size of Certain
COP and MOX Pigments

COP Materials Sample Designation	Particle Size COP Materials	Comments
As precipitated	1-5μ	Needle-like, as well as equiaxed shapes
600°C/2 hrs	Submicron to about 5μ	Agglomeration, caking effect
900°C/8 hr	Submicron to about 5μ	Rounding of particles, less agglomeration than 600°C material
1050°C/2 hr	1-5μ	Some necking between particles. No evidence of submicron material
1200°C/2 hr	2-5μ	Moderate necking. Rounded particles, no sharp edge effects.
1400°C/2 hr	2-5μ	Strong necking. Further rounding of particles.
ZnOx precursor	2-5μ	
TiOx precursor	0.5-3μ	More irregularly shaped than ZnOx
MOX, as mixed	0.5-4μ	
MOX(6)	Submicron to about 2μ	Mostly submicron
MOX(6-10.5/2)	0.5-2μ	
MOX-A	0.5-5μ	
MOX-A (6)	0.5-3μ	
MOX-A(6-9/4)	1-3μ	
MOX-A(6-9/8)	1-3μ	
MOX-A(6-9/16)	1-3μ	Some necking

C6233-44

Table 1 (Cont'd)

MOX-A(6-10.5/1)   1-4μ ⎫
MOX-A(6-10.5/2)   1-4μ ⎬————— Agglomeration
MOX-A(6-10.5/4)   1-4μ ⎬
MOX-A(6-10.5/8)   1-4μ ⎭
MOX-A(6-12/0.5)   1-5μ ⎫
MOX-A(6-12/1)   1-5μ ⎬————— Agglomeration and necking
MOX-A(6-12/2)   1-5μ ⎭

MOX-B(6)   0.5-3μ
MOX-B(6-9/4)   Submicron - 3μ ⎫————— Agglomeration
MOX-B(6-9/16)   Submicron - 3μ ⎭
MOX-B(6-10.5/1)   1-5μ ⎫
MOX-B(6-10.5/4)   1-5μ ⎬————— Agglomeration and necking
MOX-B(6-10.5/8)   1-5μ ⎭
MOX-B(6-12/0.5)   1-5μ ⎫————— Strong necking
MOX-B(6-12/2)   1-5μ ⎭

9   C6233-44

3. IRRADIATION TESTING

A total of five ultraviolet irradiation tests have been completed and analyzed during the report period. These tests and one previously unreported are described.

3.1 IRIF Test I-68

3.1.1 Test Conditions

IRIF Test I-68 was conducted at an intensity of six suns using a compact Mercury 1000w ultraviolet source, (Pek AH-6), operating at an average input power of 950 watts. A pressure level of less than 2×10^{-7} torr was maintained during irradiation. Spectral hemispherical reflectance measurements in the spectral region 325-2600 nm were made of each sample prior to irradiation, after an ultraviolet radiation exposure of 1340 ESH and of 2570 ESH; after irradiation, the IRIF was backfilled to 760 Torr with oxygen and reflectance measurements were again made of each sample.

3.1.2 Test Results

The sample descriptions and test results are summarized in Table 2. The spectral data are given in figs. 3-11. The Tektronix zinc orthotitanate pigments obviously are quite stable. The ZnO and TiO_2 pigments were irradiated for comparison, and, as expected, they degrade moderately when irradiated as powders. Like many other surface-active pigments, they degrade severely in an organic binder. The zinc orthosilicate pigments are carefully prepared CRT phosphors manufactured by Tektronix, one of which is intrinsically doped with manganese to improve its luminescence properties.

Table 2

IRIF TEST I-68

TEST RESULTS

Sample Description	Solar Absorptance Values			
	Initial	1340 ESH	2570 ESH	O_2 Bleach
Zn_2TiO_4 (No fire)*	.236	.268	.294	.269
Zn_2TiO_4 (900°C/9 hr)*	.150	.162	.183	.176
Zn_2TiO_4 (1200°C/1 hr)*	.225	.245	.250	.244
Zn_2TiO_4 (1250°C/24 hr)*	.268	.282	.285	.300
Zn_2SiO_4**	.229	.252	.272	.247
Zn_2SiO_4:Mn**	.159	.176	.209	.214
ZnO (N.J. Zinc SP-500)	.259	.258	.282	.264
a-TiO_2 (DuPont FF)	.206	.289	.356	.253
r-TiO_2 (DuPont R-900)	.286	.321	.341	.310

*Samples obtained from Tektronix, Inc., Beaverton, Ore.
**CRT phosphors from Tektronix, Inc., Beaverton, Ore.

The performance of the Zn_2TiO_4 pigments in OI-650G vehicles has already been determined and reported (Ref. 1). Their performance here, however, especially the bleaching behavior, confirms that these pigments are inherently quite stable.

3.1.3 Analyses

Figures 3 through 6 show the reflectance spectra of zinc orthotitanate samples prepared by Tektronix. The spectra in Fig. 3 pertain to a basic mixture of 2.05:1 $ZnO:TiO_2$ which was spray dried at 250°C. The spectra belie the presence of con-
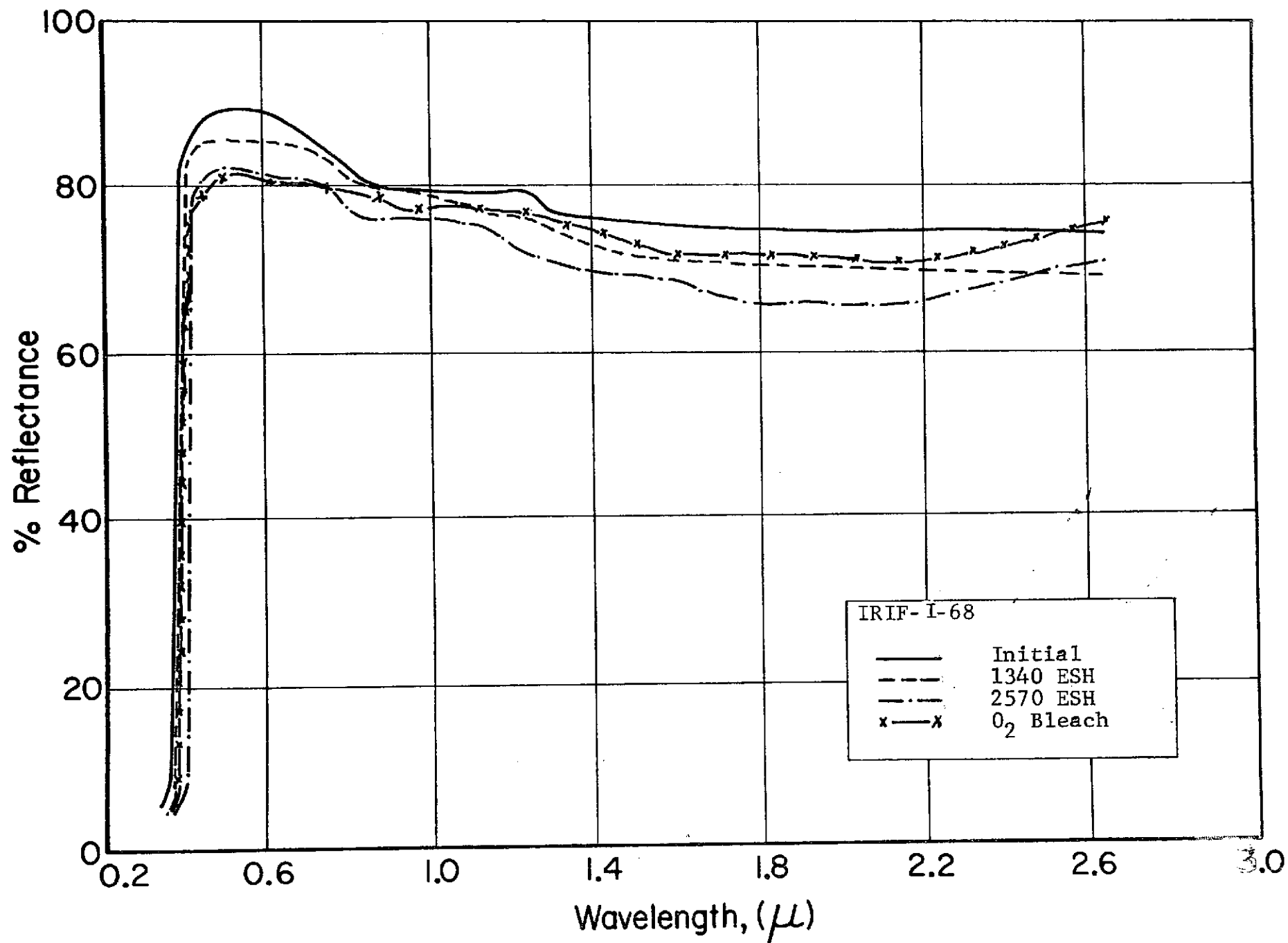
Fig. 3, REFLECTANCE SPECTRA OF TEKTRONIX Zn_2TiO_4 PRE-MIX (NO FIRE)
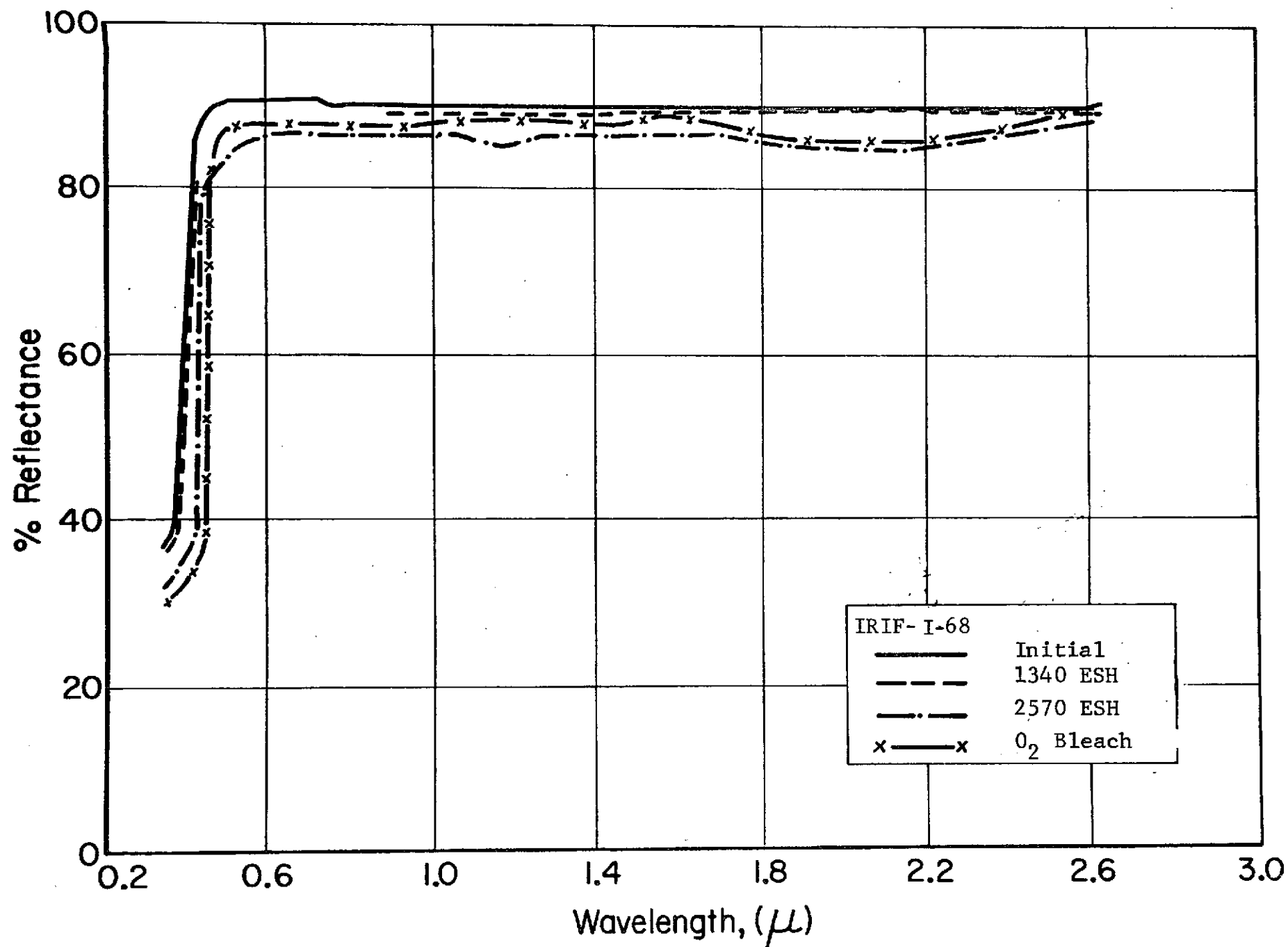
Fig. 4, REFLECTANCE SPECTRA OF TEKTRONIX Zn_2TiO_4 (900°C/9 hr)

C6233-44
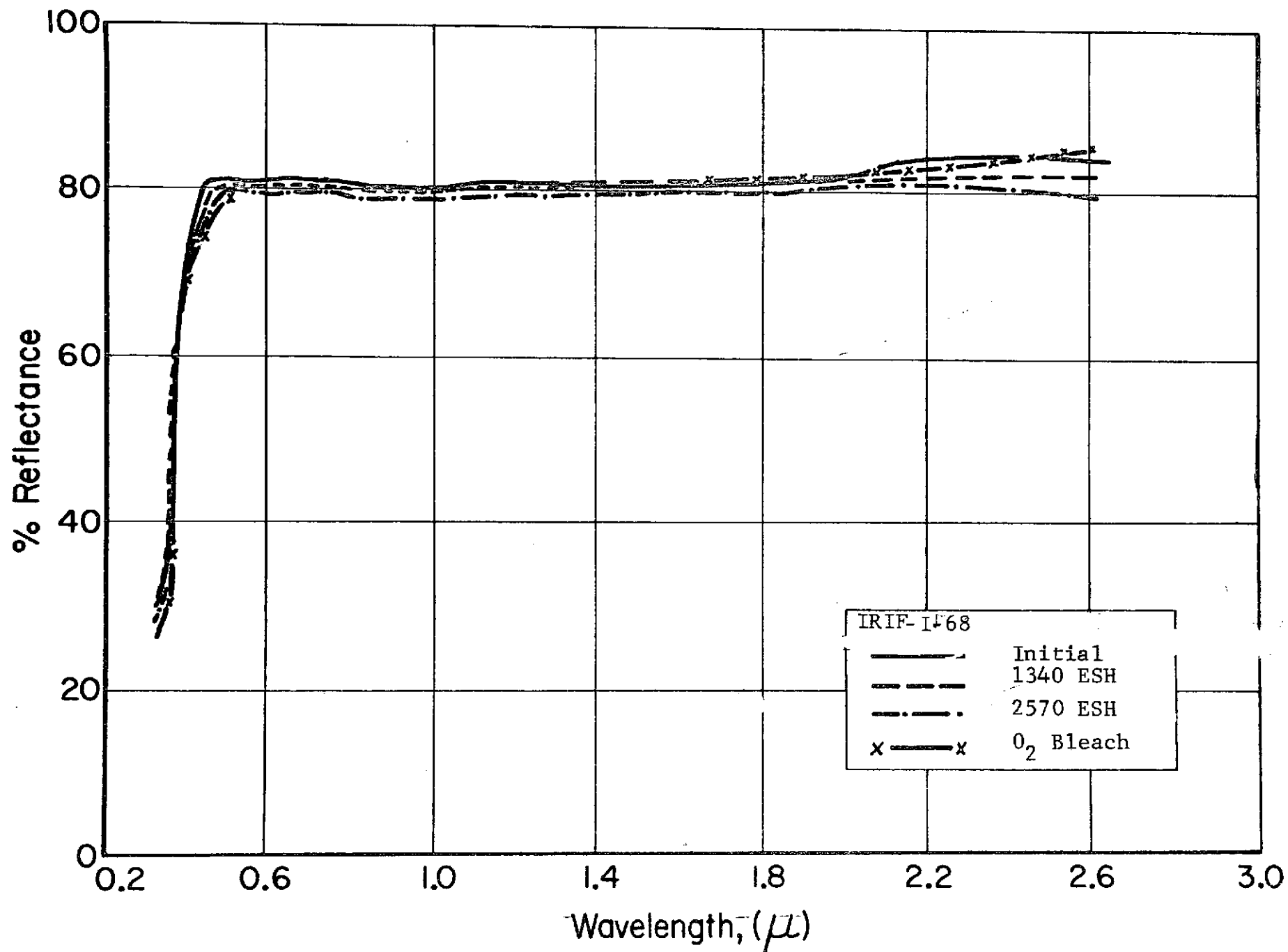
Fig. 5, REFLECTANCE SPECTRA OF TEKTRONIX Zn_2TiO_4 (1200°C/1 hr)

14

C6233-44
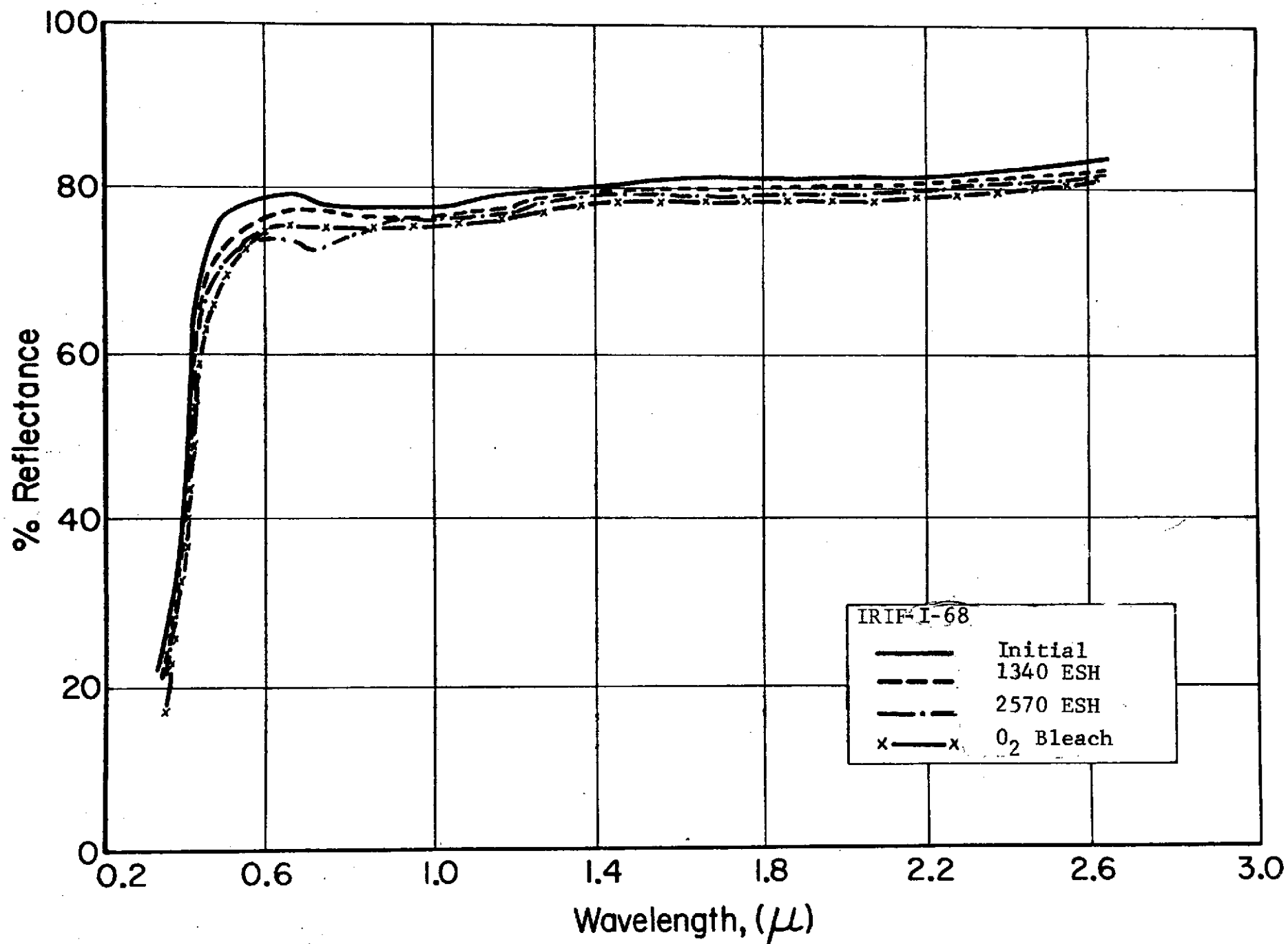
Fig. 6, REFLECTANCE SPECTRA OF TEKTRONIX Zn_2TiO_4 (1250°C/24 hr)

siderable free ZnO; the infrared bleaching very probably occurs as a direct result of (and may even be a measure of) this free ZnO content. The spectra of the same material which has been fired at 900°C/9 hrs has been presented in fig. 4. Here the stability is excellent. The spectra also reveal slight bleaching, again probably because of the moderate free ZnO content. The latter is also evident from the "dog leg" in the shape of the ultraviolet reflectance spectrum. Materials fired at 1200°C/1 hr and at 1250°C/24 hrs. exhibit excellent stability as figs. 5 and 6, respectively, show. The 1200°C/1 hr material remained reasonably powdery, while the 1250°C/24 hr material formed large and very hard "clinkers" in the firing process. Both, however, exhibit very little bleaching, while the 1250°C/24 hr material shows a substantially greater proportion of free ZnO, as indicated by the knee in the ultraviolet reflectance spectrum. The zinc orthosilicate samples, also supplied by Tektronix, are not as stable as zinc orthotitanate. From a comparison of the spectra in fig's 7 and 8, it is obvious that manganese doping stabilizes Zn_2SiO_4 against the production of bleachable infrared damage but does little if anything to confer any degree of overall optical stability upon this material.

The curves for ZnO and for anatase and rutile TiO_2 in figs. 9-11 are for comparison. The behavior in each case is typical. In particular these reflectance curves can be compared with those of the MOX-A pigments, which will be discussed later.
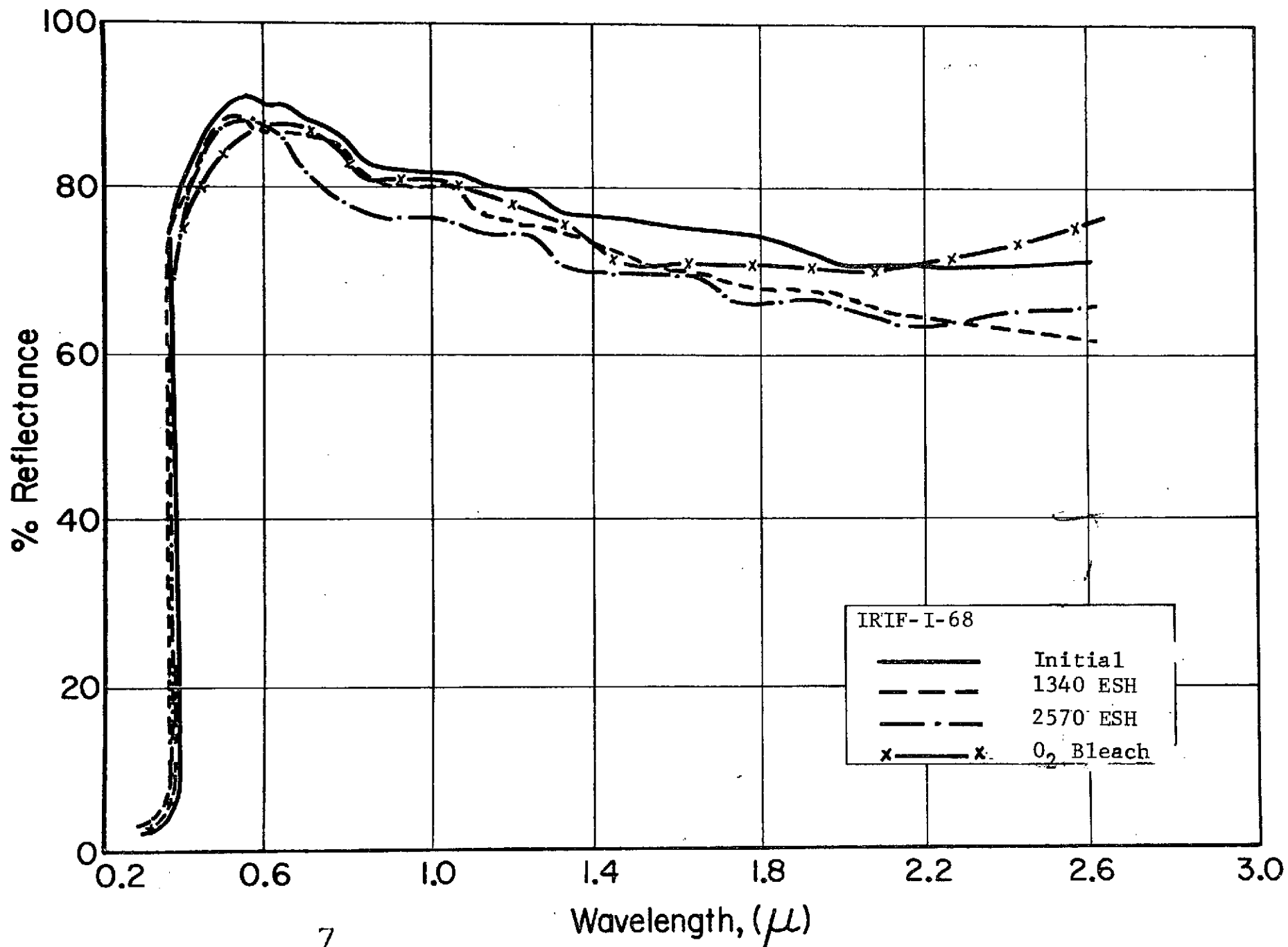
Fig. 7, REFLECTANCE SPECTRA OF TEKTRONIX Zn_2SiO_4
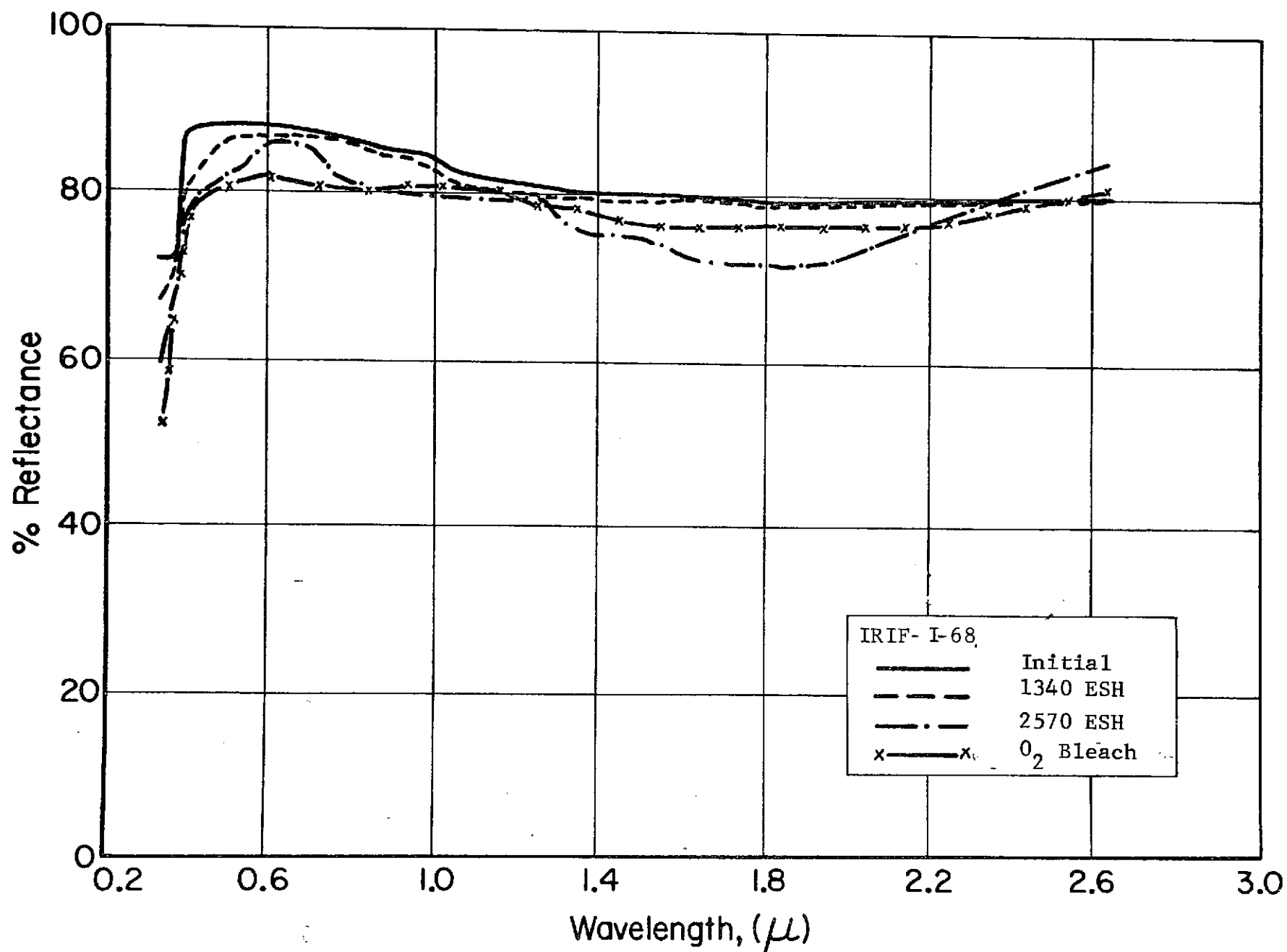
Fig. 8, REFLECTANCE SPECTRA OF TEKTRONIX Zn_2SiO_4:Mn
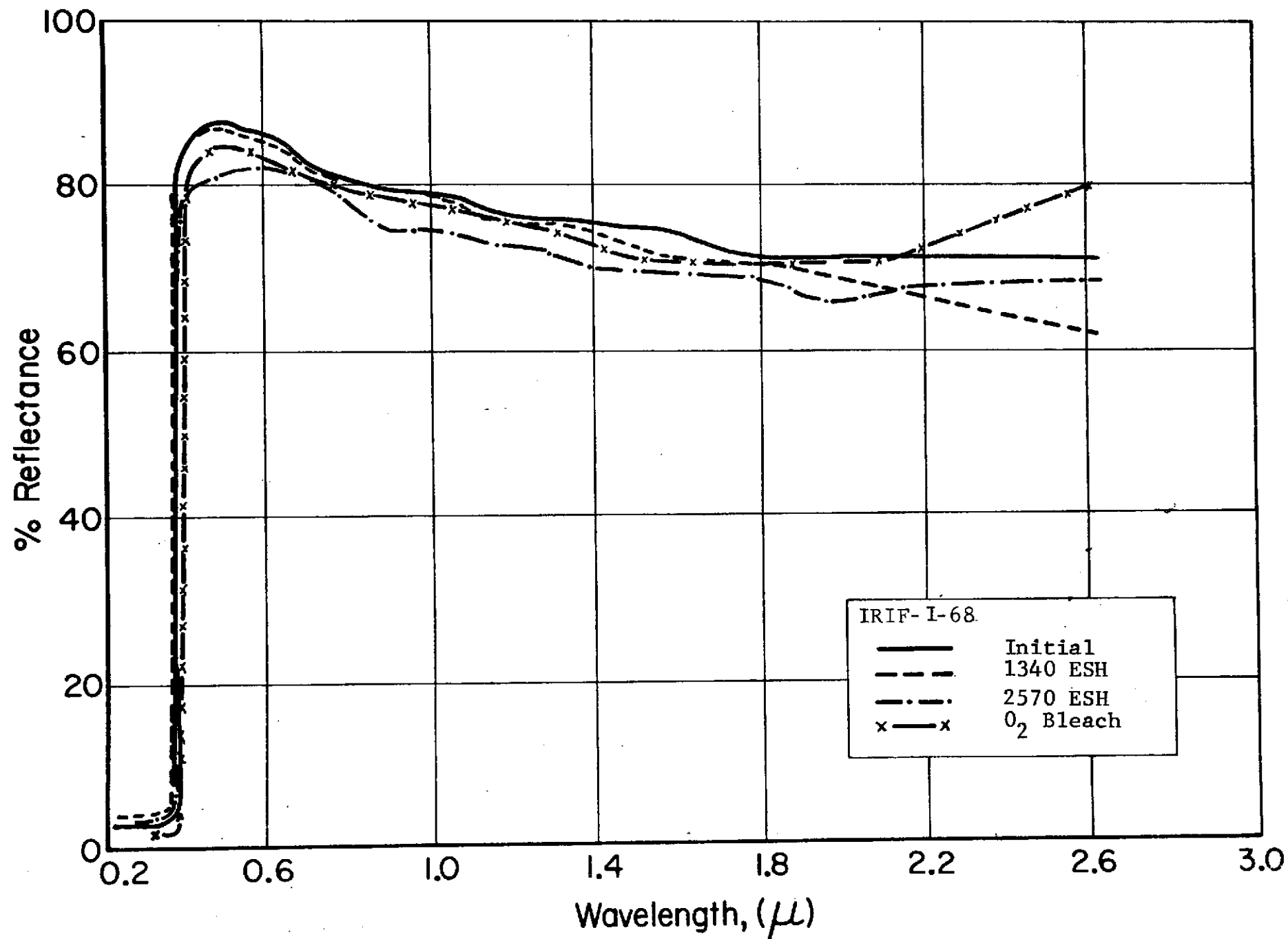
Fig. 9, REFLECTANCE SPECTRA OF ZnO (NEW JERSEY ZINC SP-500)

C6233-44
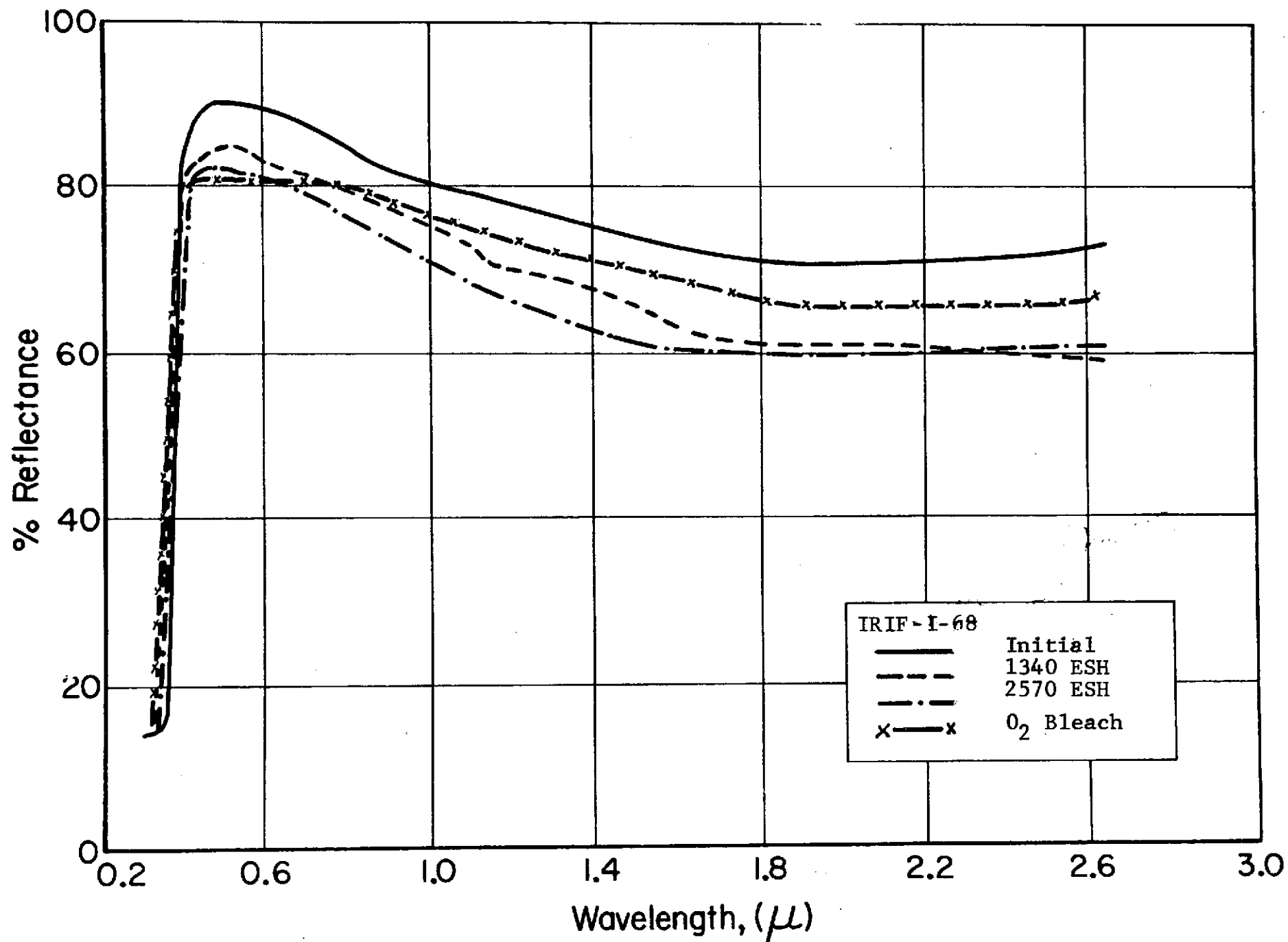
Fig. 10 REFLECTANCE SPECTRA OF ANATASE TiO$_2$ (DU PONT FF)
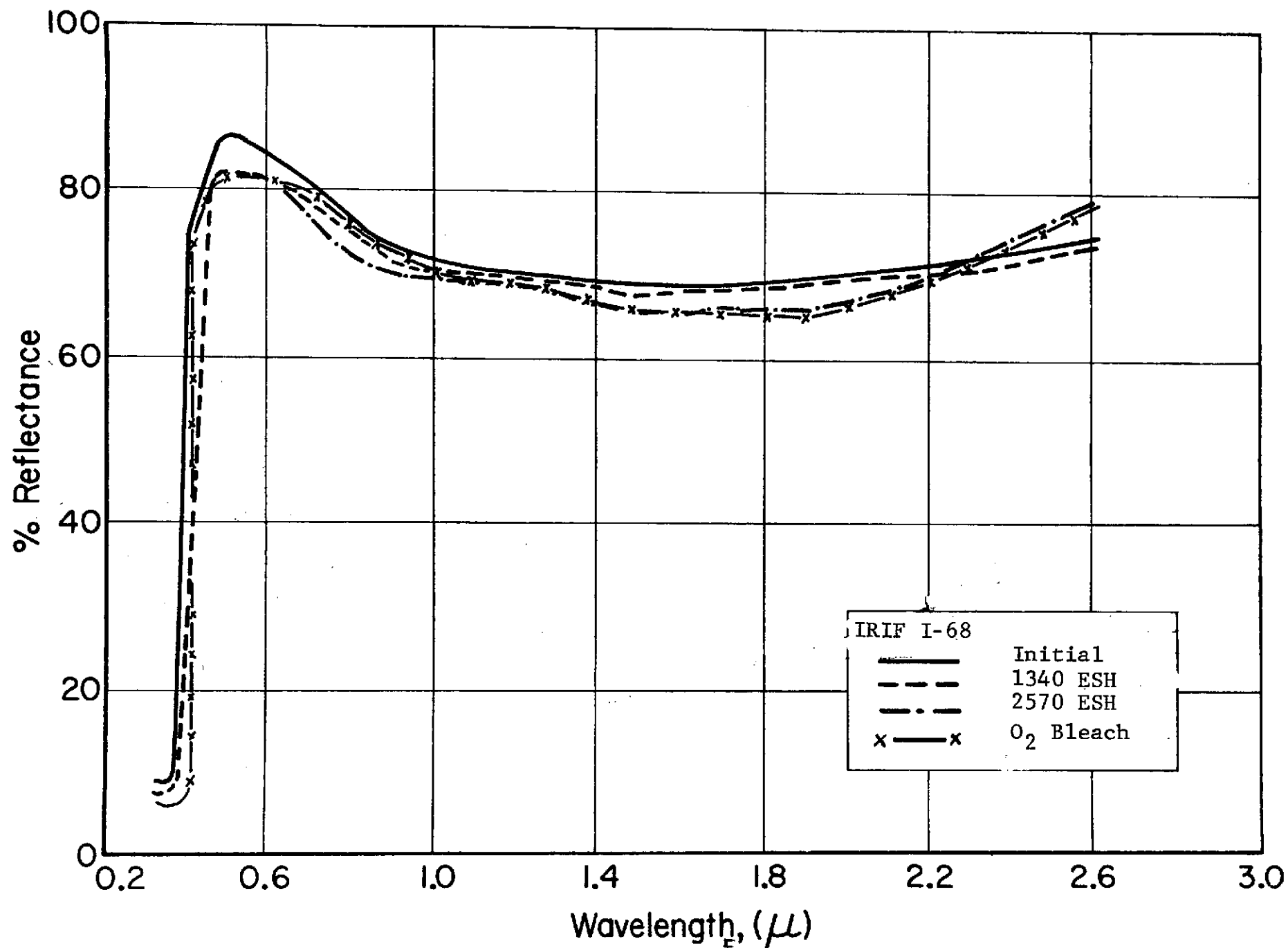
Fig. 11, REFLECTANCE SPECTRA OF RUTILE TiO$_2$ (DU PONT R-900)

3.2 IRIF TEST I-70

3.2.1 Test Conditions

In IRIF Test I-70 the samples were exposed to a total of 3130 ESH. The test was carried out using an A-H6 compact mercury arc illuminator at a solar factor of 6 (equivalent) ultraviolet (UV) suns. A pressure of less than $2x10^{-7}$ Torr was maintained during irradiation. Reflectance measurements, accomplished in the spectral range from 325nm to 2600nm, were made under vacuum prior to UV irradiation, after 540 ESH, 1060 ESH and after 3130 ESH; a final scan was made of certain samples after the system pressure was increased to 760 torr using pure O_2.

3.2.2 Materials Descriptions and Test Results

The materials tested in IRIF I-70 are described in Table 3, wherein also are pertinent test results. The notation used is that which we have used consistently to describe Zn_2TiO_4 pigments. In this case all the pigments have been derived from batch LH-106 and all samples are OI650G paints. The full description of sample No. 6, for example, would be LH-106(6-12-A-10):Li_2SiO_3/OI650G. This notation describes a paint whose pigment was made from a coprecipitate (COP) precursor (LH-106), which was precalcined at 600°C/2hr, calcined at 1200°C/2hr., acetic acid washed, re-calcined at 1000°C/2hr, and encapsulated in Li_2SiO_3. The binder is an IITRI-modified OI650 silicone resin, designated OI-650G.

The spectral reflectance curves are presented in Fig's 12-23, inclusive. The notation used to describe the samples remains the same as previously given and is directly relatable to the data in table 3. The basic purpose of this test was to discern optimum treatments for a baseline pigment, i.e. a "6-12" pigment. Table 3 and the figures are organized to show progressively the effects of acetic acid washes, recalcinations and encapsulants.

Table 3
IRIF TEST I-70
ULTRAVIOLET RADIATION TEST RESULTS

No.	Sample Description*	ΔR_{400}	ΔR_{900}	Solar Absorptance Values					$\Delta\alpha_s$
					Exposure (ESH)			O_2 Bleach	
				Initial	540	1060	3130		
1	(6-12)	.04	.065	.152	.173	.173	.171	.161	.019
2	(6-12-10)	.045	.06	.180	.204	.203	.214	.189	.034
3	(6-12-A-10)**	.025	.065	.213	.220	.221	.243	.226	.030
4	(6-12):Li_2SiO_3**	.03	.05	.203	.209	.211	.224	.216	.021
5	(6-12-10):Li_2SiO_3**	.03	.025	.194	.204	.209	.212		.018
6	(6-12-A-10):Li_2SiO_3**	.03	.02	.180	.188	.190	.194		.014
7	(6-12):K_2SiO_3**	.025	.02	.232	.239	.242	.244		.012
8	(6-12-10):K_2SiO_3	.025	.02	.187	.191	.196	.203		.016
9	(6-12-A-10):K_2SiO_3**	.025	.02	.210	.219	.220	.225		.015
10	(6-12):K_2SiF_6**	.03	.03	.192	.202	.207	.213	.206	.021
11	(6-12-10):K_2SiF_6**	.03	.025	.215	.225	.230	.231		.016
12	(6-12-A-10):K_2SiF_6	.03	.05	.206	.228	.226	.234	.210	.028

*All samples contain Zn_2TiO_4 from batch LH106 and treated as indicated; all are OI-650G paints

**Also irradiated in CREF Test No. 16

23
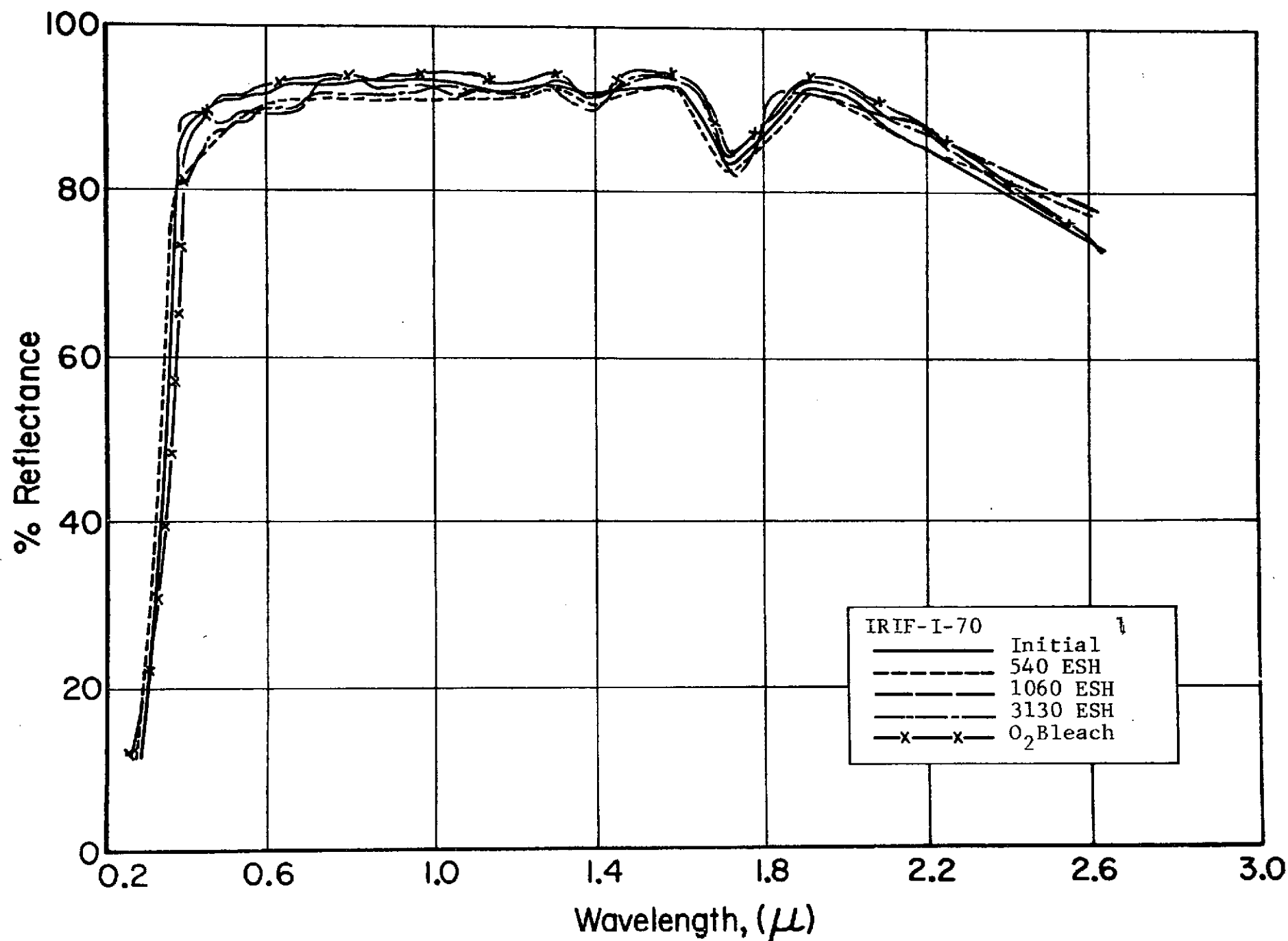
Figure No. 12 REFLECTANCE SPECTRA OF LH-106(6-12)/G

Legend (IRIF-I-70):
- Initial
- 540 ESH
- 1060 ESH
- 3130 ESH
- —x—x— O_2 Bleach
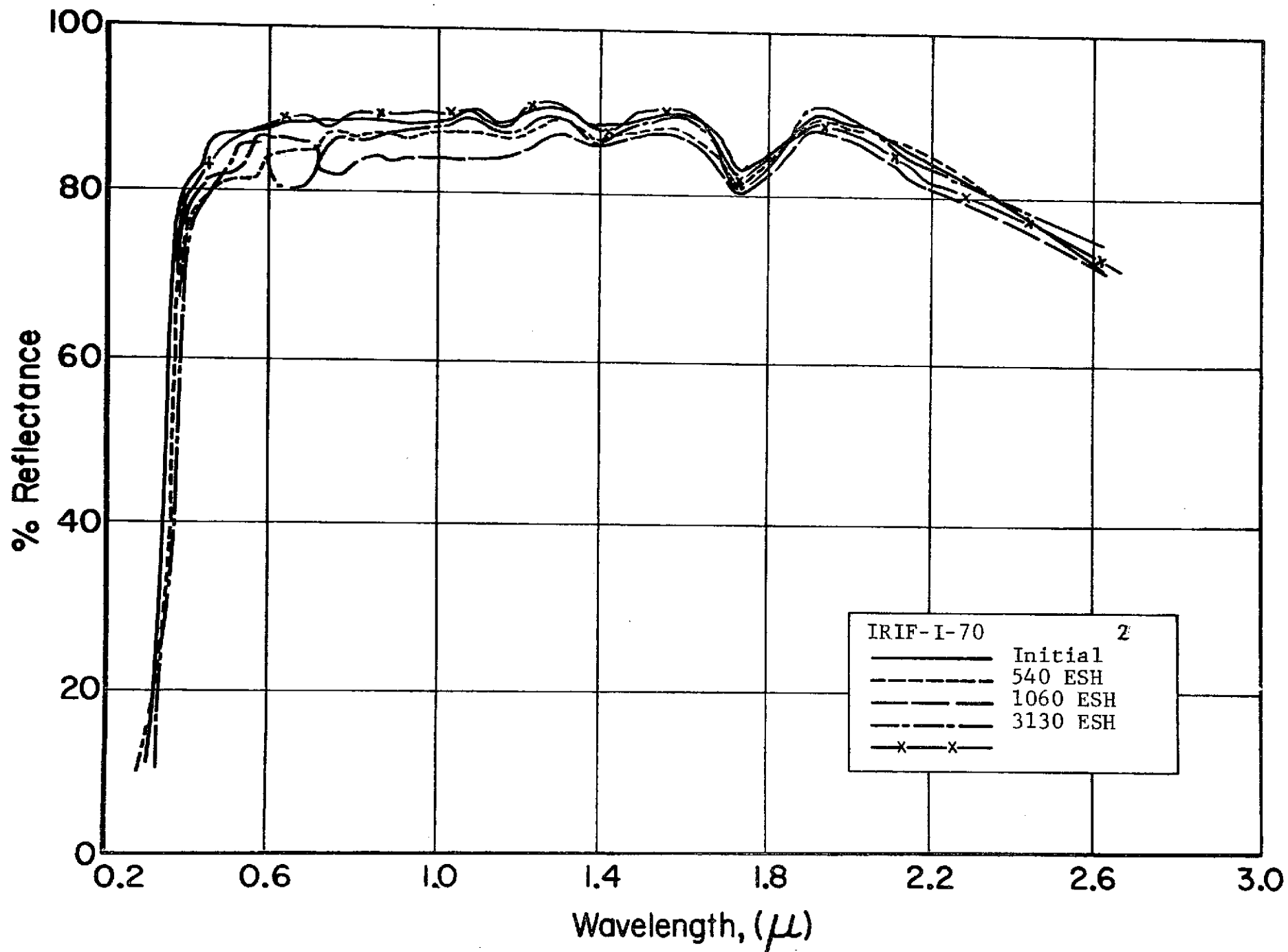
Figure No. 13 REFLECTANCE SPECTRA OF LH-106(6-12-10)/G
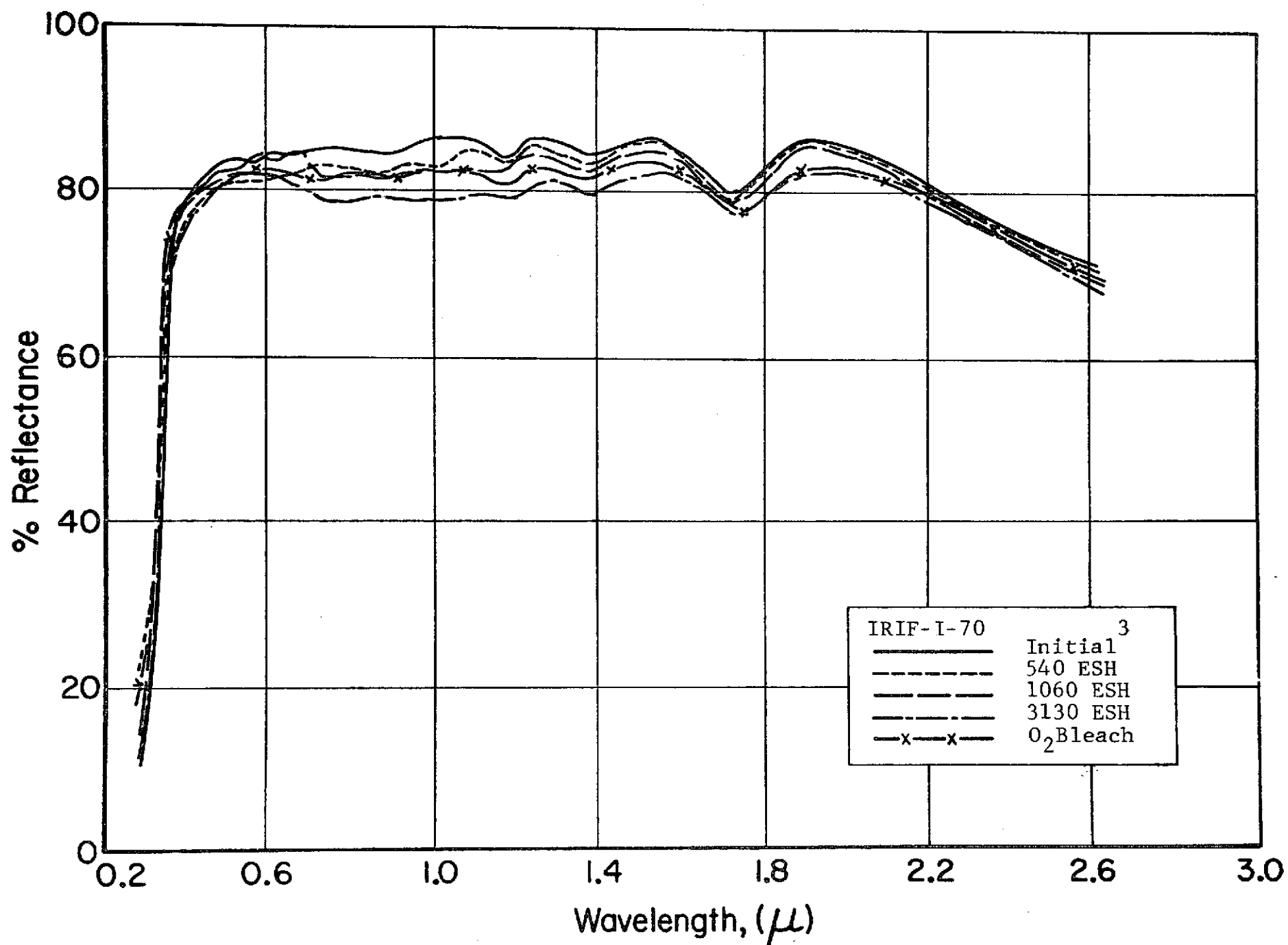
Figure No. 14   REFLECTANCE SPECTRA OF LH-106(6-12-A-10)/G
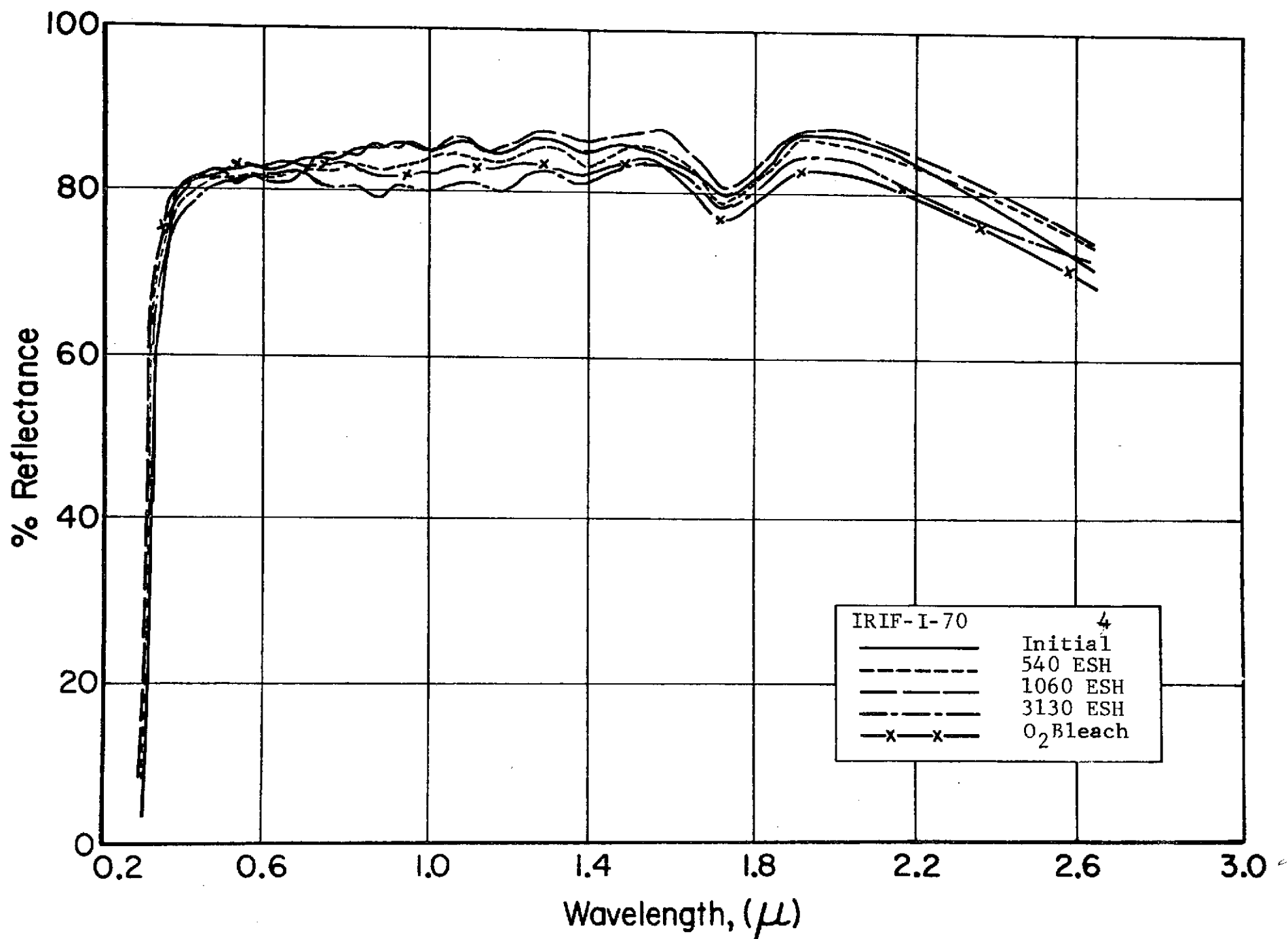
Figure No. 15   REFLECTANCE SPECTRA OF LH-106(6-12):Li$_2$SiO$_3$/G
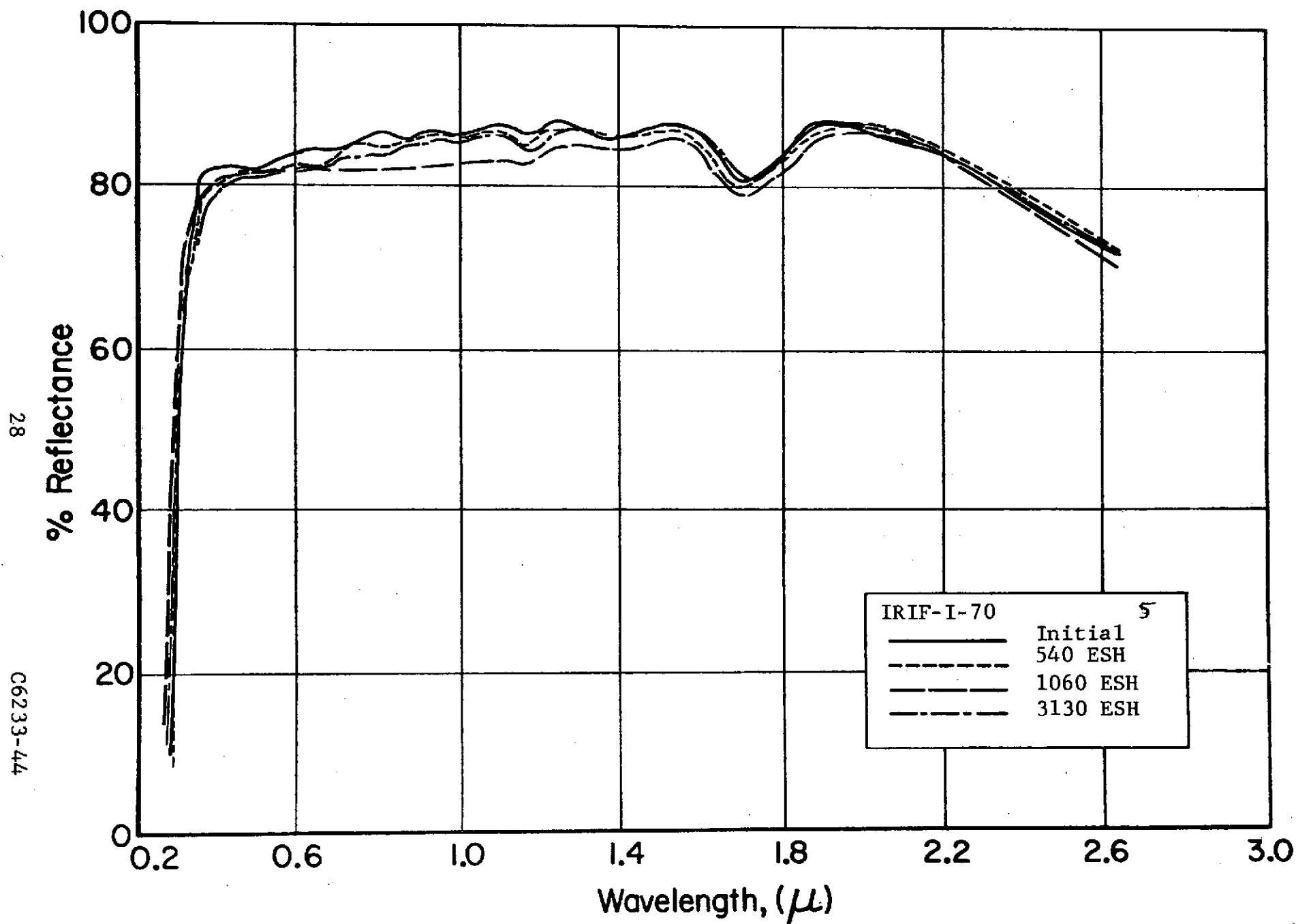
Figure No. 16   REFLECTANCE SPECTRA OF LH-106(6-12-10):Li$_2$SiO$_3$/G
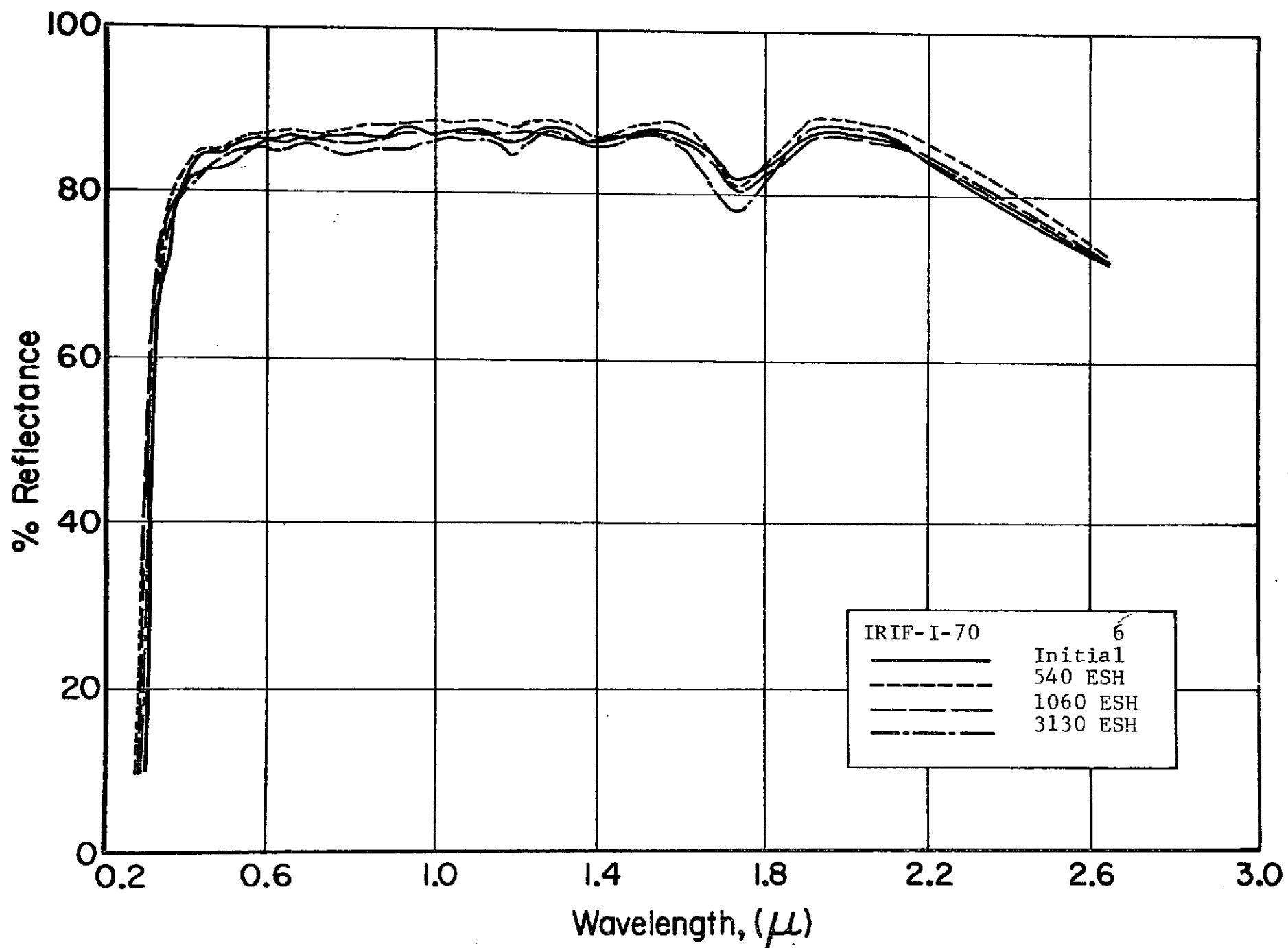
Figure No. 17 REFLECTANCE SPECTRA OF LH-106(6-12-A-10):Li_2SiO_3/G

30
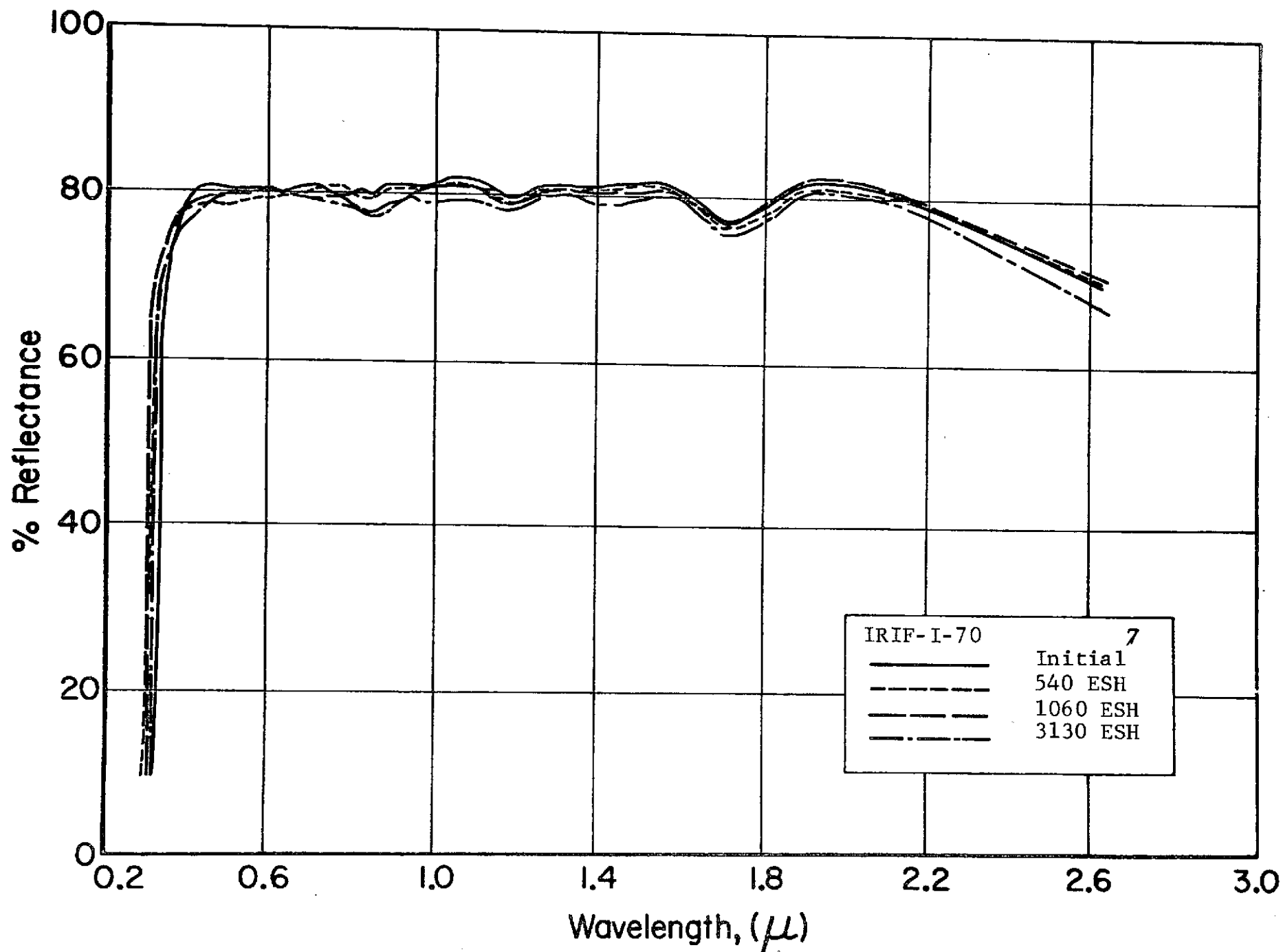
Figure No. 18   REFLECTANCE SPECTRA OF LH-106(6-12):K_2SiO_3/G
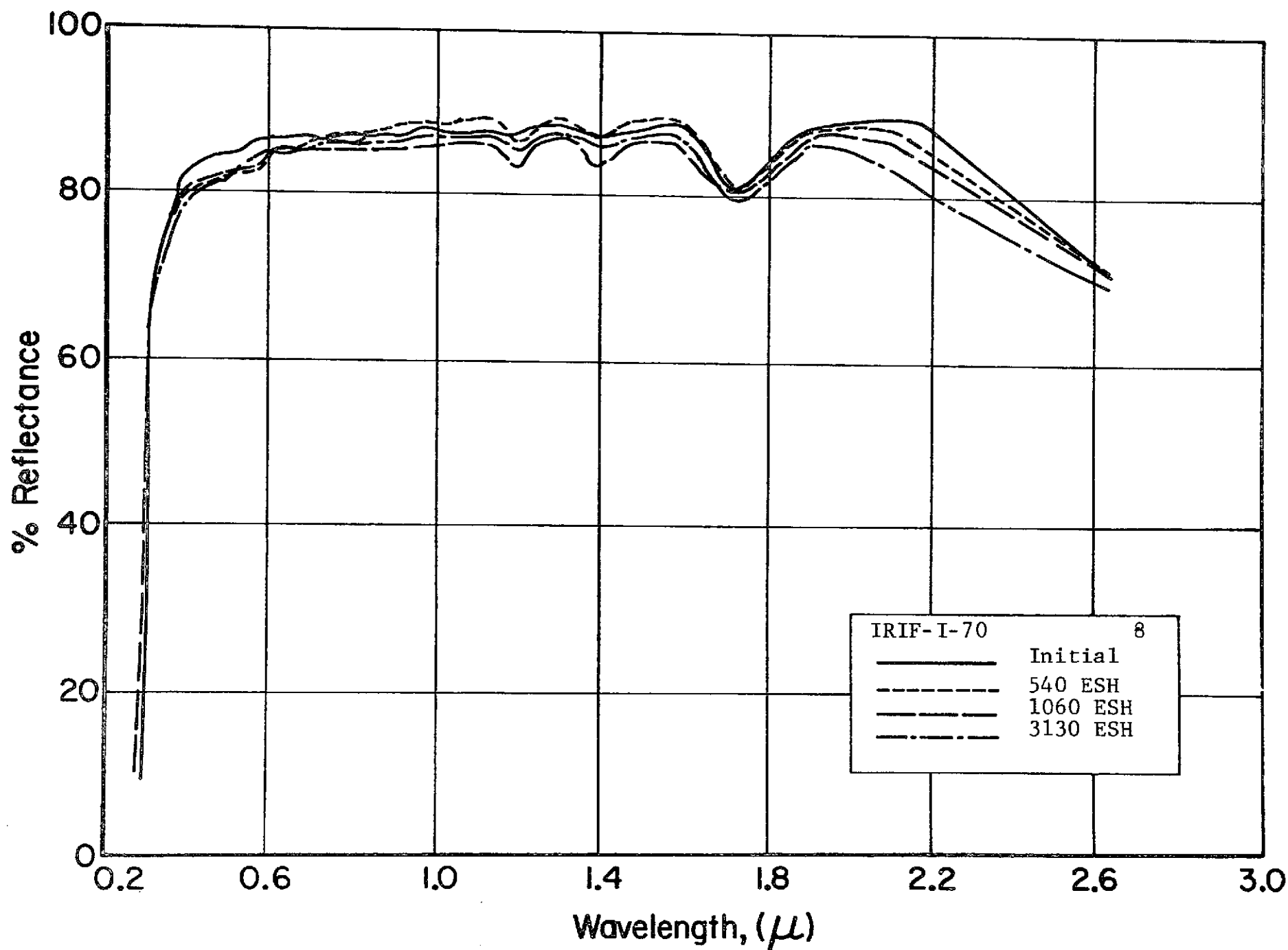
Figure No. 19   REFLECTANCE SPECTRA OF LH-106(6-12-10):K_2SiO_3/G
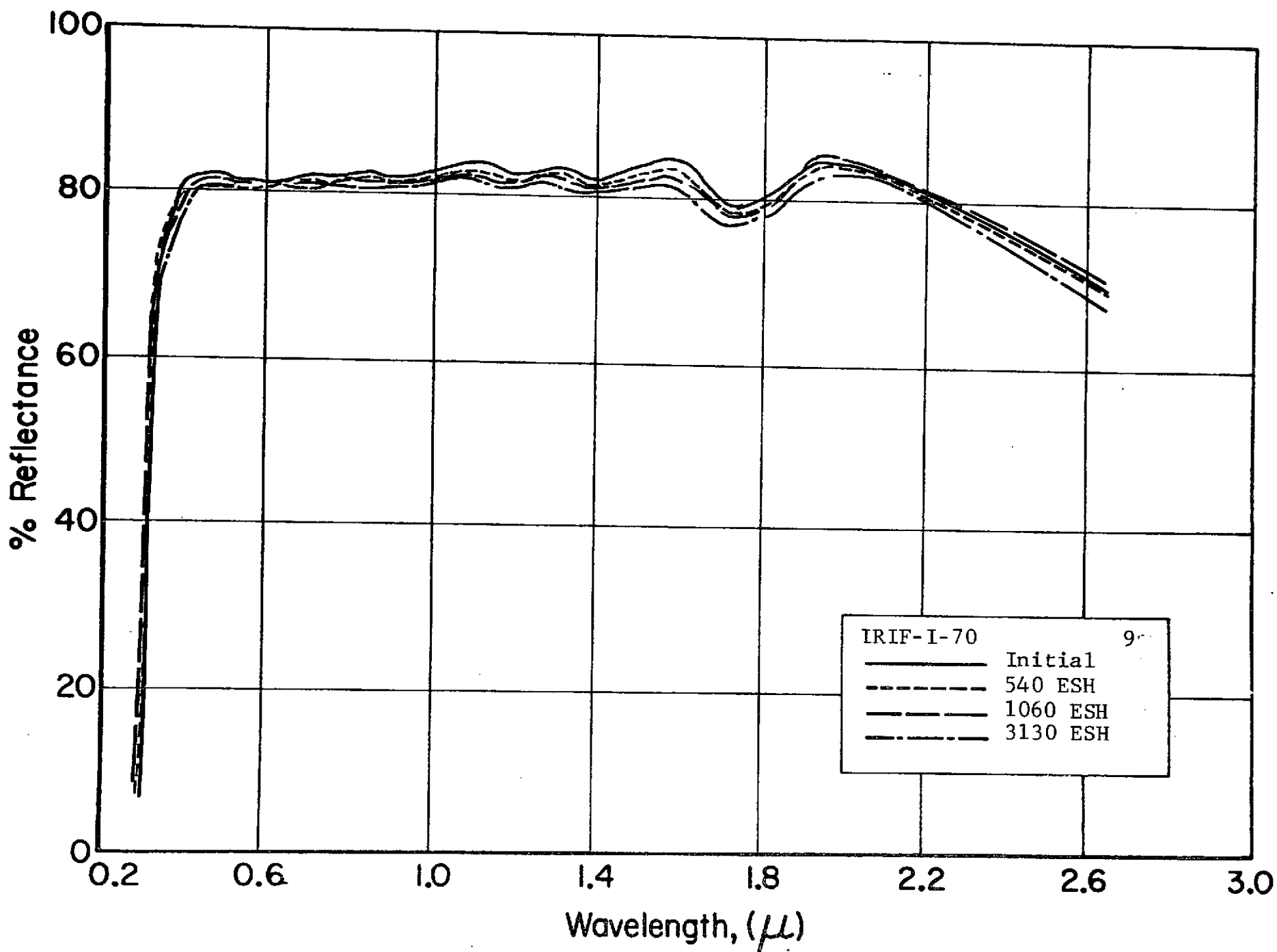
Figure No. 20   REFLECTANCE SPECTRA OF LH-106(6-12-A-10):K$_2$SiO$_3$/G
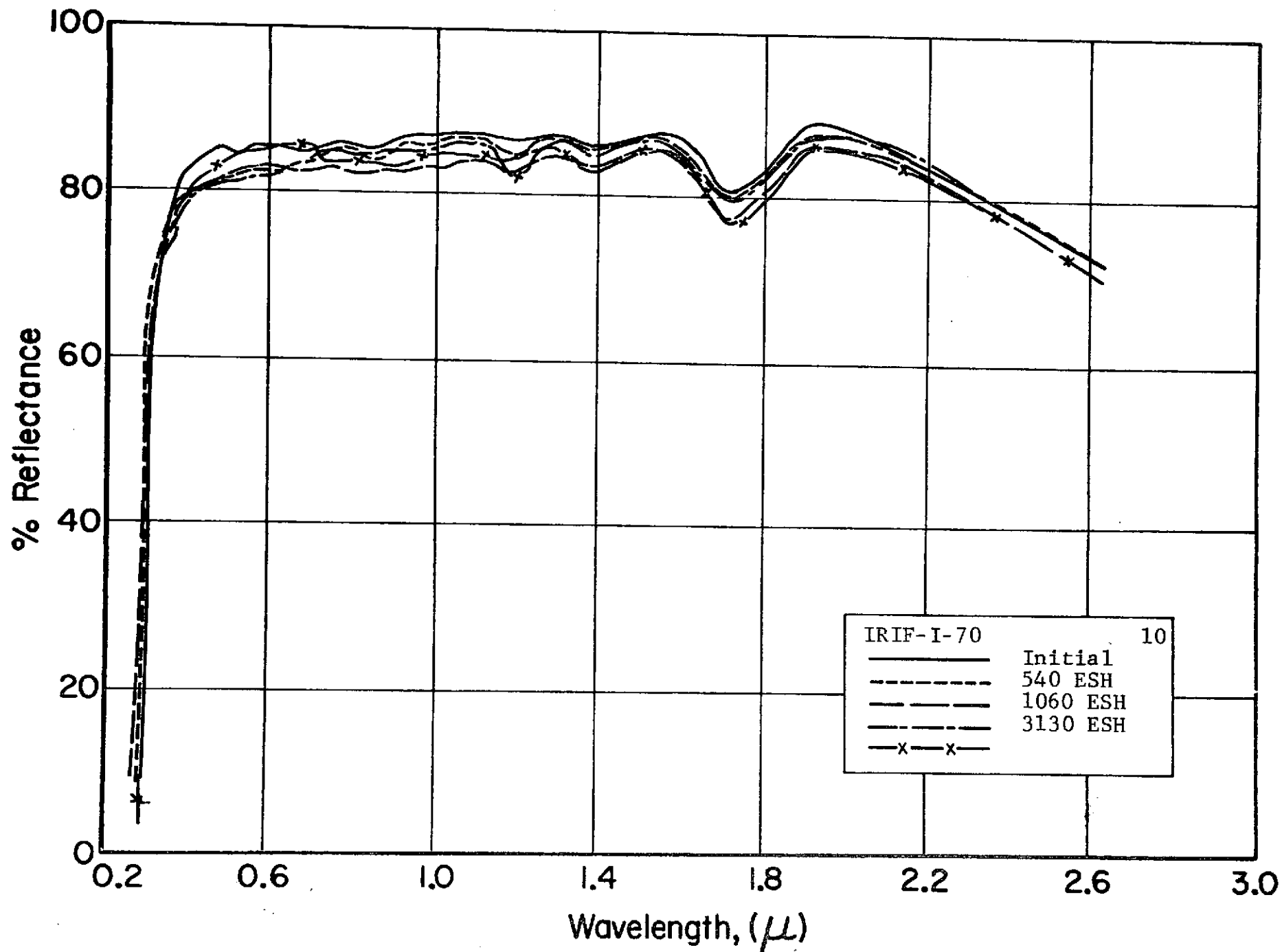
Figure No. 21   REFLECTANCE SPECTRA OF LH-106(6-12):K_2SiF_6/G
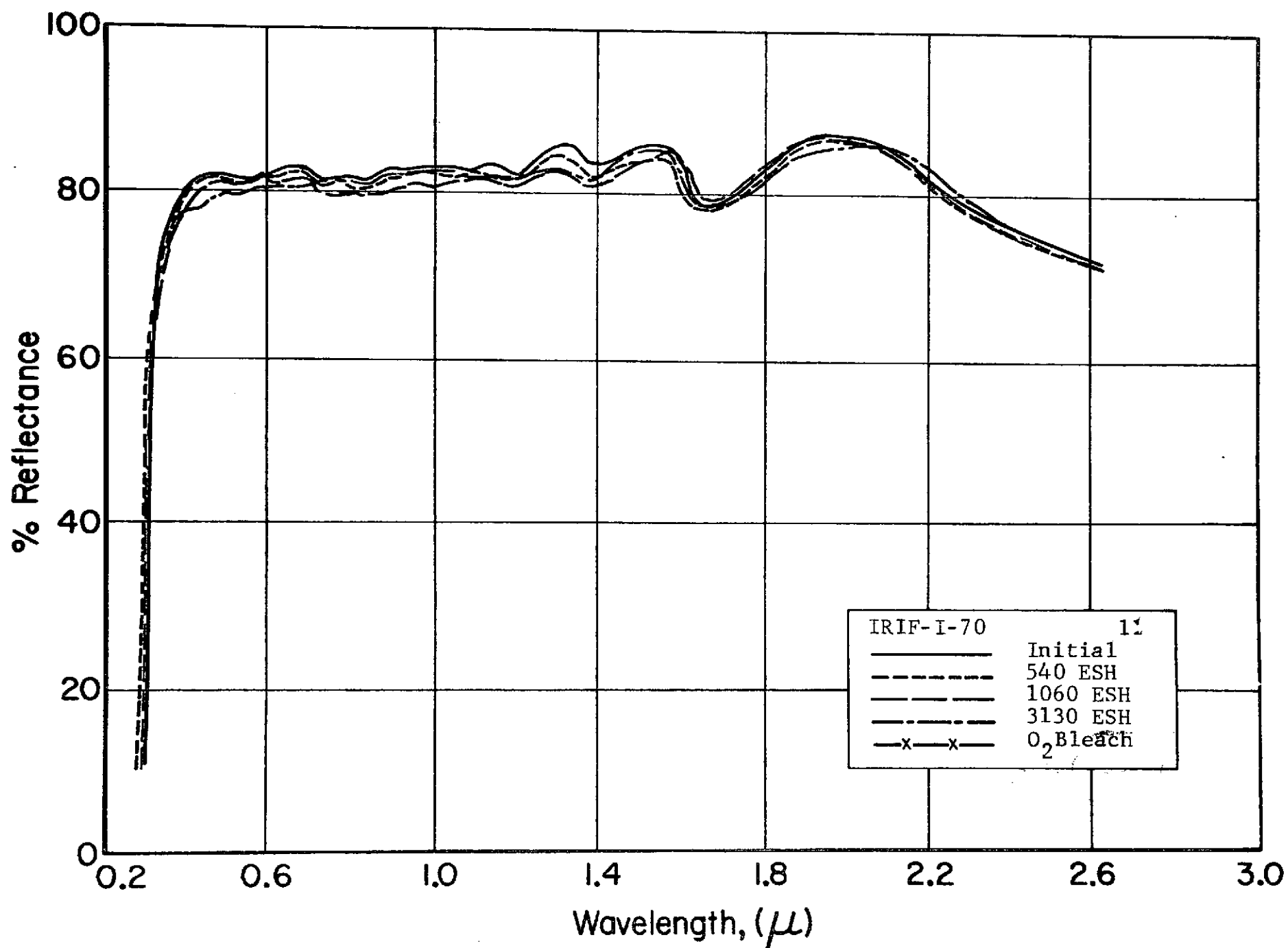
Figure No. 22 REFLECTANCE SPECTRA OF LH-106(6-12-10):K_2SiF_6/G
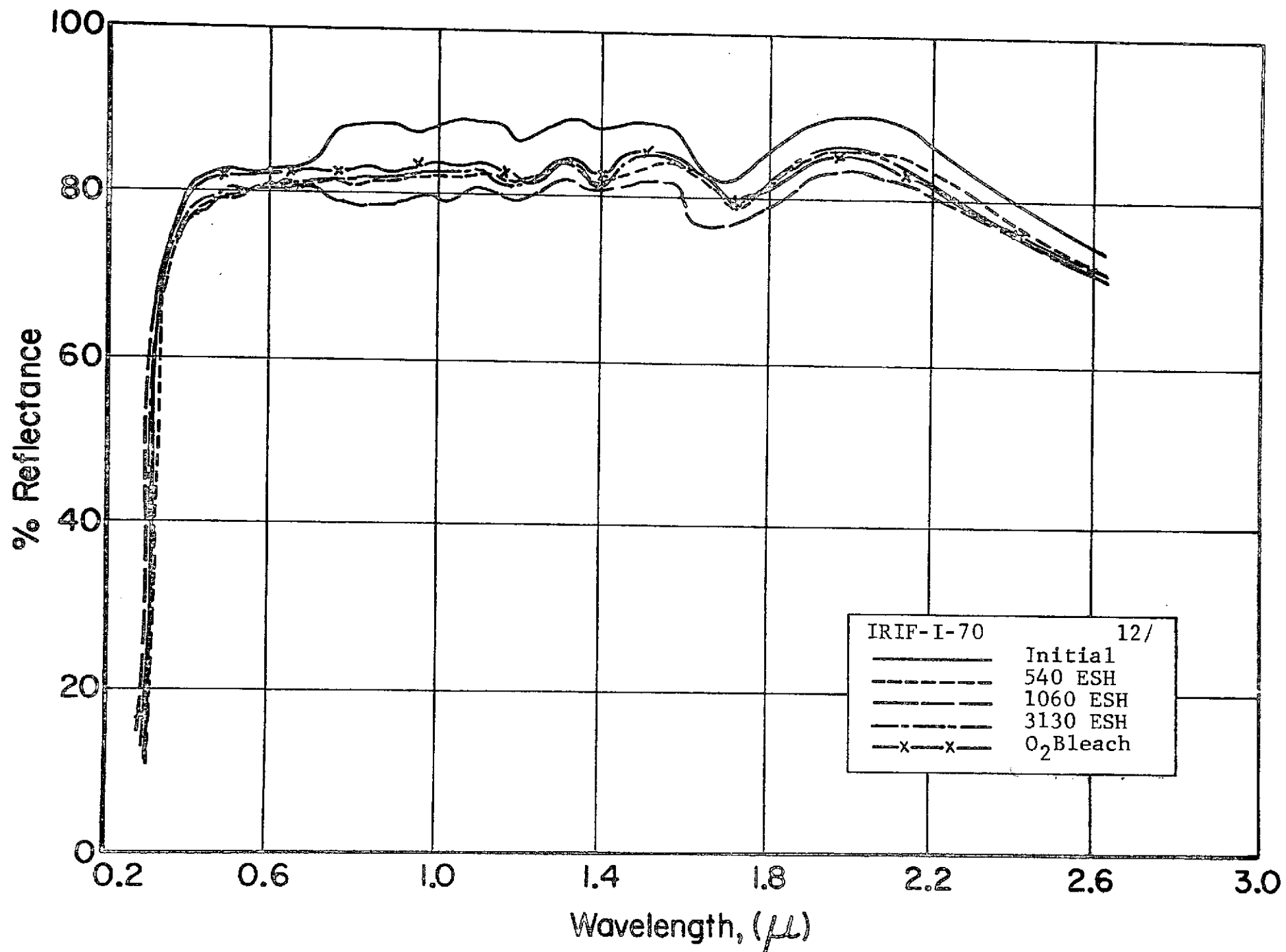
Figure No. 23   REFLECTANCE SPECTRA OF LH-106(6-12-A-10):K_2SiF_6/G

3.2.3 Analyses and Discussions

From a general survey of the spectra of the paints irradiated in I-70, and as Table 3 also shows, it is apparent that most of these paints are relatively stable. The induced changes range from .012 for the paint with the pigment (6-12):K_2SiO_3 to 0.34 for that with (6-12-10). The 6-12 pigments of LH-106 do not exhibit a "knee" in the near ultraviolet region of the spectrum. Consequently, the resulting "knee" reflectances (at 370nm) range from 72 to 76%. Surprisingly, the A-10 treatment of the 6-12 pigmented paint reduced the degradation at 400nm while not affecting it at 900nm, compared to the 6-12 and 6-12-10 pigmented paints. In Table 4 we summarize some of the relevant data.

An analysis of table 4 leads to the conclusions that, in the LH-106(6-12) pigments, acid washing has no significant effects, and, most importantly that K_2SiO_3 provides much better protection than do any of the other encapsulants. This may be seen both at 400nm and at 900nm in all 3 series. The spectra of these samples show the effect of oxygen bleaching, and in general bleaching, when it does occur, has a greater effect in the 900nm region than in the 400nm region. The ΔR data of table 4 represent the change in reflectance (with respect to the initial reflectance) before and after a post-irradiation exposure to 760 Torr of pure O_2. The ΔR_{900} data are particularly important because they indicate the effectiveness of an encapsulant. Compare, for example, the ΔR_{900} data for the 6-12 series. The untreated 6-12 pigment displays an ultraviolet radiation induced degradation (D) at 900nm of .07 and upon exposure to O_2 a recovery (R) to .01, thus the notation .07/.01. Ideally, in the degradation/recovery index, D would be minimal and R would be somewhat less. The .07/.01 ratio reflects the fact that the pigment was

unencapsulated. In the same series the K_2SiO_3 permitted only .05 degradation (O_2 bleaching spectra were not taken for this sample.), while K_2SiF_6 is next best. The D/R index at 900nm measures the effectiveness of an encapsulant, primarily in the value of D, but as verified by R. The rationale for using this index derives from the fact that the ΔR_{900} damage is known to be oxygen-related. Under UV irradiation the pigment surface undergoes photodesorption of the oxygen. An encapsulant prevents or deters this desorption. Thus D relates to the optical effect of photo desorption (diffusion away) from the surface, and R relates to the optical effect of oxygen re-absorption, and consequently

both are a measure of how good a barrier the encapsulant is to O_2. Both values are necessary in determining this, because in some instances absorption bands in other spectral regions affect the ΔR_{900} value. Thus, we consider also the D/R values at 400nm, where the oxygen effect very likely results from an oxygen-related defect in the siloxane resin, and equally likely may be provoked by the encapsulant or the surface defects of an unprotected pigment (Ref. 3). The oxygen may induce a significant recovery at 400nm, effecting a partial recovery at 900nm which is not necessarily due to an ineffective encapsulant.

The LH-106 series quite obviously produce highly stable paint systems. The fact that none of the 3 series prepared evidences a knee may bear upon the explanation for this stability. We should observe also that acid washing should not be expected to produce any significant results in a pigment which has no "knee", and obviously in this test the A-10 treatment hasn't. Further, a stoichiometry in which an excess of either ZnO, TiO_2 or other reaction product(s) is not evident may also create a different defect structure, thus changing the amount and nature of the surface defects whose optical effects an encapsulant must mitigate or prevent.

3.3 IRIF Test I-71

3.3.1 Test Conditions

Samples irradiated in IRIF Test I-71 received an ultraviolet exposure of 460 ESH. Two samples were measured after an additional exposure of 600 ESH - a total of 1060 ESH. The test was carried out in a vacuum whose pressure level was maintained well below 10^{-6} Torr. The samples were irradiated at an average intensity level of 6 ultraviolet suns using a high pressure 1000w Pek AH-6 Mercury lamp. Reflectance measurements, in the spectral

range from 325 to 2600nm, were made prior to irradiation, at exposures of 130 ESH, 460 ESH, and (for 2 selected samples) at 1060 ESH, and (again for the same 2 samples) after a post-irradiation O_2 bleach.

3.3.2 Materials Descriptions and Test Results

The samples, with the exception of S-13G, are all Zn_2TiO_4 powder films on IRIF coupons. The full complement of test samples is listed in Table 5, along with their associated solar absorptance values. The MOX-A materials (where MOX refers to "mixed oxalates" and "A", to a specific batch) differ from previous Zn_2TiO_4 pigments in two important ways. Firstly, the MOX-A pigments were prepared by mixing individually precipitated zinc and titanium "oxalates" and then converting the mixture to Zn_2TiO_4. This differs from previous Zn_2TiO_4 pigments in that their precursors were coprecipitated and then converted. Secondly, an error was made in the formulation of the MOX-A resulting in a 1.49 Zn:Ti mole ratio rather than the theoretically required 2.0 value.

Also in the test complement is a sample of MOX, (No. 6), the original mixed oxalate batch, one which has a Zn:Ti mole ratio of 2.05 (to provide a slight Zn excess). For comparison purposes two samples of a COP pigment are also included.

An experimental pigment, silicon nitride, was included because of its very high purity and good whiteness, S-13G was placed in the test as a control to indicate whether the exposures were within nominal, expected values. The reflectance spectra for all of the samples appear in Figures 24-35, inclusive.

3.3.3 Analyses and Discussions

In view of the substantially different Zn:Ti mole ratio of the MOX-A pigments, it is indeed very surprising to note that most of the MOX-A samples display much less of a "knee" effect

Table 5

IRIF TEST I-71

ULTRAVIOLET RADIATION TEST RESULTS

Sample No.	Description*	Solar Absorptance Values					$\Delta\alpha_{s\ 460}$
		Initial	130 ESH	460 ESH	1060 ESH	O_2 Bleach	
7	MOX-A(6-9/4)	.170	.190	.194			.024
8	MOX-A(6-9/16)	.157	.176	.173			.016
9	MOX-A(6-10.5/2)	.124	.150	.158			.034
10	MOX-A(6-10.5/4)	.143	.163	.173			.030
5	MOX-A(6-10.5/8)	.160	.190	.209			.049
6	MOX(6-10.5/2)	.132	.140	.138	.172	.158	.008
3	LH-103(6-10.5/2)	.165	.181	.198			.033
4	LH-103(C6-10.5/2)**	.160	.181	.182			.022
2	MOX-A(6-12/0.5)	.116	.167	.184			.068
11	MOX-A(6-12/2)	.114	.143	.148			.034
12	S-13G (D274)	.165	.178	.193	.216	.226	.028
1	Si_3N_4	.178	.203	.241			.063

*All samples, except for S-13G, are powders

**C6 indicates precursor oxalates were compressed at 5000 psi prior to 600°C pre-calcination
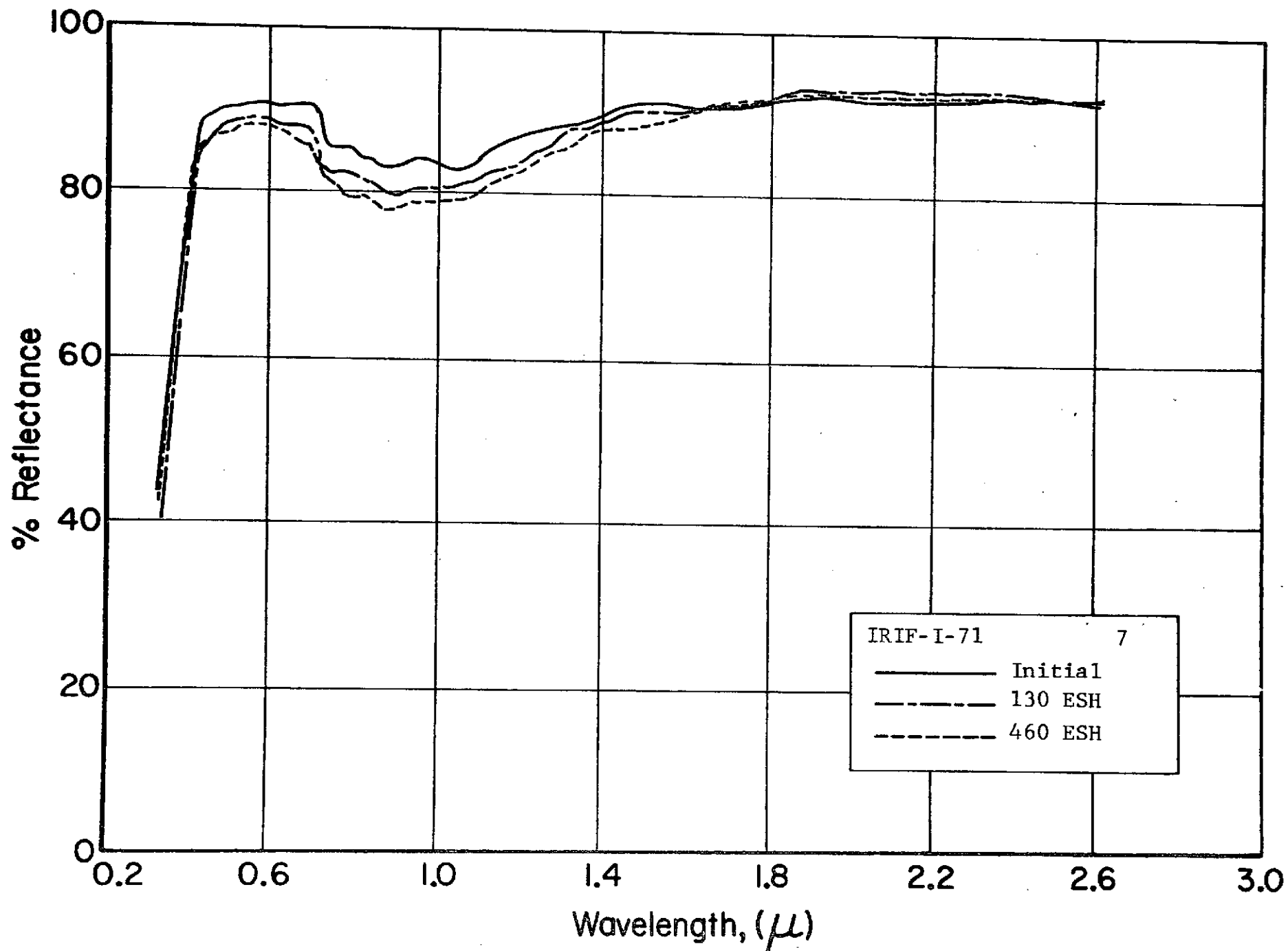
Figure No. 24   REFLECTANCE SPECTRA OF MOX-A(6-9/4) (Powder)
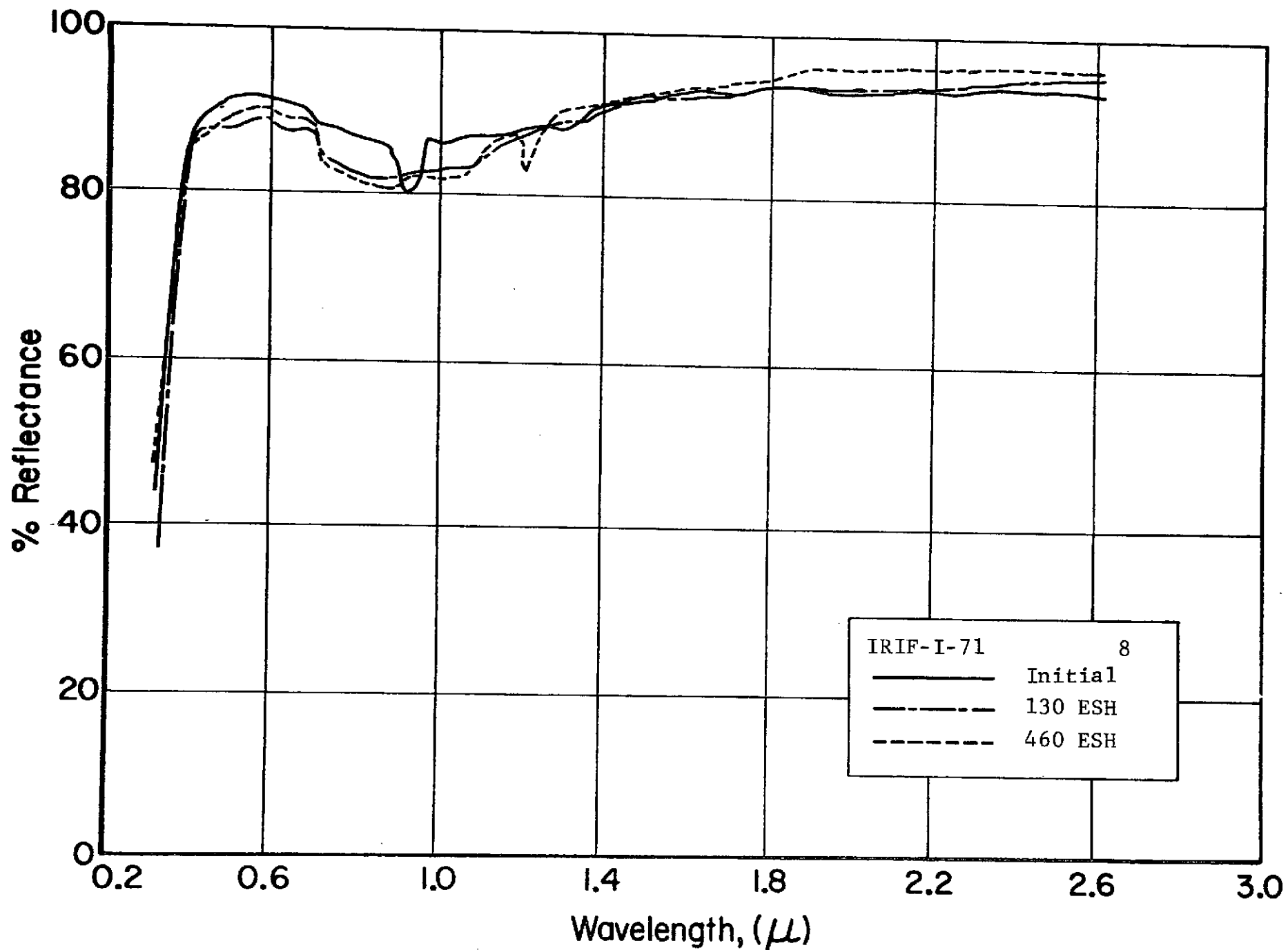
Figure No. 25   REFLECTANCE SPECTRA OF MOX-A(6-9/16) (Powder)
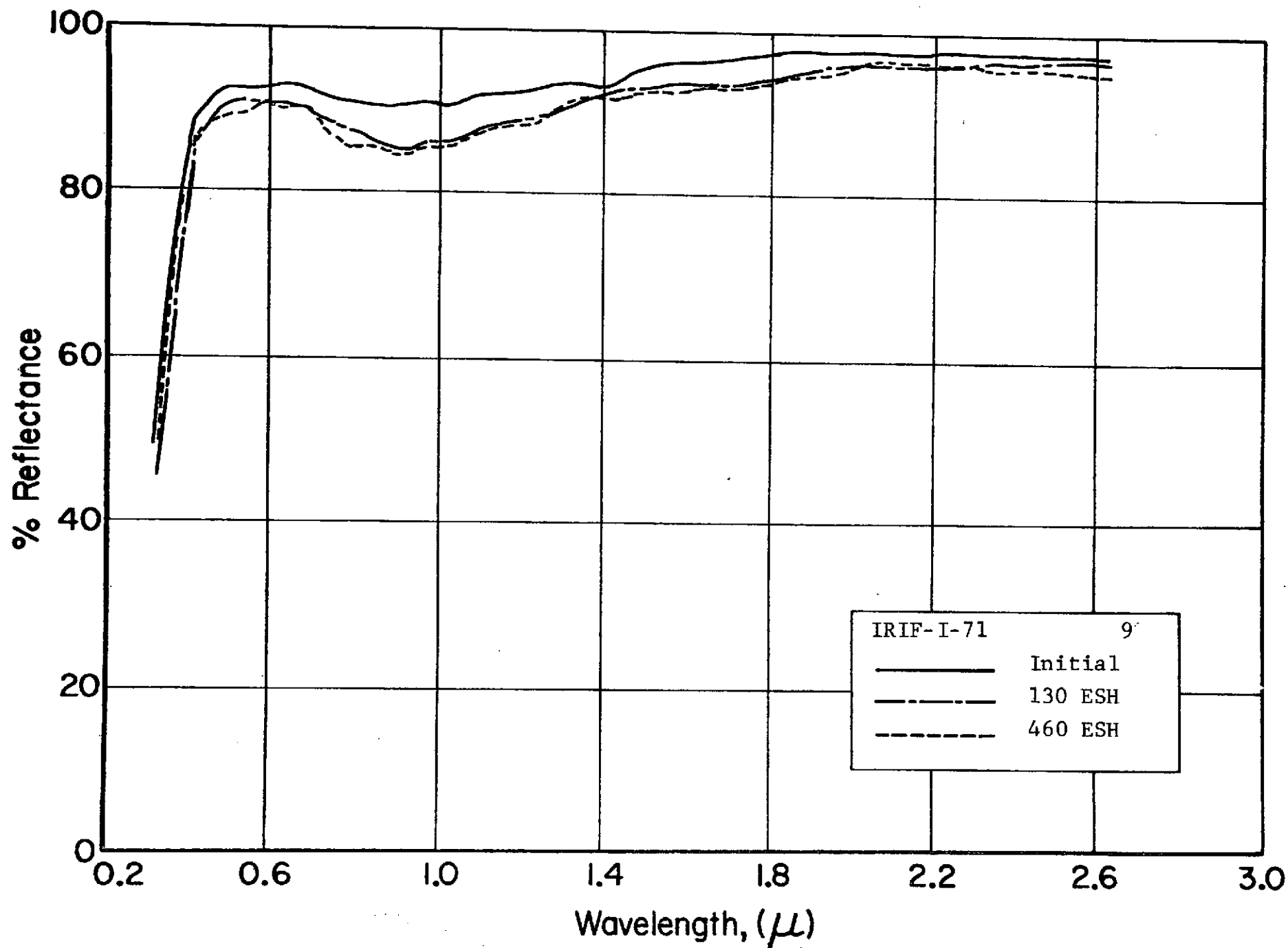
Figure No. 26 REFLECTANCE SPECTRA OF MOX-A(6-10.5/2) (Powder)
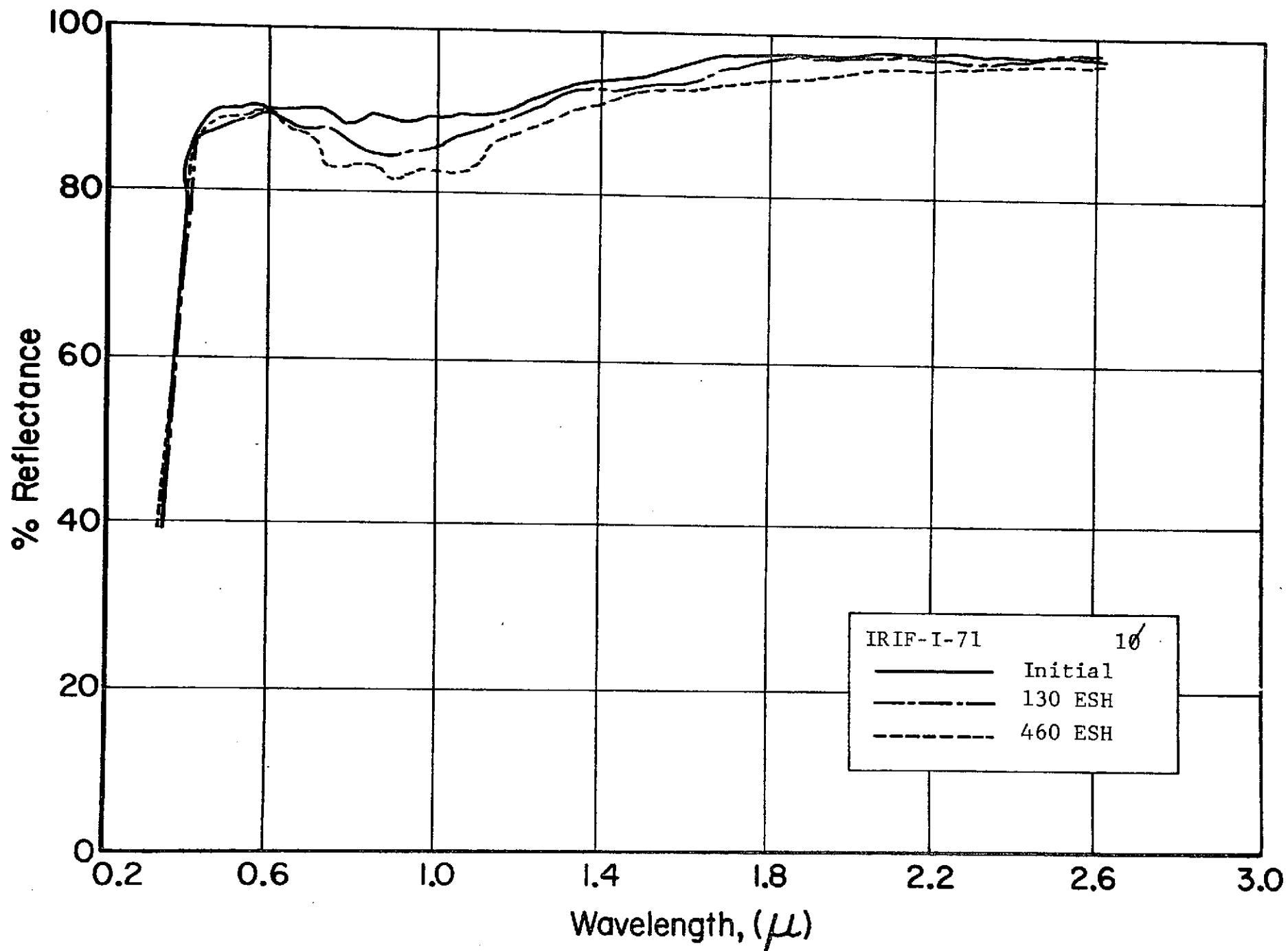
Figure No. 27   REFLECTANCE SPECTRA OF MOX-A(6-10.5/4) (Powder)
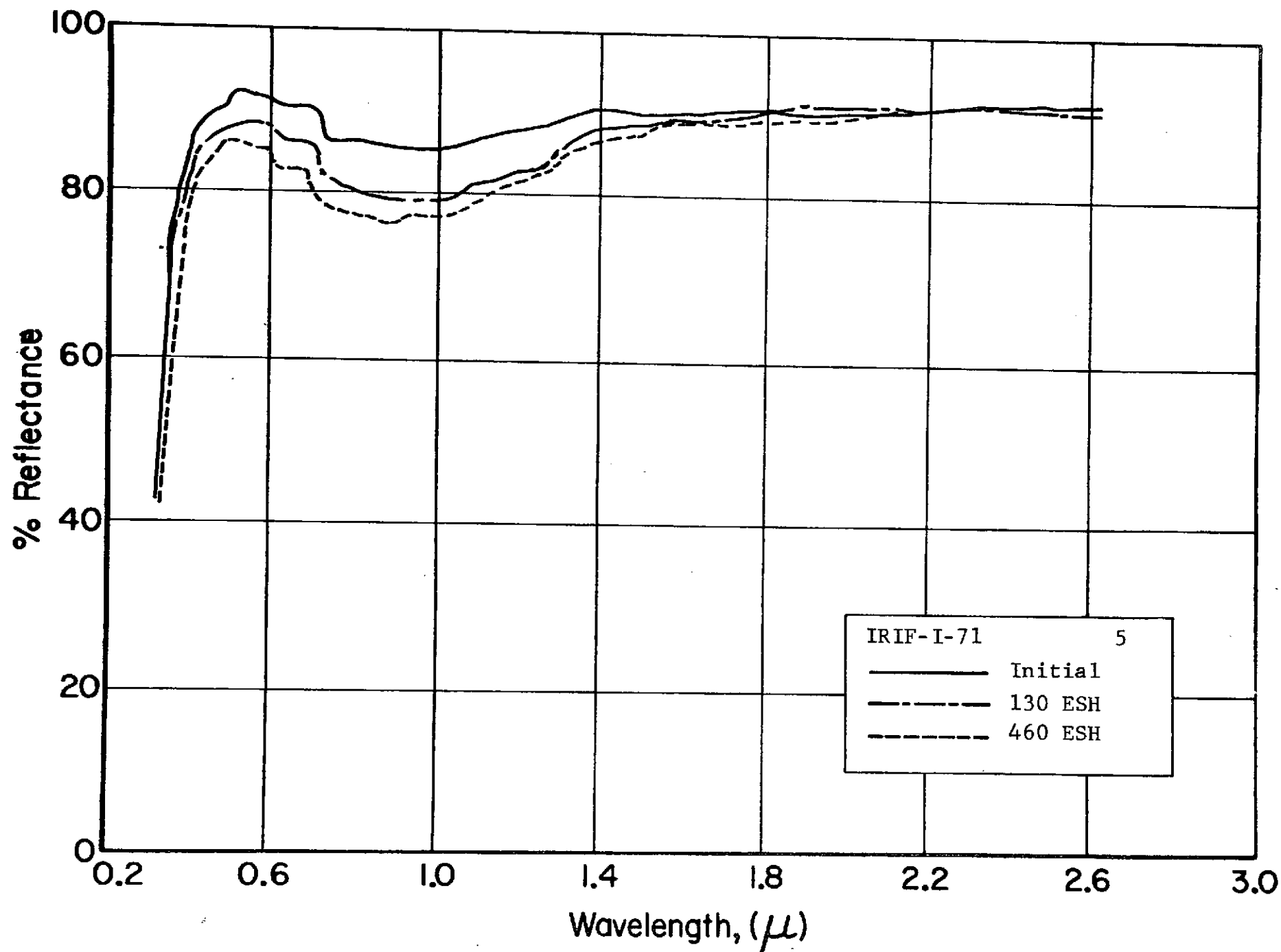
Figure No. 28   REFLECTANCE SPECTRA OF MOX-A(6-10.5/8) (Powder)

C6233-44
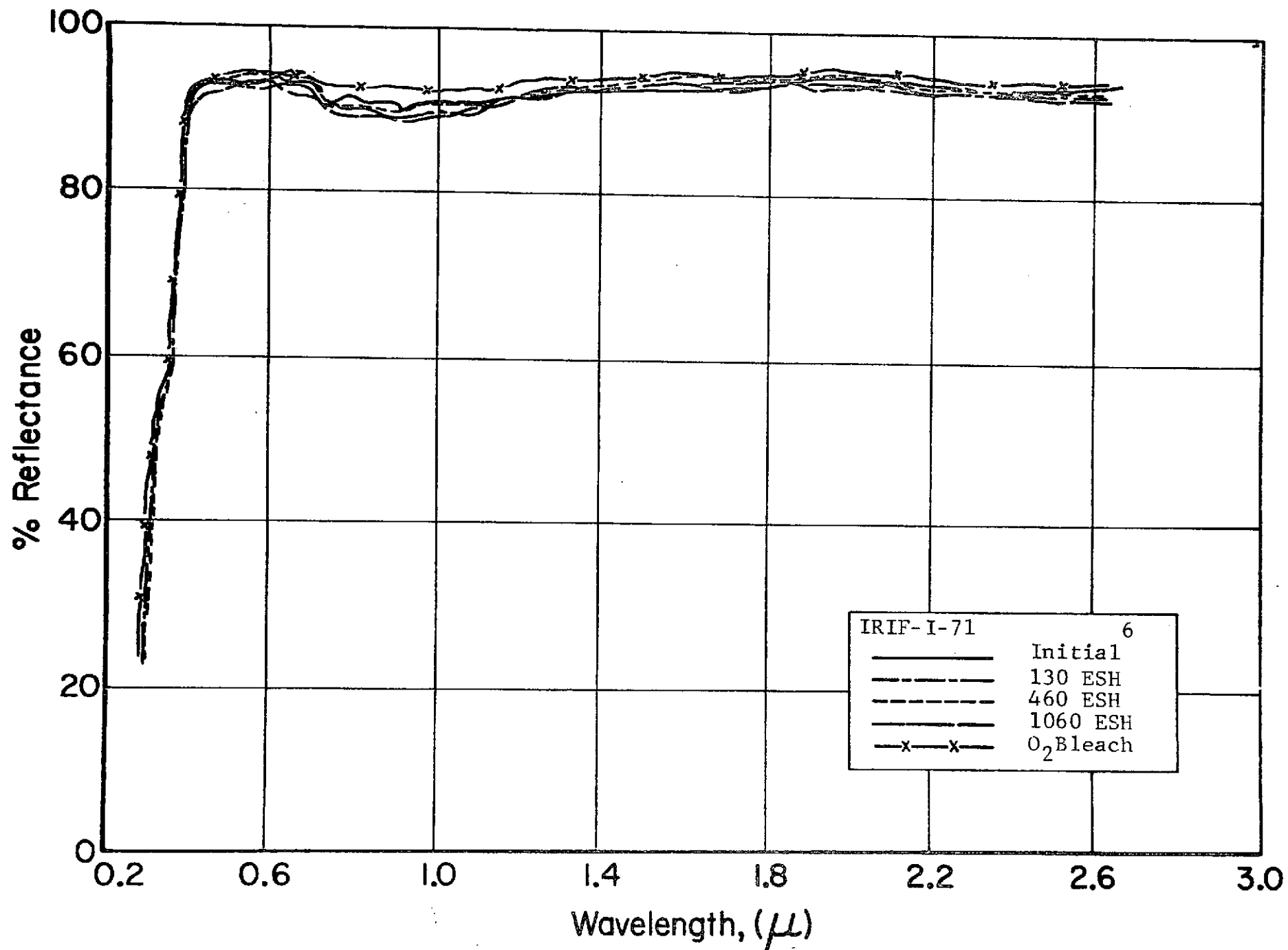
Figure No. 29   REFLECTANCE SPECTRA OF MOX(6-10.5/2) (Powder)
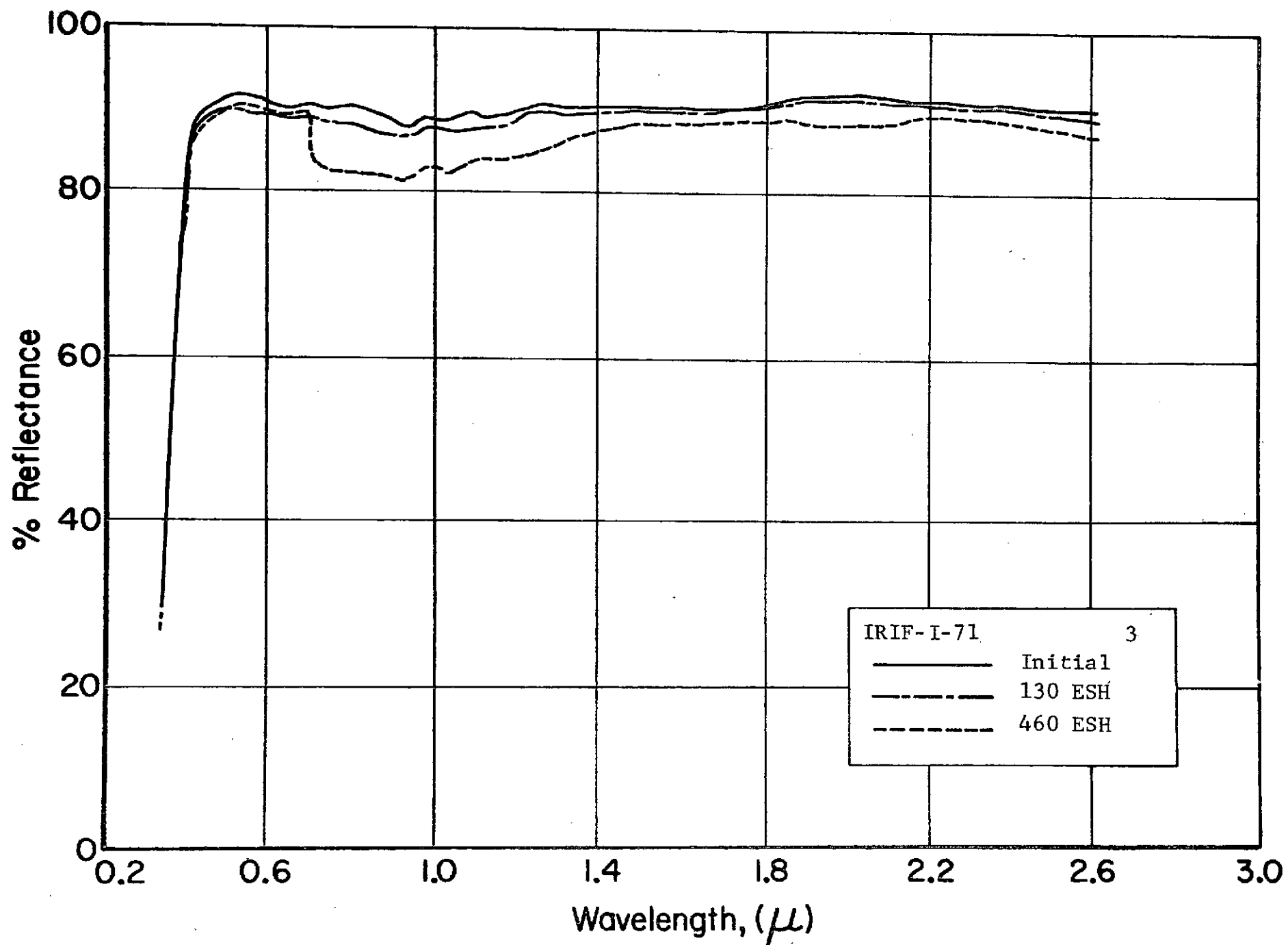
Figure No. 30   REFLECTANCE SPECTRA OF LH-103(6-10.5/2) (Powder)

Legend (within plot):

IRIF-I-71   3
—————————— Initial
—·—·—·—·— 130 ESH
— — — — — 460 ESH
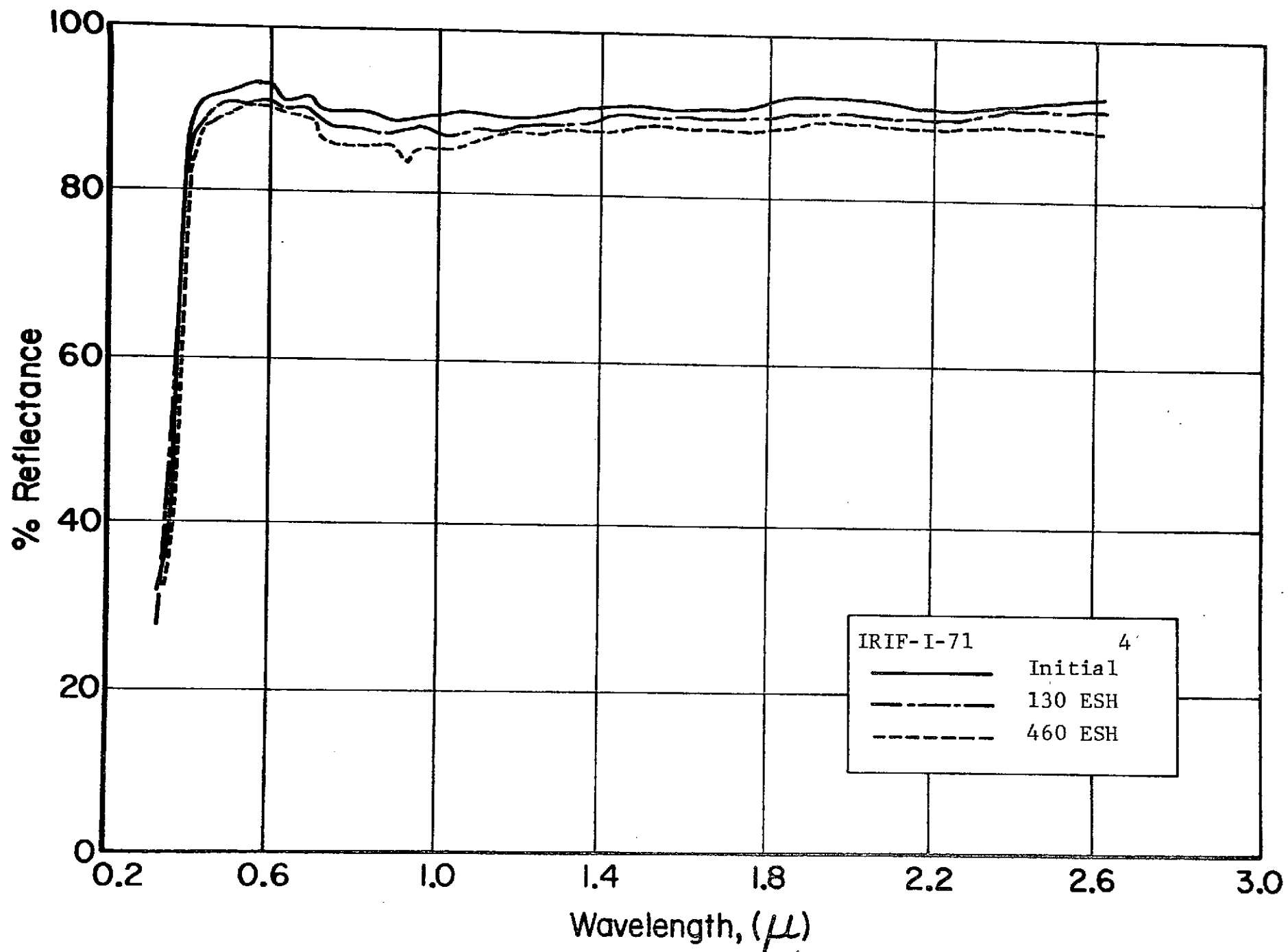
Figure No. 31 REFLECTANCE SPECTRA OF LH-103(C6-10.5/2) (Powder)
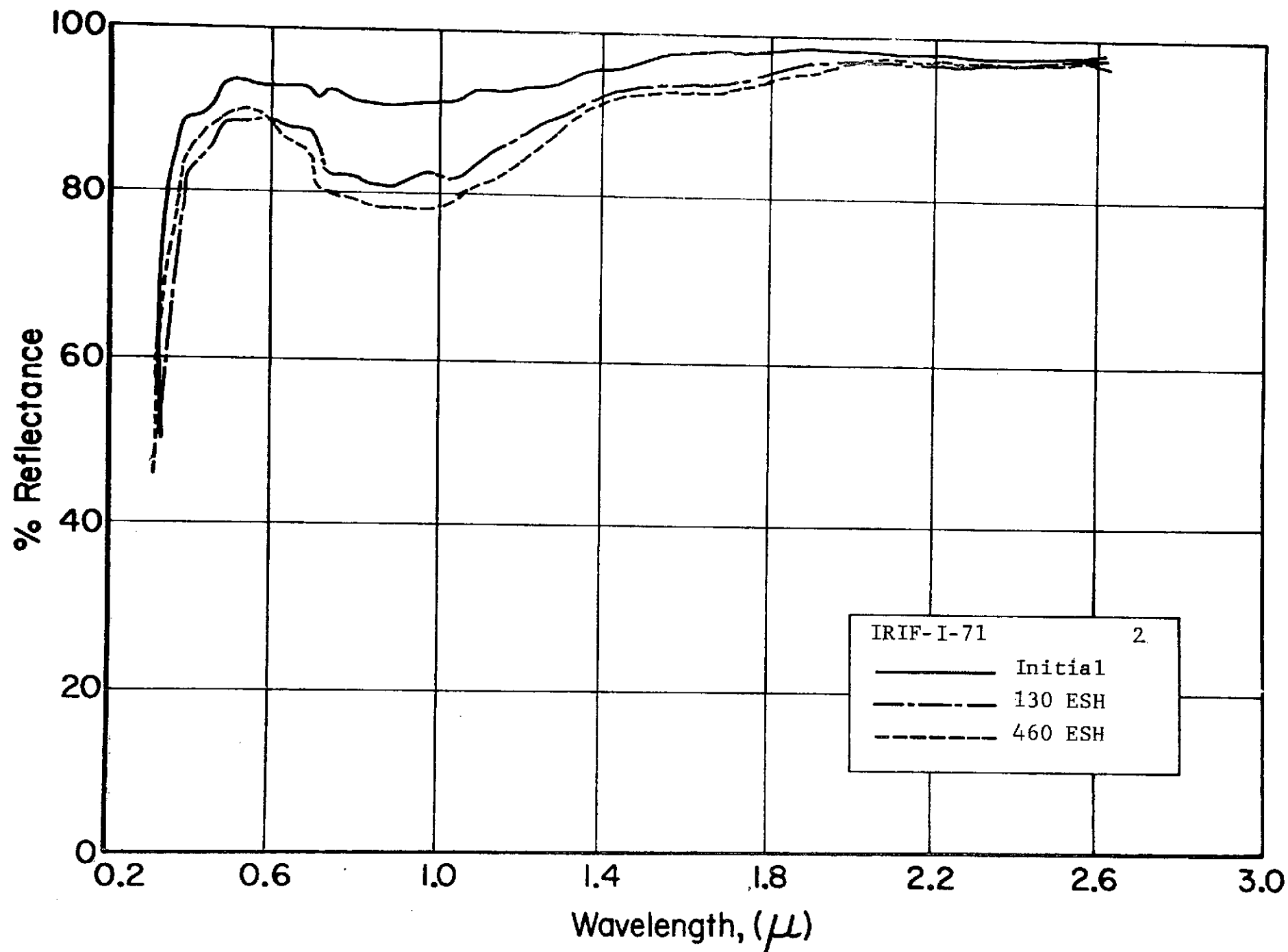
Figure No. 32   REFLECTANCE SPECTRA OF MOX-A(6-12/0.5) (Powder)
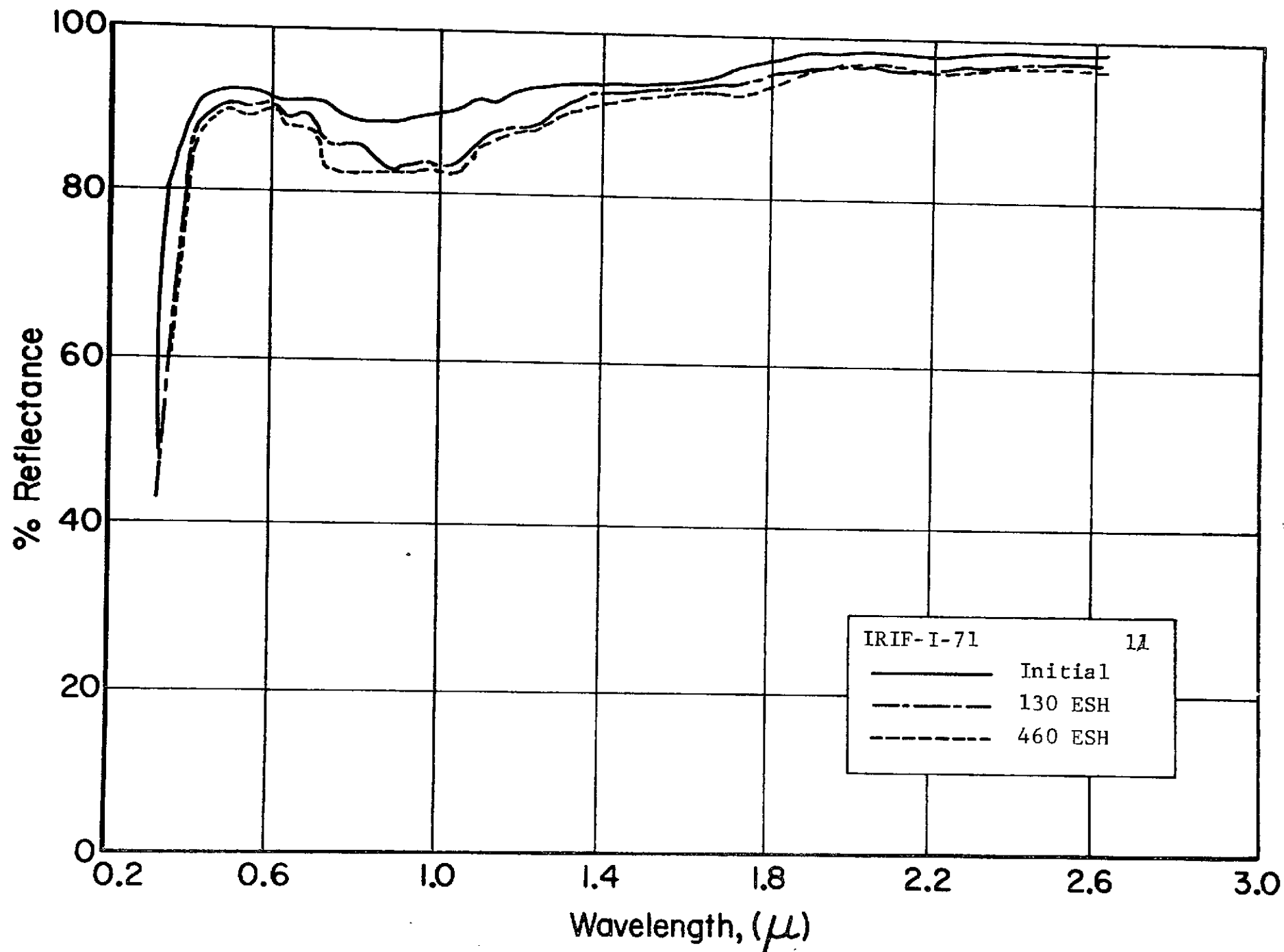
Figure No. 33   REFLECTANCE SPECTRA OF MOX-A(6-12/2) (Powder)
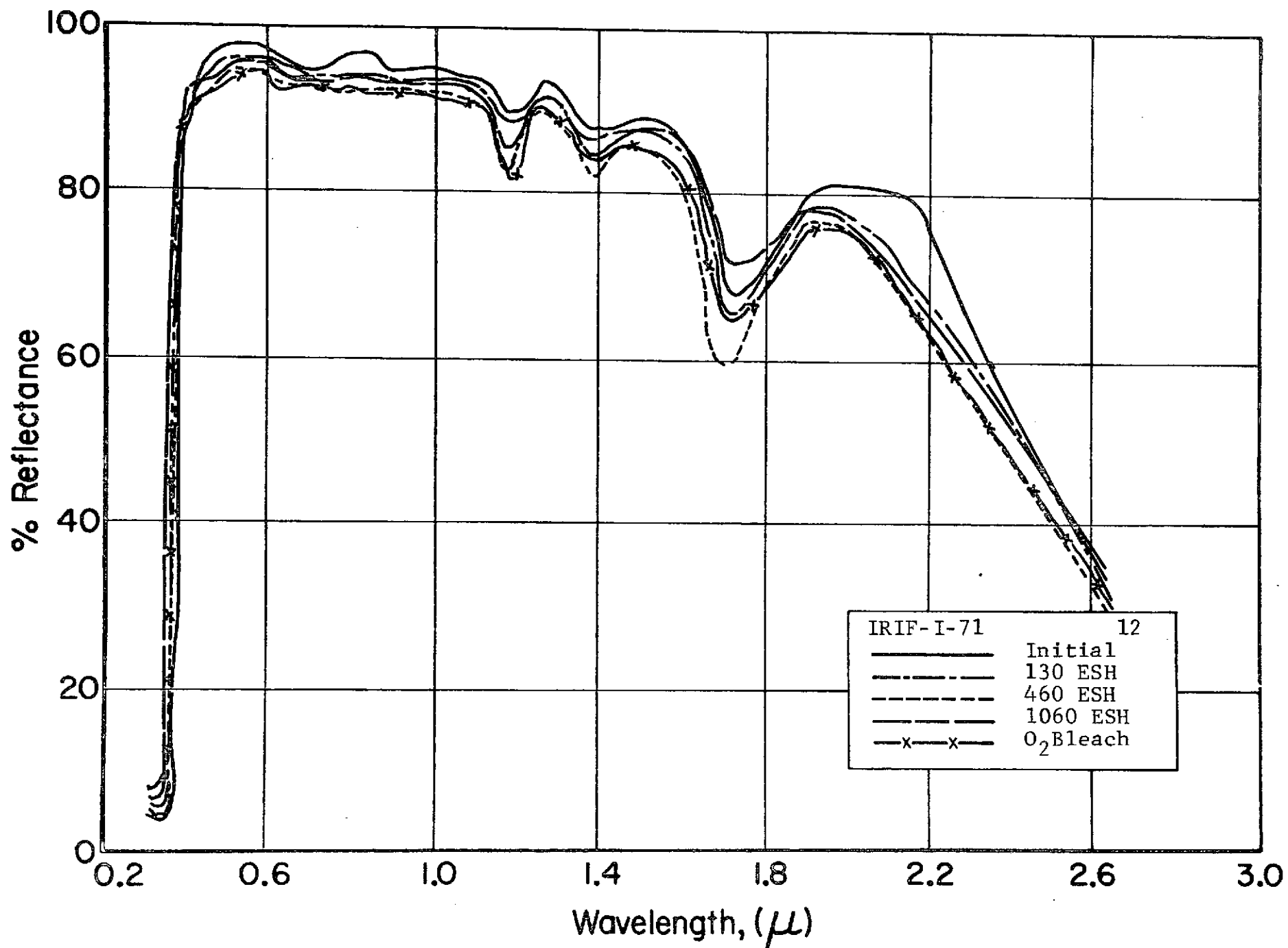
Figure No. 34   REFLECTANCE SPECTRA OF S-13G (D-274)
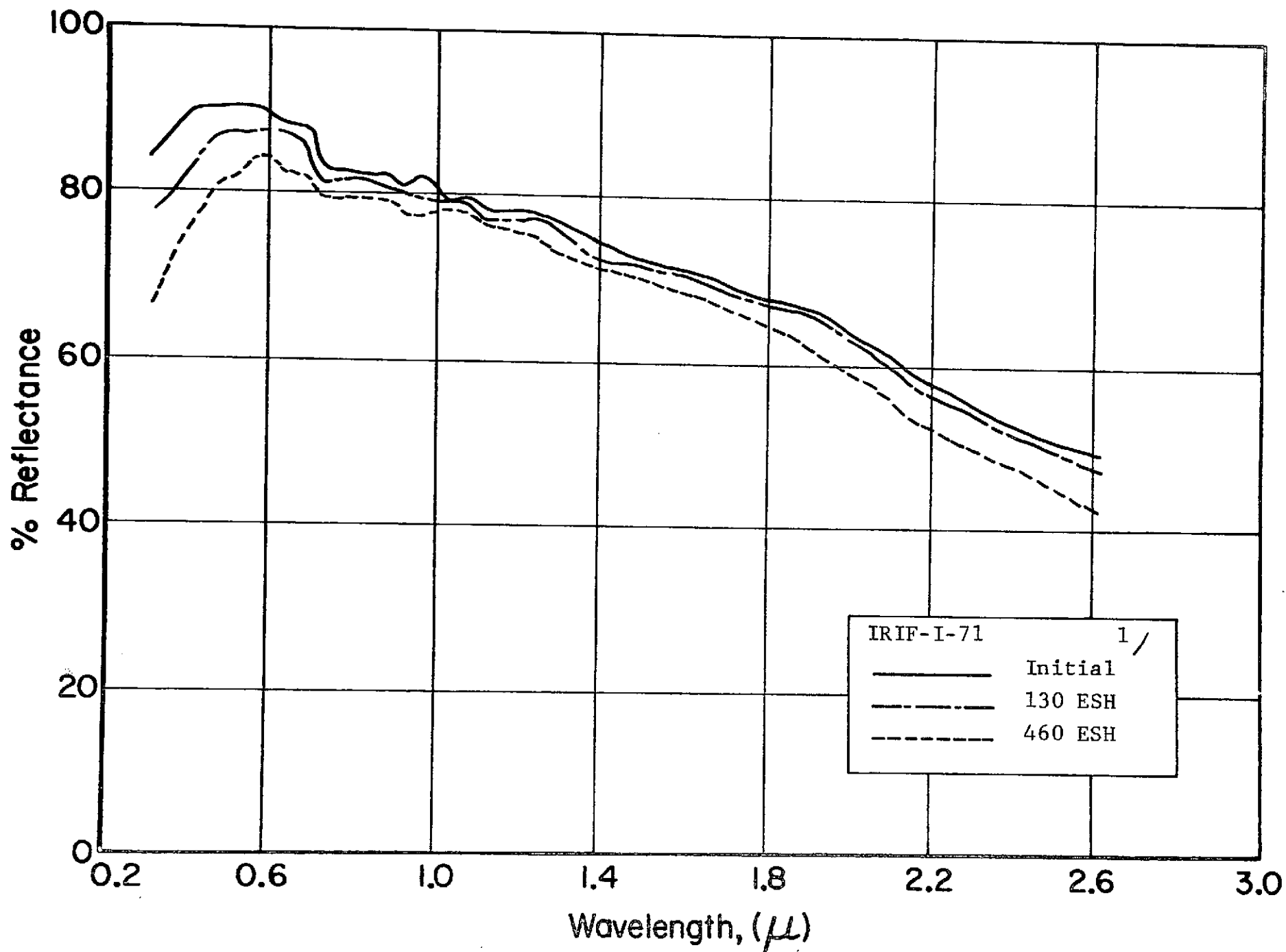
Figure No. 35   REFLECTANCE SPECTRA OF Si_3N_4 (Powder)

Chart axes:
- Y-axis: % Reflectance (0 to 100)
- X-axis: Wavelength, (μ) (0.2 to 3.0)

Legend:
IRIF-I-71   1/
——————— Initial
— · — · — 130 ESH
— — — — 460 ESH

than expected. A comparison of some of the performance data, as shown in Table 6, points up some of the more important differences between MOX-A, MOX and LH-103 pigments.

As table 5 also shows, the degradation of the MOX-A pigments exceeds reasonable limits and explains why the test for all but the S-13G and the MOX pigment samples was terminated after only 460 ESH. This was done since the degradation of Zn_2TiO_4 pigments in OI-650G is always greater than that of the pigment alone. The results, nonetheless, are very informative. The absence of substantial damage in the 900nm region of the MOX-A pigments will undoubtedly require serious appraisal of our earlier requirement for a 2.05 Zn:Ti mole ratio. This requirement was based on two observations: one, that a Zn excess in the Zn_2TiO_4 product can be chemically extracted, while a Ti excess can not; and, second, that a Ti excess would promote the damage evidenced at 900nm, presumably caused by photo-induction of the reaction $Ti^{+4} \rightarrow Ti^{+3}$.

Table 6A contains some data which are somewhat anomalous. If we associate R_k with absorption due to excess ZnO or of TiO_2, we would expect that R_k would be much lower in the case of MOX-A, than in the case of either MOX or LH-103, mainly because MOX-A contains a 25% excess of Ti while the latter pigments contain approximately 2% excess of Zn. Significantly, the R_k values of these pigments differ substantially from one another and, rather than being lower, R_k of the MOX-A pigment is higher.

The influence of temperature and time on the properties and performance of MOX-A pigments is shown in Table 6B. The improvement of R_k with increasing calcination temperature stands out clearly. Generally, while the effect of temperature is as expected, it considerably surpasses that of time at temperature, but the net effect of time may be either beneficial or adverse. The adverse effects of time at temperature on the ΔR_{900} of the 6-10.5 series

C6233-44

Table 6

SELECTED IRIF-I-71 TEST DATA

Table 6A

COMPARISON OF MOX-A WITH OTHER PIGMENTS

Index	Pigment: Treatment:	MOX-A (6-10.5/2)	MOX (6-10.5/2)	LH-103 (6-10.5/2)	LH-103 (C6-10.5/2)
R_k		71	56	39	41.5
R_{max}		98	93	90.5	91
ΔR_{400}		.035	.02	.03	.025
ΔR_{900}		.055	.132	.065	.04
$\Delta \alpha_s$		.034	.006	.033	.022

Table 6B

INTERCOMPARISON OF MOX-A PIGMENTS

Index	MOX-A Pigment						
	6-9/4	6-9/16	6-10.5/2	6-10.5/4	6-10.5/8	6-12/0.5	6-12/2
R_k	63	69.5	71	69	72	81.5	88.5
R_{max}	91	93	98	97.5	90.5	97	97.5
ΔR_{400}	.03	.02	.035	.02	.03	.05	.025
ΔR_{900}	.05	.045	.055	.055	.085	.12	.055
α_s	.170	.157	.124	.143	.160	.116	.114
$\Delta \alpha_s$	.024	.016	.034	.030	.049	.058	.032

contrasts with its desirable affects on the ΔR_{900} of the 6-12 series.

In summary, IRIF-I-71 test results, primarily those of $\Delta\alpha_s$, clearly show the inherent instability of MOX-A pigments. The properties and performance of these pigments, whose Zn:Ti mole ratio is at substantial variance from the theoretically necessary stoichiometry of Zn_2TiO_4, raise fundamental and serious questions about the true nature of the precursor oxalates, the chemistry of their conversion to titanates, and the sensitivity of optical properties and environmental stability to pigment stoichiometry.

3.4 IRIF Test I-72

3.4.1 Test Conditions

IRIF Test I-72 was accomplished in a vacuum whose pressure level averaged about $5-8\times10^{-7}$ Torr. The samples were irradiated at an intensity of 6 ultraviolet suns with radiation from a high pressure 1000 watt mercury compact source (Pek AH-6). Diffuse hemispherical reflectance measurements in the wavelength range 325nm to 2600nm were made in-situ on each sample. Reflectance scans were taken immediately prior to radiation exposure, after exposure to 175 ESH, 560 ESH, 1560 ESH and to 2630 ESH, and subsequently after exposure to 760 Torr of pure O_2.

3.4.2 Materials Descriptions and Test Results

The unusually high reflectance of "MOX" Zn_2TiO_4 pigments along with an appreciation of the stoichiometric deficiencies of MOX-A Zn_2TiO_4 pigments prompted the production and testing of another "MOX" pigment batch,* in this case designated MOX-B.

---

*In the text we distinguish the meaning of the term MOX: "MOX" refers to the preparation method, and MOX, to the designation of the first batch of pigment made by the "MOX" method.

The MOX-B pigments were prepared at three different calcination temperatures and (each) at different calcination times. The majority of the samples, as Table 7 shows, are OI-650G paints. The remainder are MOX-B powder films, a MOX (original "MOX") pigment, and a sample of S-13G paint. The notation in the table is standard; the G designation refers to IITRI-modified OI-650 resin. Reflectance spectra of all these samples are given in figures 36-47, inclusive.

3.4.3 Analyses and Discussions

The results, as even a cursory analysis of Table 7 would show, confirm the fact that OI650G paints are always less stable than the pigments from which they are made and always inferior to them in reflectance properties as well. Also evident is the better stability of the 6-12 pigments. The stability of MOX-B paints, however, is only moderate, since neither do they significantly outperform S-13G or exhibit lower initial α_s values.

The various properties and environmental performance indices compiled in table 8 support the above conclusions and several others of importance. The earlier statement regarding the superior properties of pigments vs paints made from them is shown to be valid on several bases. R_k, the "knee" reflectance, of powders tends to remain rather independent of temperature and time, but the inferiority of the paint with respect to the pigment alone tends to decrease with increasing calcination temperature (table 8B). The improvement of ΔR_{400}, ΔR_{900}, and of $\Delta \alpha_s$ exhibit clear trends in the same direction. Though $\Delta \alpha_s$ of powders increases mildly with increasing calcination temperature, that of corresponding paints decreases substantially. The factors which tend to amplify the absorption effect when a MOX-B pigment is dispersed in OI-650G quite obviously diminish with increasing

Table 7

IRIF TEST I-72
ULTRAVIOLET RADIATION TEST RESULTS

No.	Sample Description	Solar Absorptance Values					O_2 Bleach	$\Delta\alpha_s$ 2630
		Initial	175 ESH	560 ESH	1560 ESH	2630 ESH		
2	MOX-B(6-9/4)/G*	.235	.305	.328	.357	.362	.288	.127
3	MOX-B(6-9/16)/G	.198	.273	.294	.333	.336	.264	.133
9	MOX-B(6-9/16)	.174	.183	.186	.192	.200	.174	.025
4	MOX-B(6-10.5/1)/G	.204	.260	.276	.311	.315	.252	.111
5	MOX-B(6-10.5/4)/G	.212	.257	.279	.308	.310	.253	.098
6	MOX-B(6-10.5/8)/G	.214	.242	.267	.287	.279	.231	.065
10	MOX(6-10.5/2)	.111	.118	.125	.126	.134	.111	.023
11	MOX-B(6-10.5/8)	.207	.228	.229	.233	.237	.215	.030
7	MOX-B(6-12/0.5)/G	.228	.261	.282	.297	.302	.252	.074
8	MOX-B(6-12/2)/G	.216	.245	.260	.267	.276	.240	.060
12	MOX-B(6-12/2)	.141	.168	.194	.188	.190	.155	.049
1	S-13G (D-375)	.191	.221	.242	.267	.276	.246	.085

*Designates Paint Binder is OI-650G

57
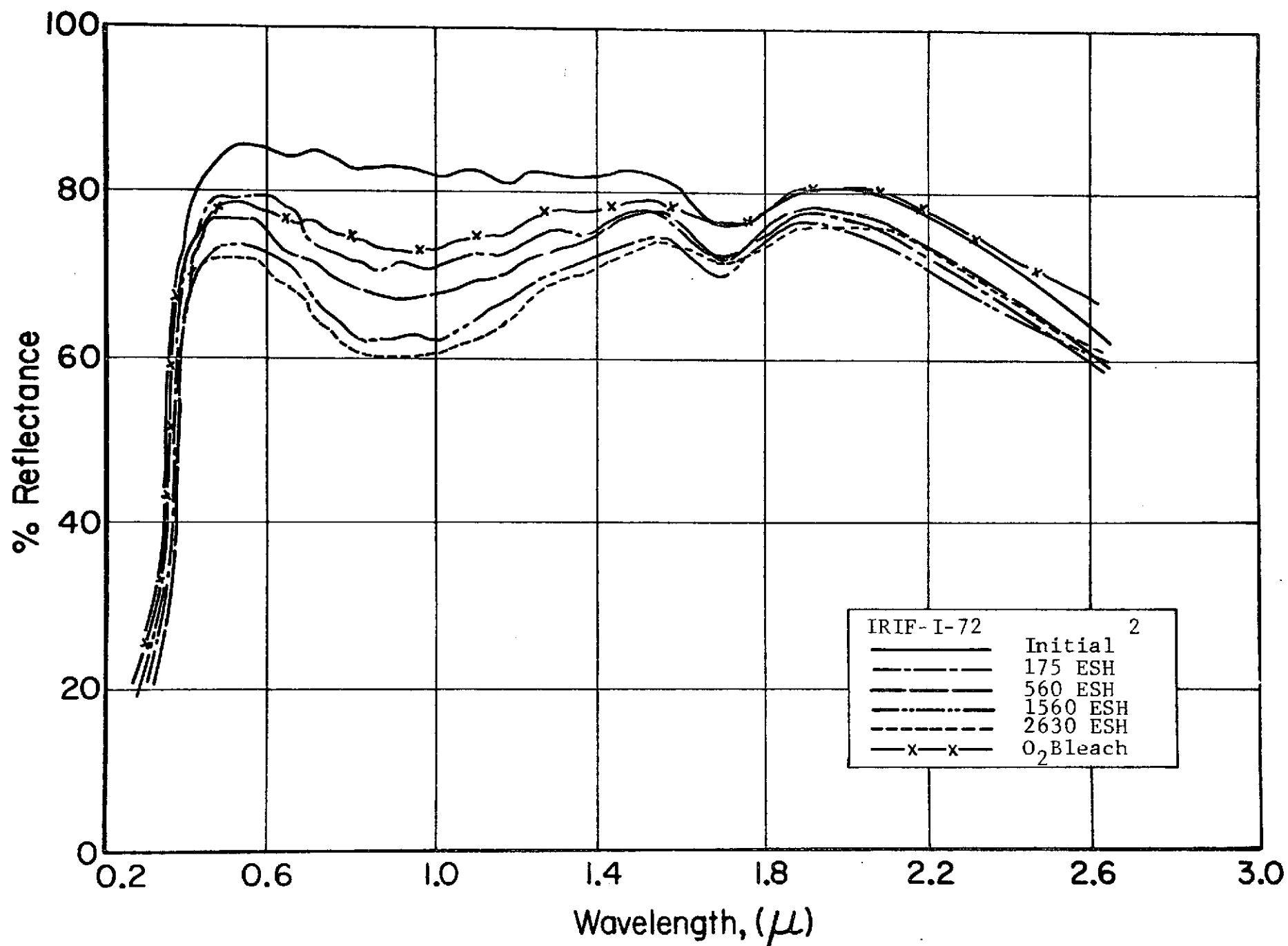
Figure No. 36   REFLECTANCE SPECTRA OF MOX-B(6-9/4)/G

The legend within the figure reads:

IRIF-I-72   2
——————————— Initial
— · — · — · — 175 ESH
——————————— 560 ESH
— · · — · · — 1560 ESH
— — — — — — 2630 ESH
— x — x — O₂ Bleach

Axis labels: % Reflectance (vertical), Wavelength, (μ) (horizontal)

58

C6233-44
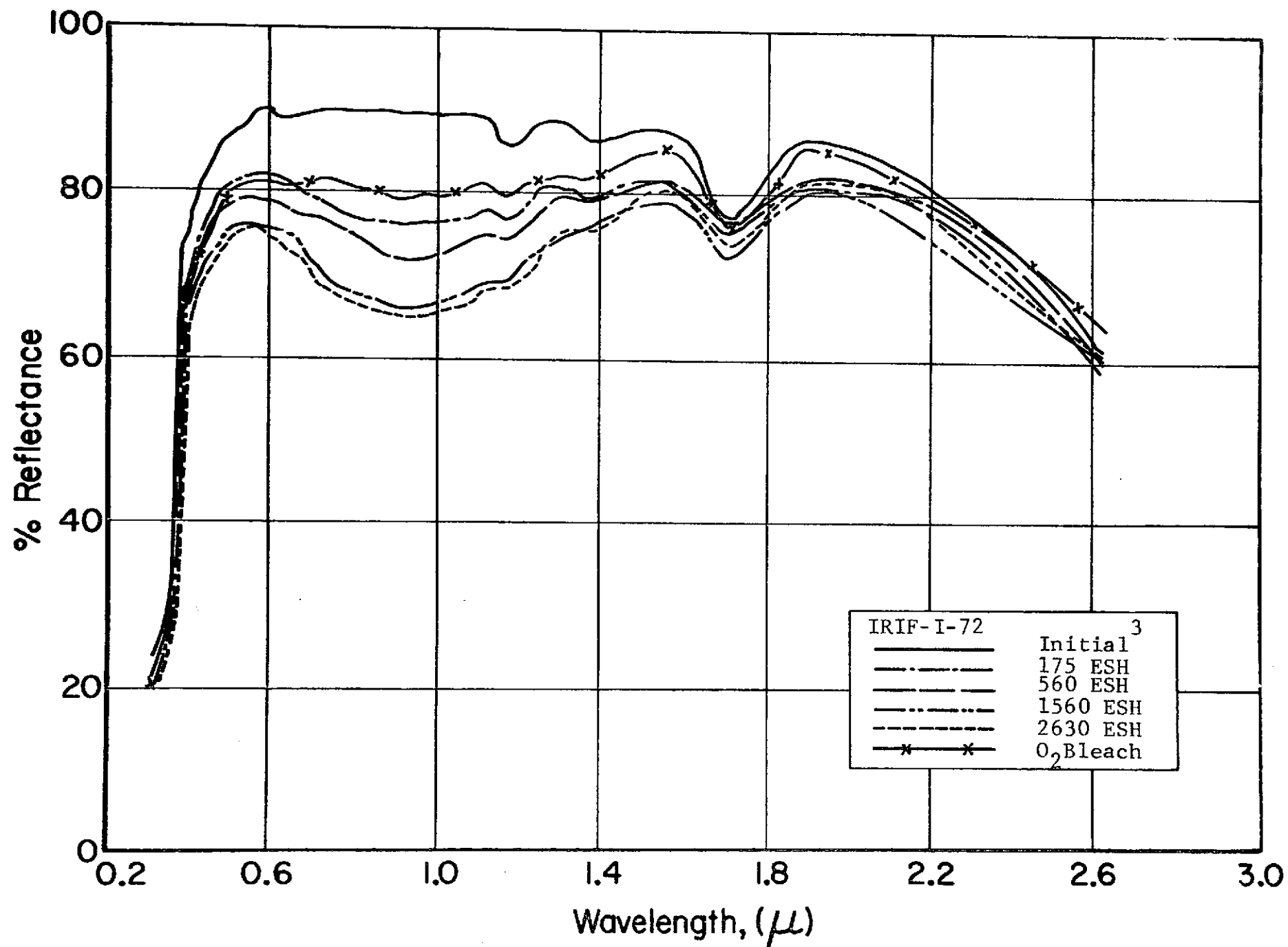
Figure No. 37   REFLECTANCE SPECTRA OF MOX-B(6-9/16)/G

Legend (inset):

IRIF-I-72
Initial[3]
175 ESH
560 ESH
1560 ESH
2630 ESH
O_2 Bleach

Y-axis: % Reflectance (0 to 100)

X-axis: Wavelength, (μ) (0.2 to 3.0)
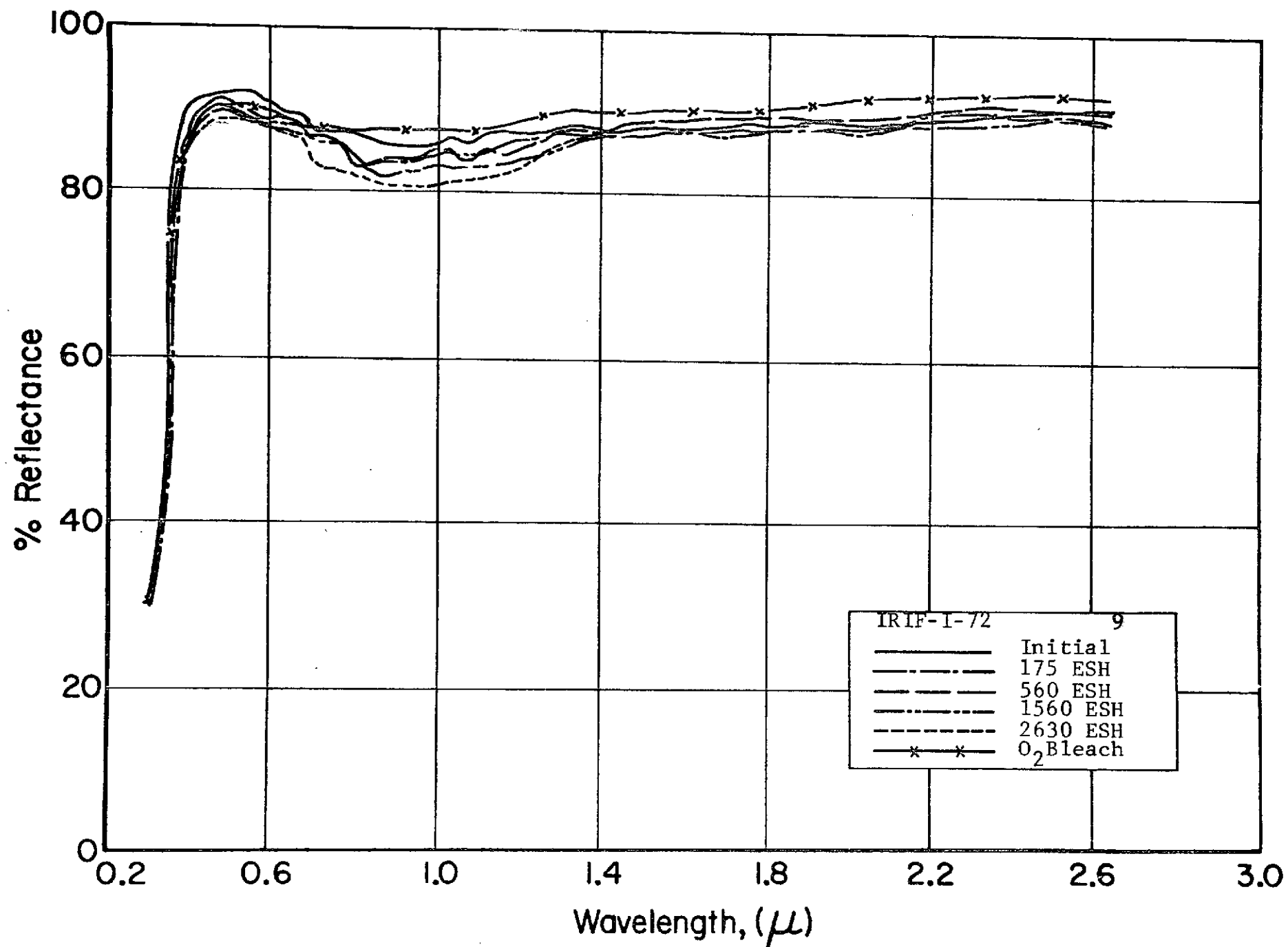
Figure No. 38   REFLECTANCE SPECTRA OF MOX-B(6-9/16) (Powder)

C6233-44

Legend (IRIF-1-72, 9):
- Initial
- 175 ESH
- 560 ESH
- 1560 ESH
- 2630 ESH
- O_2 Bleach
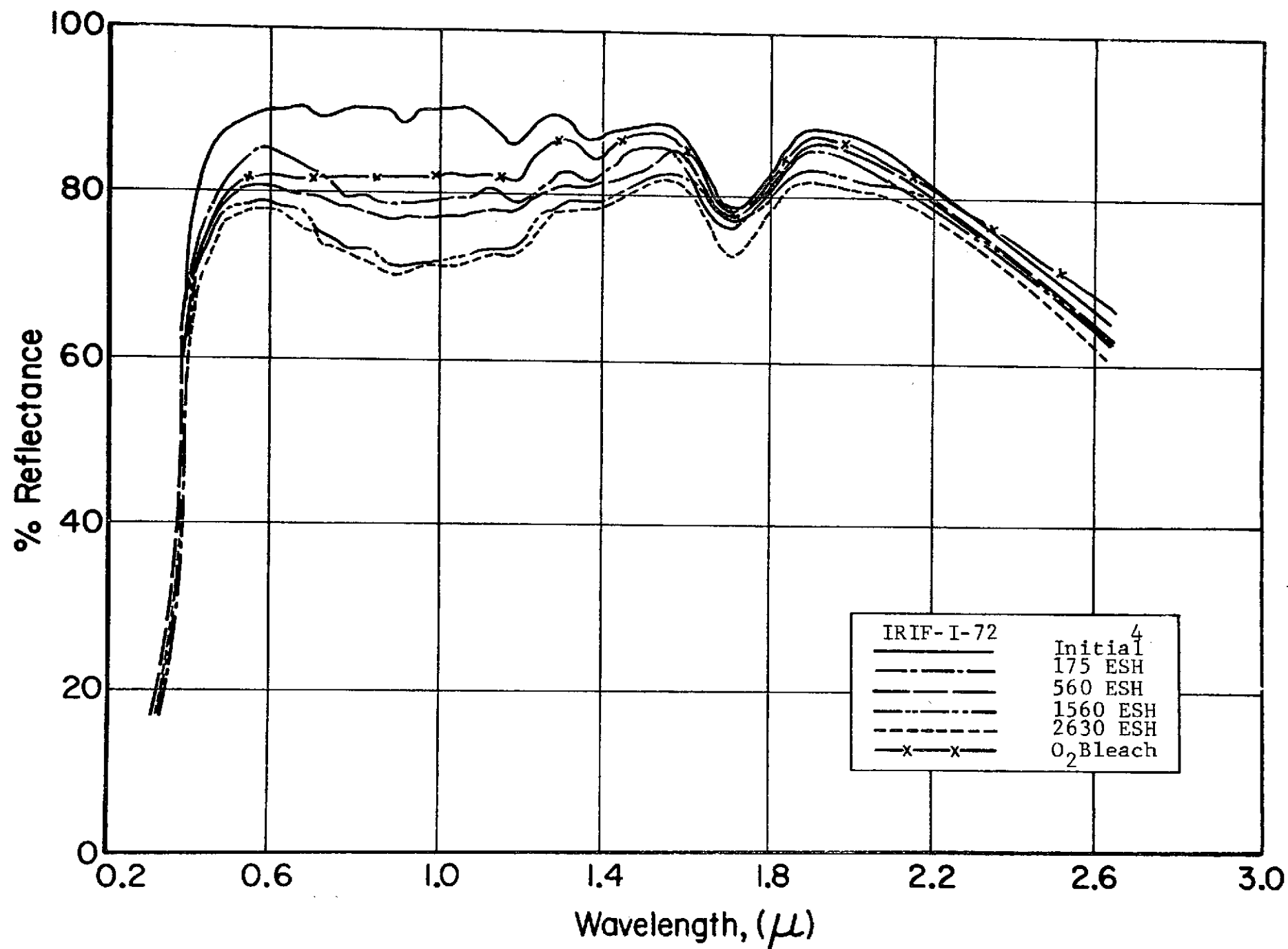
Figure No. 39   REFLECTANCE SPECTRA OF MOX-B(6-10.5/1)/G

61

C6233-44

Legend:

IRIF-I-72

	Initial
175 ESH	
560 ESH	
1560 ESH	
2630 ESH	
O$_2$Bleach	

% Reflectance (y-axis)

Wavelength, (μ) (x-axis)

IRIF-I-72   5
Initial
175 ESH
560 ESH
1560 ESH
2630 ESH
O_2 Bleach
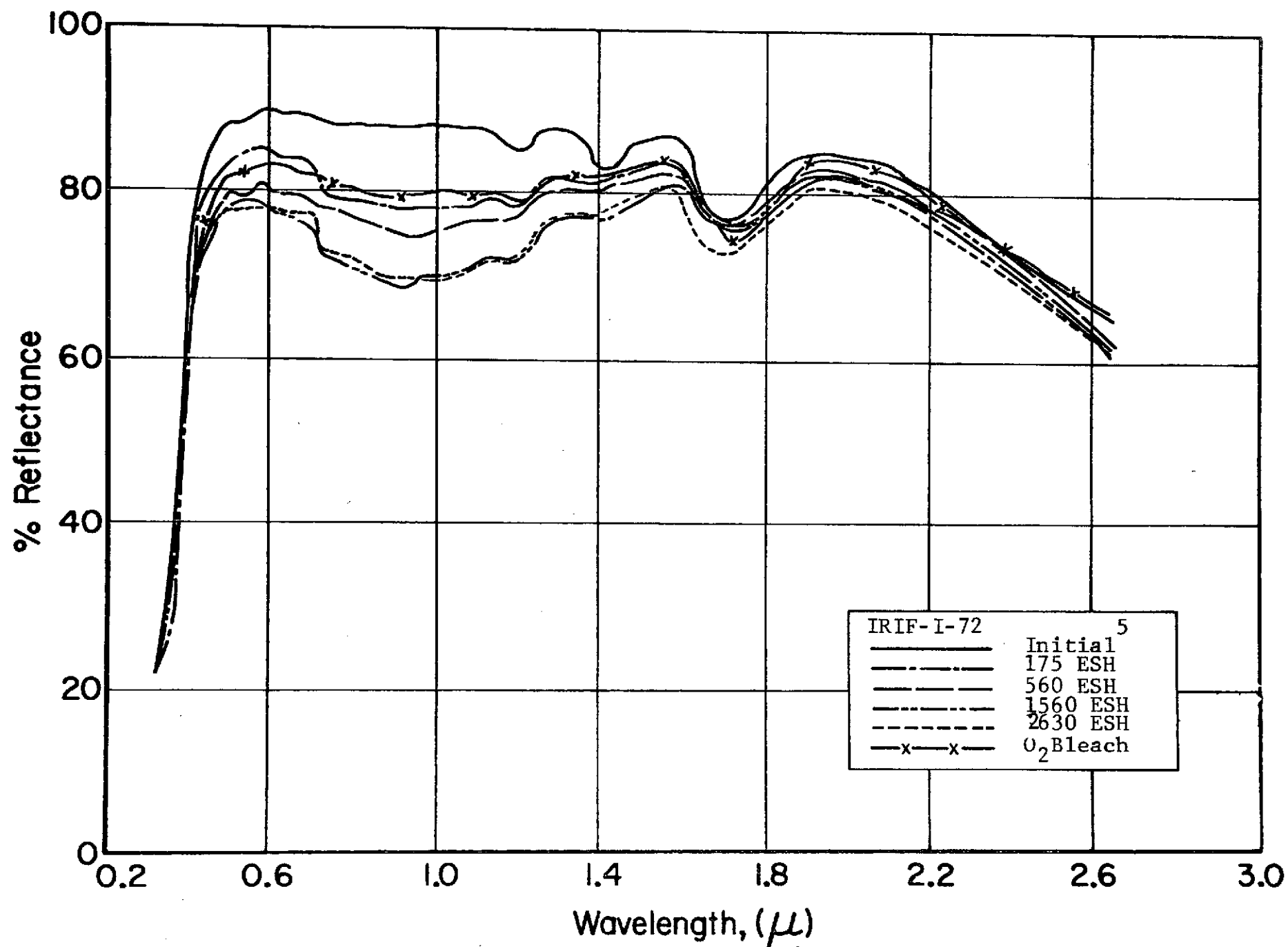
Figure No. 40   REFLECTANCE SPECTRA OF MOX-B(6-10.5/4)/G
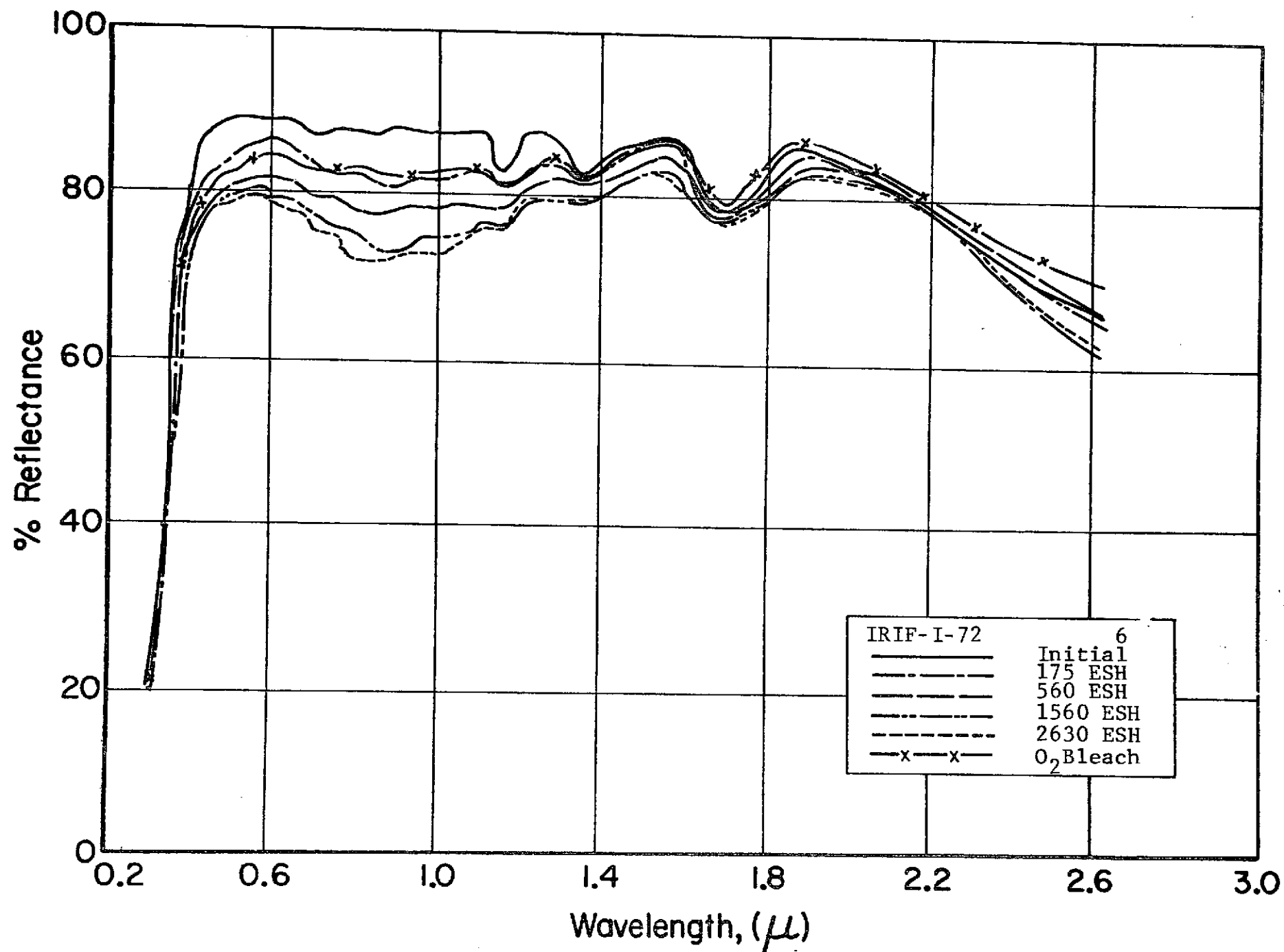
Figure No. 41   REFLECTANCE SPECTRA OF MOX-B(6-10.5/8)/G
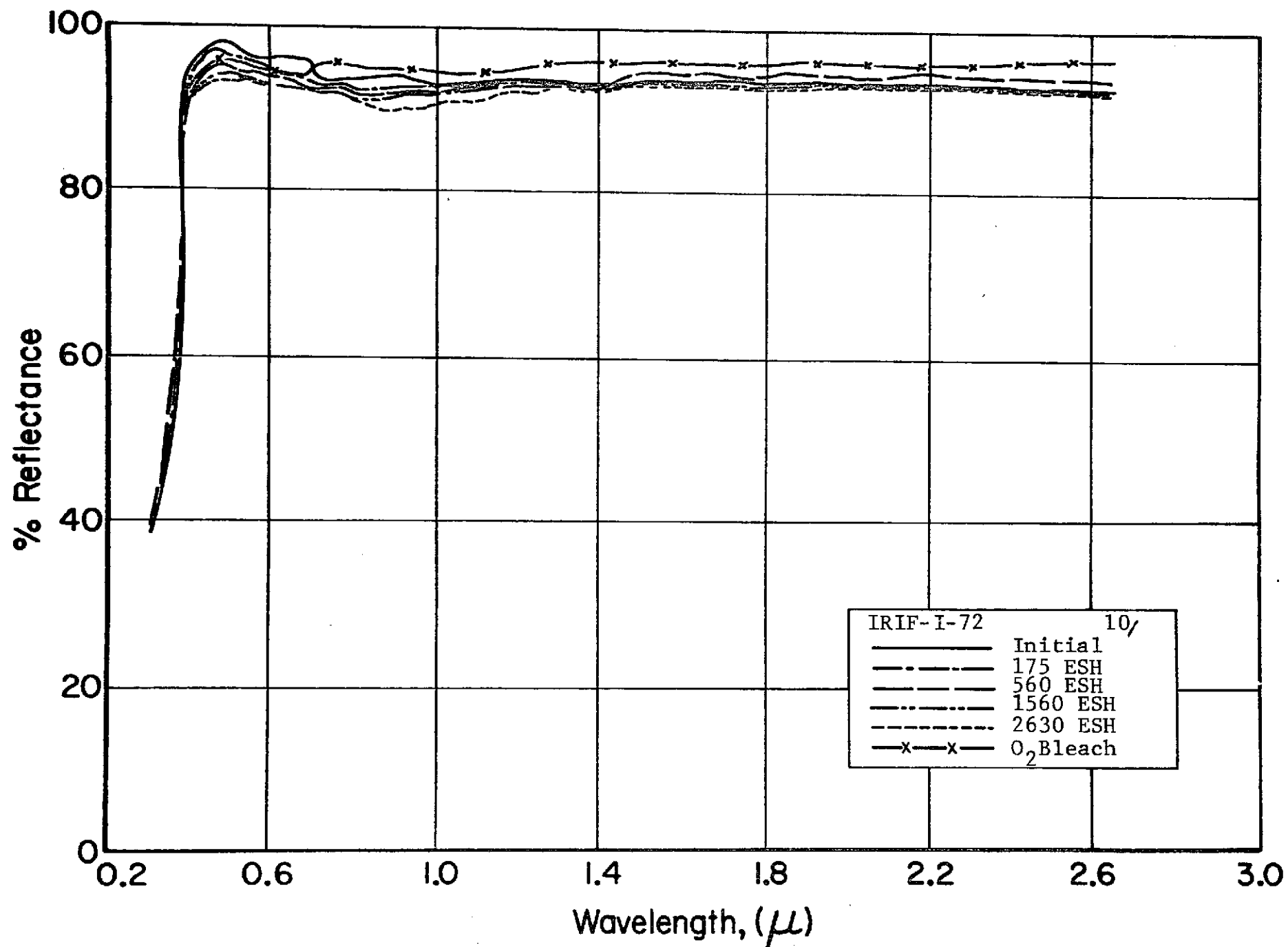
Figure No. 42   REFLECTANCE SPECTRA OF MOX(6-10.5/2) (Powder)
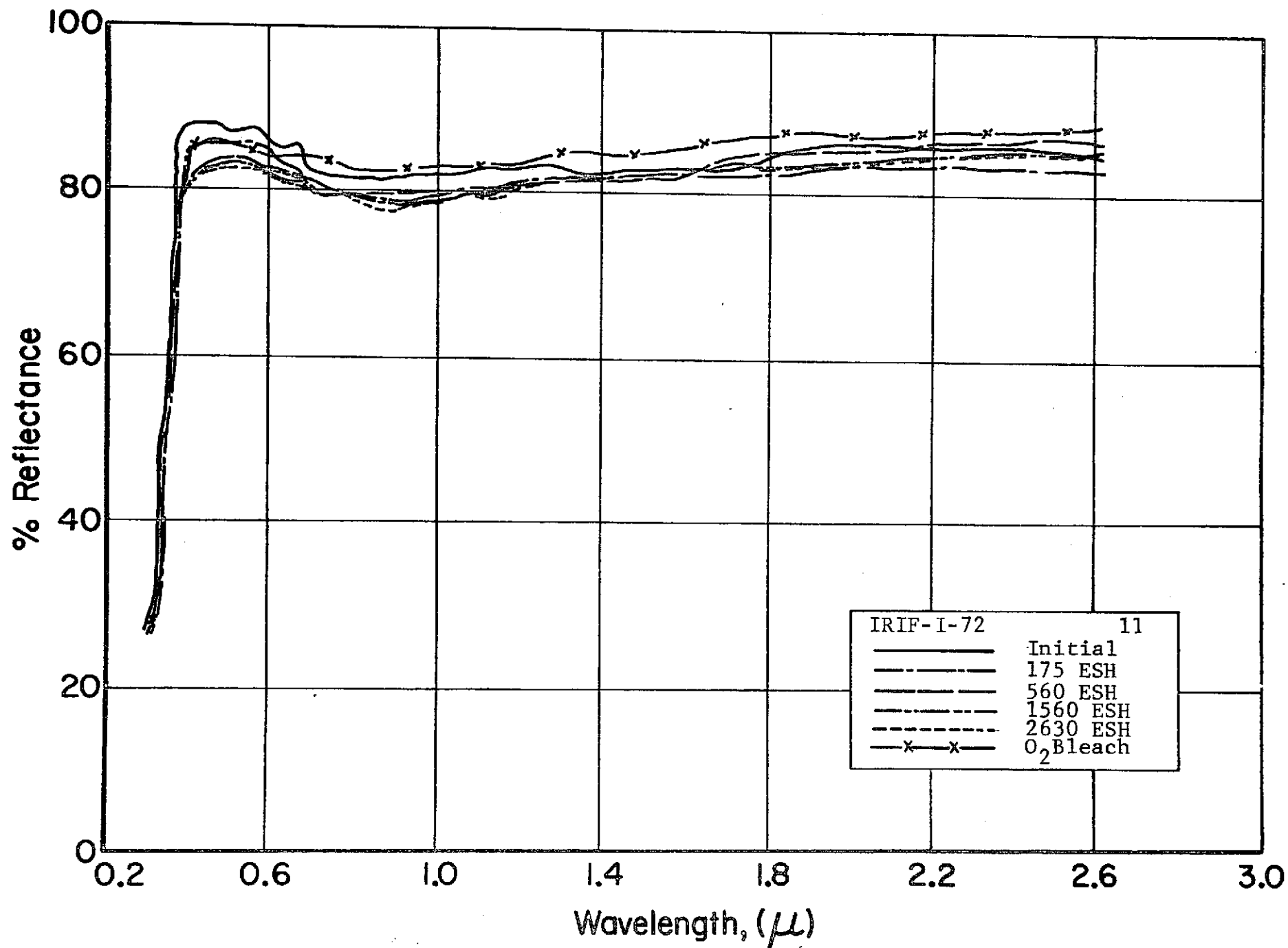
Figure No. 43   REFLECTANCE SPECTRA OF MOX-B(6-10.5/8) (Powder)

% Reflectance (vertical axis)

Wavelength, (μ) (horizontal axis)

IRIF-I-72   7
                Initial
175 ESH
560 ESH
1560 ESH
2630 ESH
O_2 Bleach
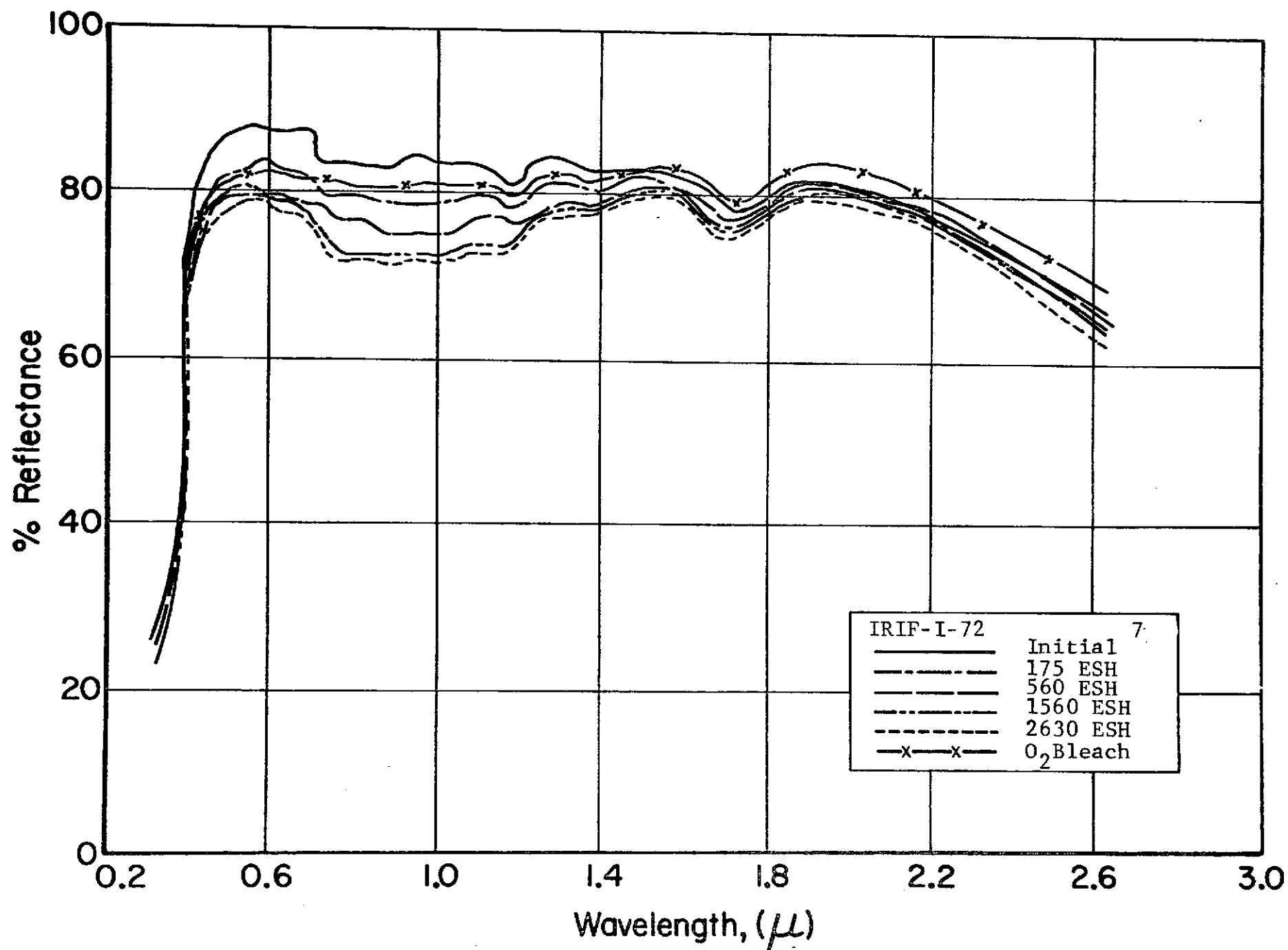
Figure No. 44   REFLECTANCE SPECTRA OF MOX-B(6-12/0.5)/G
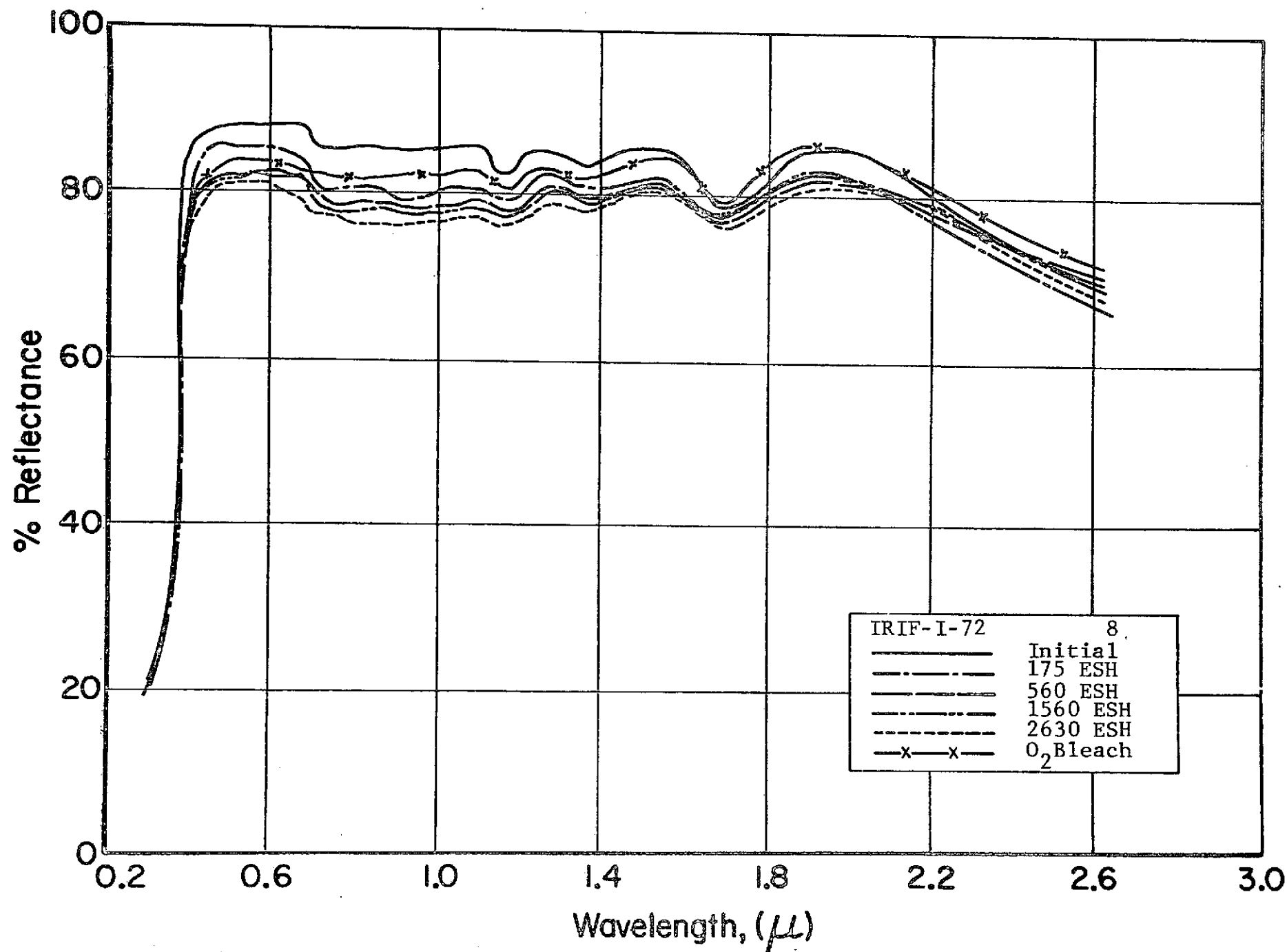
Figure No. 45   REFLECTANCE SPECTRA OF MOX-B(6-12/2)/G

The figure shows a plot of % Reflectance (y-axis, 0 to 100) versus Wavelength, (μ) (x-axis, 0.2 to 3.0).

Legend:
IRIF-I-72   8
———————— Initial
—·—·—·— 175 ESH
———————— 560 ESH
—··—··— 1560 ESH
- - - - - 2630 ESH
—x—x— O$_2$Bleach
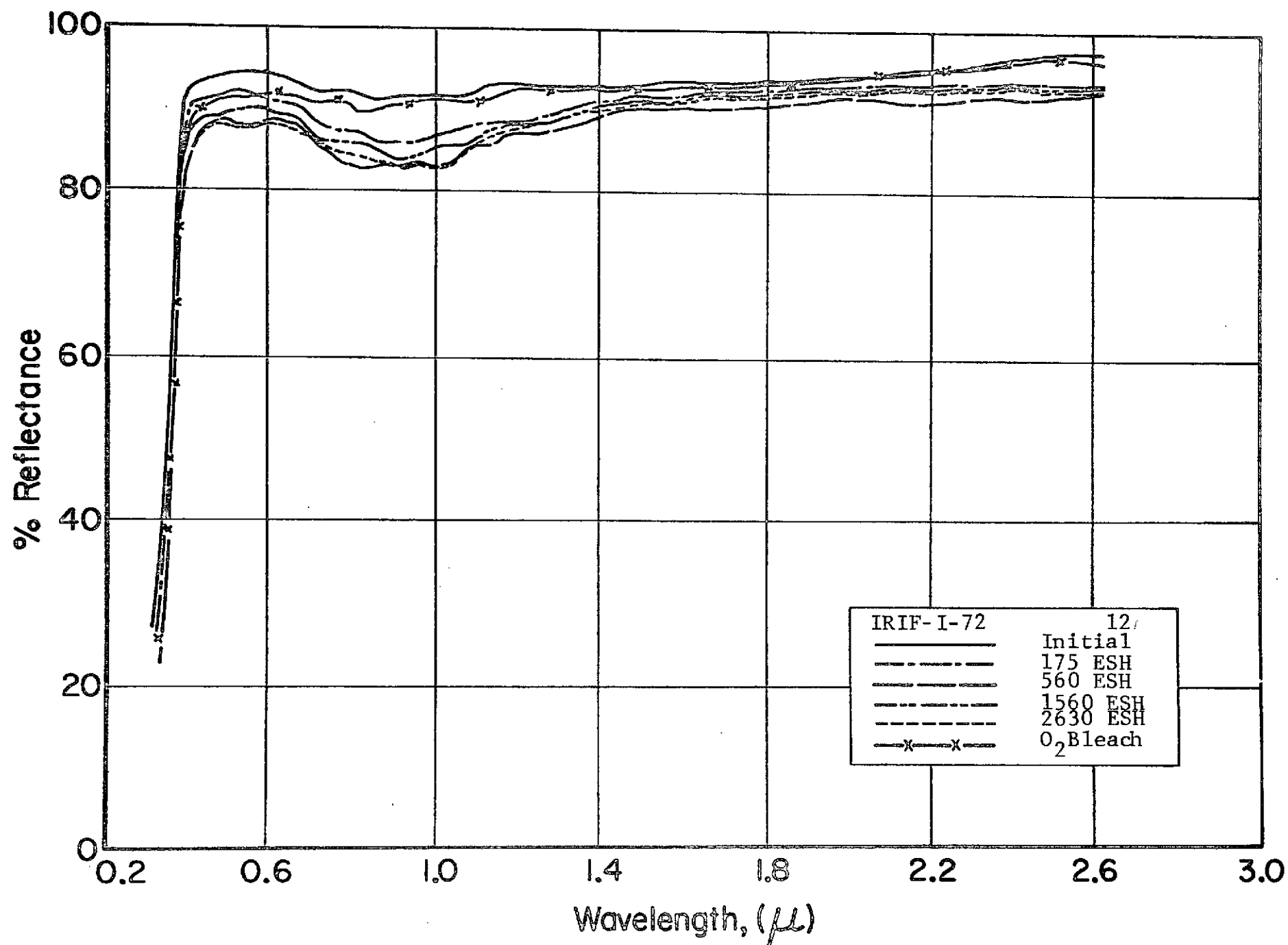
Figure No. 46   REFLECTANCE SPECTRA OF MOX-B(6-12/2) (Powder)

The graph's axes and legend:

- Y-axis: % Reflectance (0 to 100)
- X-axis: Wavelength, (μ) (0.2 to 3.0)

Legend:
IRIF-I-72   12
Initial
175 ESH
560 ESH
1560 ESH
2630 ESH
O_2Bleach

C6233-44

68
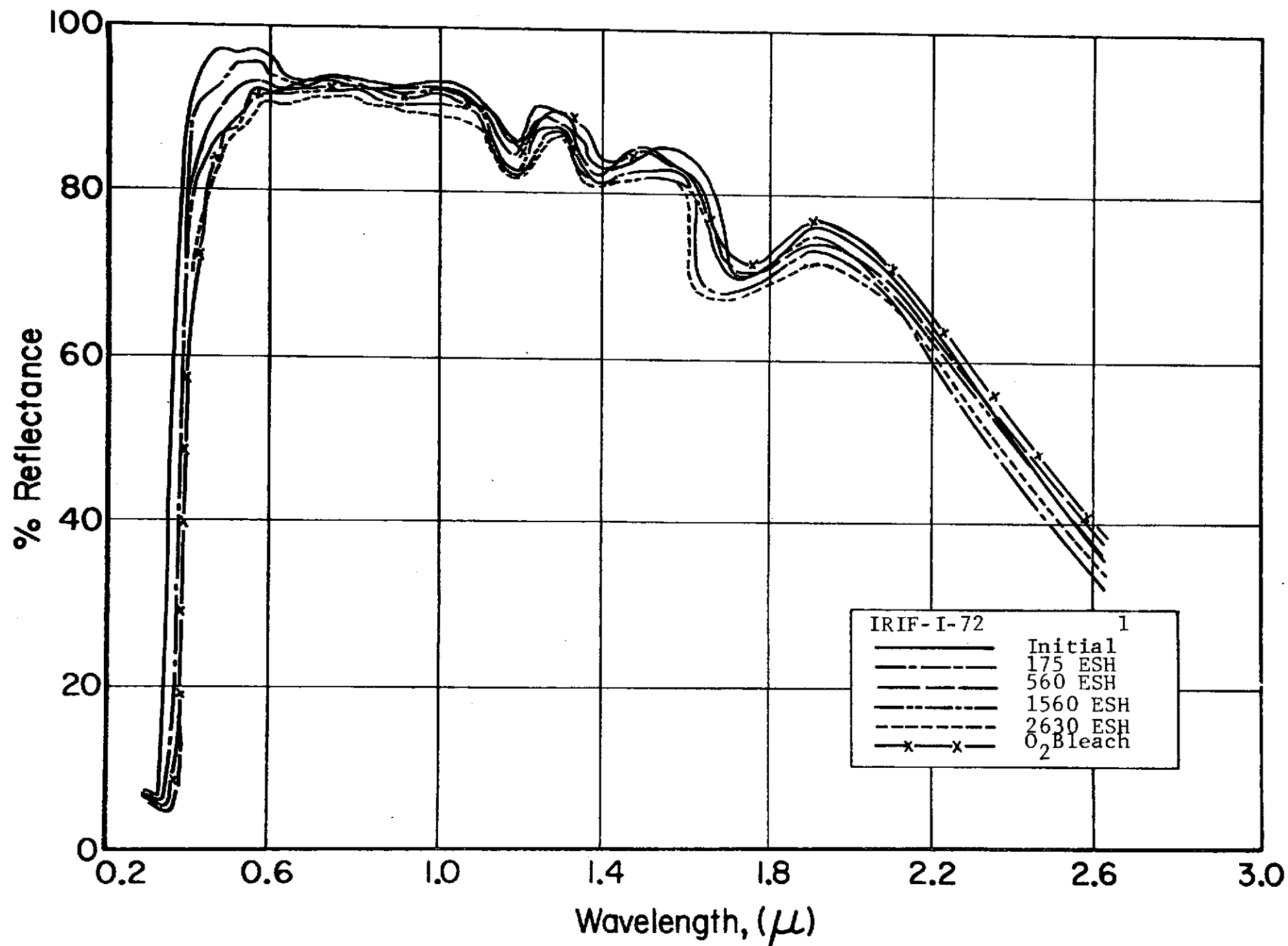
Figure No. 47 REFLECTANCE SPECTRA OF S-13G

C6233-44

Table 8

SELECTED IRIF-I-72 DATA

Table 8A
COMPARISON OF MOX-B POWDERS AND PAINTS
Powder/Paint Properties

Index	6-9/16	6-10.5/2*	6-10.5/8	6-12/2
R_k	55.5/32	57/33.5	56/36	51/34
R_{max}	89/89	96/89	86/87.5	95/87
ΔR_{400}	.045/.130	.030/.115	.040/.089	.055/.050
ΔR_{900}	.040/.124	.035/.182	.032/.124	.070/.095
α_s	.174/.198	.111/.204	.207/.214	.141/.216
$\Delta \alpha_s$	.026/.138	.023/.111	.030/0.65	.049/.060

*First column/Second column relate in this case to: 6-10.5/2 powder/
6-10.5/1 paint.

Table 8B
POWDER/PAINT RATIOS
Ratios of Powder/Paint Indices For:

Series	R_k	ΔR_{400}	ΔR_{900}	$\Delta \alpha_s$
6-9/16	1.73	0.35	0.18	0.19
6-10.5/2*	1.70	0.26	0.17	0.21
6-10.5/8	1.56	0.45	0.26	0.45
6-12/2	1.50	1.10	0.74	0.82

*Relates in this case to: 6-10.5/2 powder/6-10.5/1 paint.

Table 8C
TEMPERATURE AND TIME EFFECTS IN PAINTS

Series:	(6-9)		(6-10.5)			(6-12)	
Times:	4hrs	16hrs	1hr	4hrs	8hrs	0.5hrs	2hrs
Index							
R_k	32.5	32	33.5	36	36	37.5	34
R_{max}	85	89	89	88	87.5	86	87
ΔR_{400}	.130	.130	.115	.082	.089	.070	.050
ΔR_{900}	.230	.224	.182	.169	.125	.130	.095
α_s	.235	.298	.204	.212	.214	.228	.216
$\Delta \alpha_s$	.127	.138	.111	.098	.065	.074	.060

calcination temperature. It should be understood, however, that while we seem to impute these dependencies to temperature alone, time at temperature, though a weaker influence, also has significant effects. The $\Delta\alpha_s$ values of the two powders in the 6-10.5 series in table 8A exemplify this point; in this instance time increases $\Delta\alpha_s$ of the powder and the time effect in the paints can be seen from the data in table 8C. The most notable effect is, of course, the decreasing ΔR_{900} with increasing calcination time. Less obvious, but quite important, the full effect of time at temperature has not been attained. Thus, it would seem that lengthier calcinations would be desirable. Such, however, may be contra-indicated by other factors, such as particle size growth.

A close study of all the data presented and especially those of ΔR_{900} in table 8C lead us to believe that the chemical nature of the pigment surface, and quite possibly of the pigment bulk, differs from one series to the next. The ΔR_{900} appears to be un-affected by time at 900°C but time does influence it at 1050°C and also at 1200°C. The ratio of the ΔR_{900} values for the 6-10.5 series at 4hrs and 1hr is 1.40; for the 6-12 series at 2hrs and 0.5 hr, it is 1.37. This tempted us to investigate the fact that the ΔR_{900} for the 6-10.5/8 paint approximates that of the 6-12/0.5 paint. If we assume that the reactions are identical, then the rates should depend strictly on temperature. The rate at 1050°C times 8hrs should equal that at 1200°C times 0.5 hr. Using the Clausius-Clapeyron equation we can calculate that the activation energy is about 53.7 kcal/mole, or 2.32 eV. The energy associated with the 900nm absorption band is 1.38 eV, well within the energy calculated above. The basis of the cal-culation lies in the assumption that the number density of sur-face defect sites which are potentially convertible to optically

active defects will decrease with calcination, tantamount to the assumption that the concentration of surface defects is directly related to the degree of incompleteness of the reaction between the Zn_2TiO_4 precursors.

In summary, the MOX-B paints display poor to moderate stability, definitely not that generally observed in Zn_2TiO_4 paints. The stability of these systems, however, clearly depends upon calcination temperature and time. While the pigments alone demonstrate good performance, the vehicle "sensitizes" the pigment in the paint, causing the 900nm absorption band to be developed more strongly than in the pigment alone. The $\Delta\alpha_s$ of S-13G was slightly above nominal for an UV exposure of the magnitude achieved, indicating that the environmental parameters are valid.

3.5 CREF Test No. 15

3.5.1 Test Conditions

CREF Test No. 15 was operated at a pressure level in the range $1-5 \times 10^{-7}$ Torr. The ultraviolet radiation source, an Hanovia 5000 watt medium pressure mercury-argon burner, was operated to produce an ultraviolet radiation intensity of 4 suns at the sample location. The reflectance scans were made in the wavelength range 325 to 2600nm prior to irradiation, after exposure to 470 ESH, 1150 ESH, 1650 ESH and to 2190 ESH, and finally after a post-irradiation O_2 bleach (at 760 Torr). The samples were not subjected to proton irradiation.

3.5.2 Materials Descriptions and Test Results

In Table 9 we have listed the materials which were irradiated in CREF Test No. 15. The pigments are Zn_2TiO_4 prepared by the coprecipitation method. Most of the pigments were prepared from IITRI Batch No. LH-102; two, from IITRI Batch No. LH-103. The

Table 9

CREF-15

IRRADIATION TEST RESULTS

| | | Solar Absorptance Values | | | | | | |
| | | | Exposure (ESH) | | | | | |
Sample No.	Description*	Initial	474	1150	1650	2190	O_2 Bleach	$\Delta\alpha_s$
1	LH102(6-12):Li_2SiO_3	.192	.204	.233	.238	.247	.218	.054
2	LH102(6-12-10):Li_2SiO_3	.217	.231	.260	.264	.273	.289	.056
3	LH102(6-12-A-10):Li_2SiO_3	.224	.247	.265	.262	.268	.246	.044
4	LH102(6-12)	.183	.196	.221	.234	.230	.214	.041
5	LH102(6-12-10)	.226	.230	.252	.275	.272	.248	.046
6	LH102(6-12-A)	.272	.274	.374	.388	.387	.279	.115
7	LH102(6-12-A-10)	.214	.217	.220	.230	.235	.224	.021
8	LH103(6-12):Li_2SiO_3	.209	.222	.230	.252	.251	.241	.042
9	LH103(6-12)	.219	.222	.236	.246	.245	.241	.026
10	LH102(6-12-A):Li_2SiO_3	.229	.250	.406	.434	.457	.258	.228

*All samples are OI-650G paints containing the pigments described.

The notation used is the same as that used previously in this document. The "A" in the pigment description refers to a chemical treatment of the pigment in acetic acid, followed by water rinsing. The sequence of 6-12, 6-12-10, 6-12-A, and 6-12-A-10 is designed to elicit the effects of individual treatments. Reflectance spectra of all the test samples are presented in figures 48-57, inclusive.

3.5.3 Analyses and Discussions

One of the most obvious results of this test confirms our earlier supposition that re-calcination is necessary after an acid wash. It further confirms our contention that the 900nm absorption band arises principally from UV-activated surface defects. The degradation is much greater in the case of the Li_2SiO_3 encapsulated pigment. The encapsulant is obviously not effective and in fact appears to magnify the damage, as a comparison of the 900nm induced absorption bands in fig's 50 and 54 shows. The O_2 bleaching in the case of the Li_2SiO_3 encapsulated pigment provides further evidence of this assertion. However, the residual acid may have blocked the encapsulant and prevented its attachment to the pigment surface; other explanations including a reaction between the residual acid and the Li_2SiO_3 may also be possible. But as an encapsulant, Li_2SiO_3 does not provide protection against the formation of the optical defects causing ΔR_{900} as is evident in comparing the performances of paints with Li_2SiO_3 encapsulated pigments with those of paints with un-encapsulated pigments.

In Table 10 are some of the pertinent properties and performance indices. Using the LH-102(6-12) data as a baseline, it is evident that only the A-10 treatment produces any significant improvement that the -10 treatment alone has essentially no effect, and that the -A treatment alone increases $\Delta \alpha_s$. The
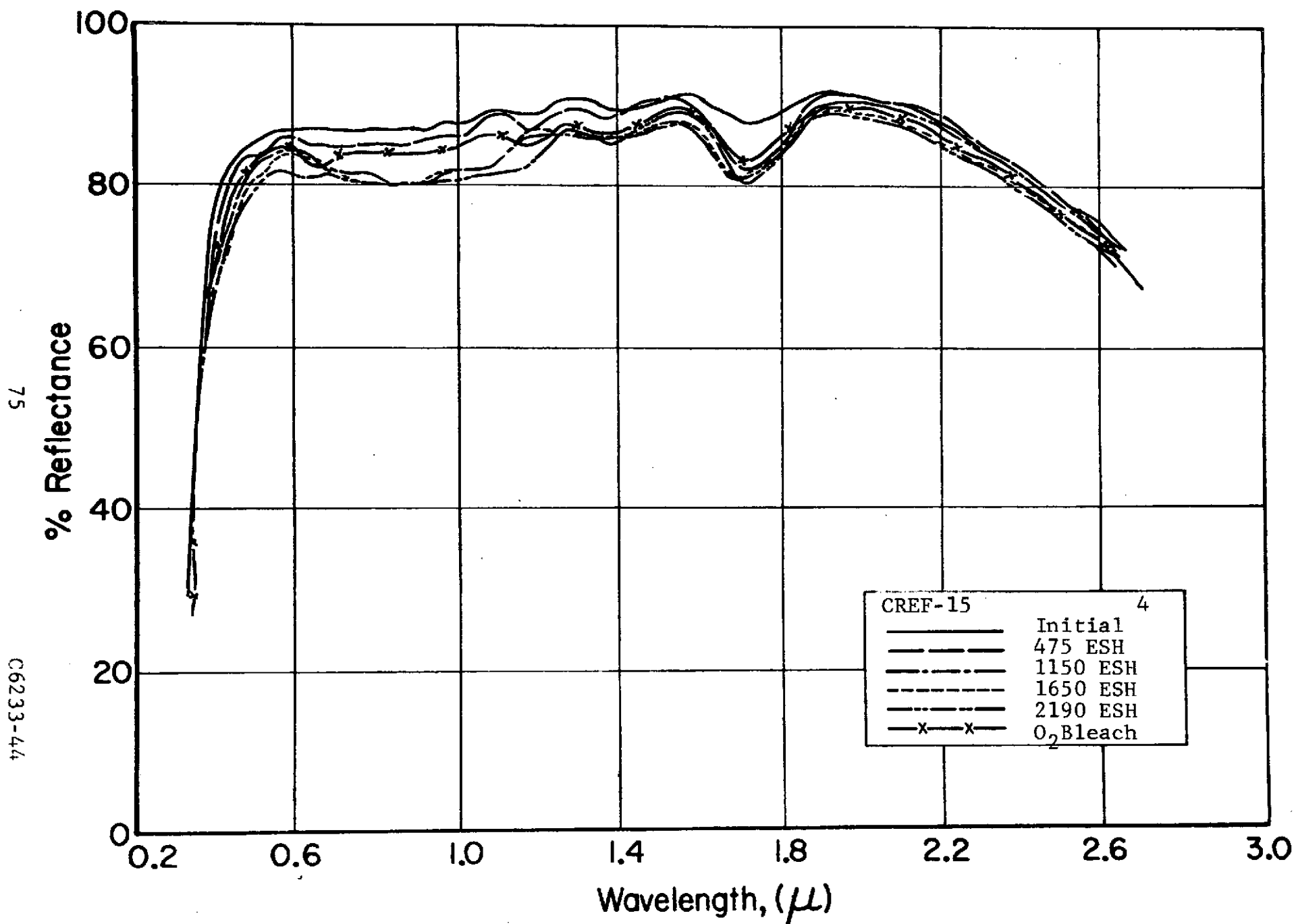
Figure No. 48   REFLECTANCE SPECTRA OF LH-102(6-12)/G

CREF-15 legend:
- Initial
- 475 ESH
- 1150 ESH
- 1650 ESH
- 2190 ESH
- O_2 Bleach

75
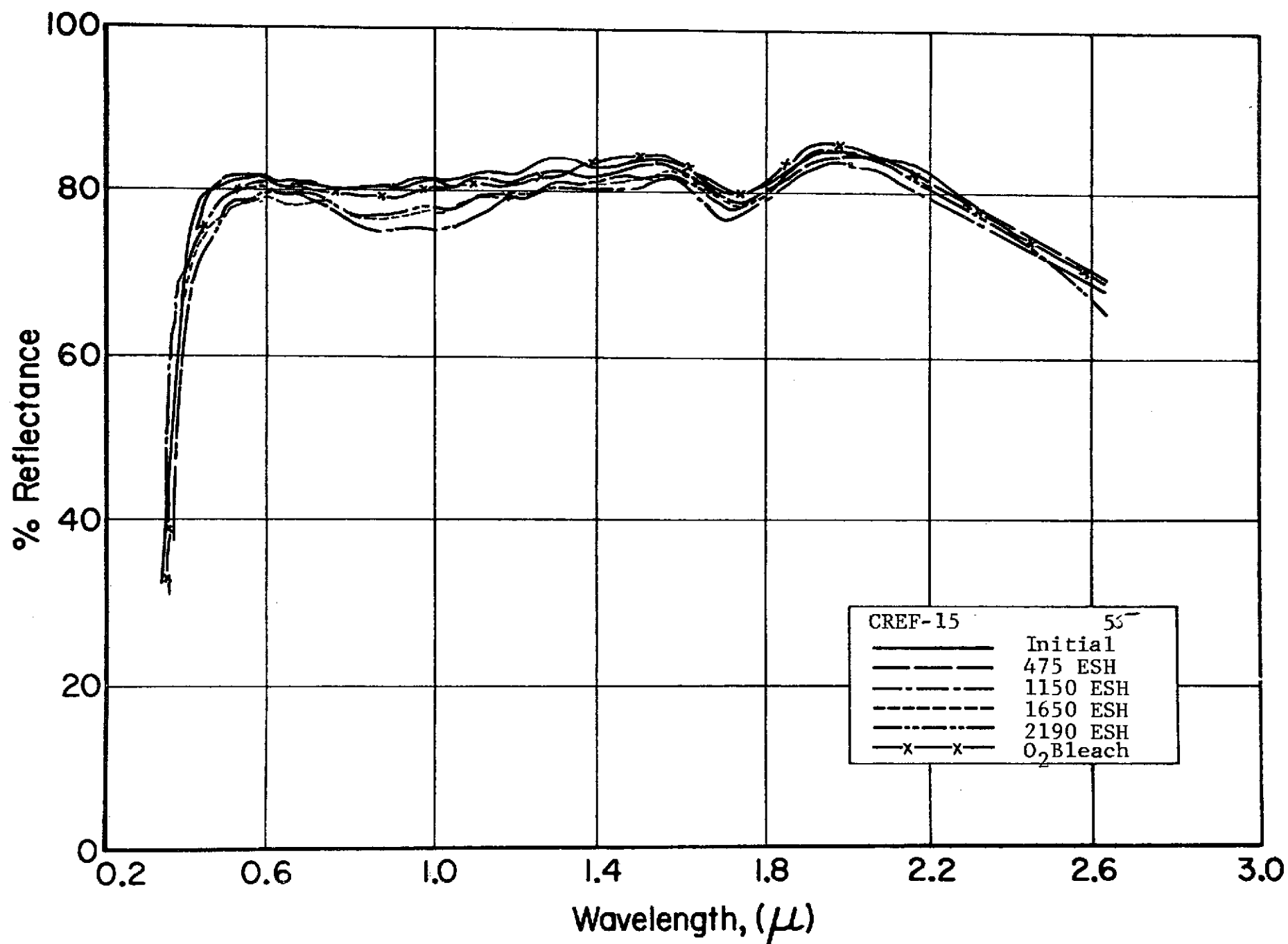
C6233-44

Figure No. 49   REFLECTANCE SPECTRA OF LH-102(6-12-10)/G
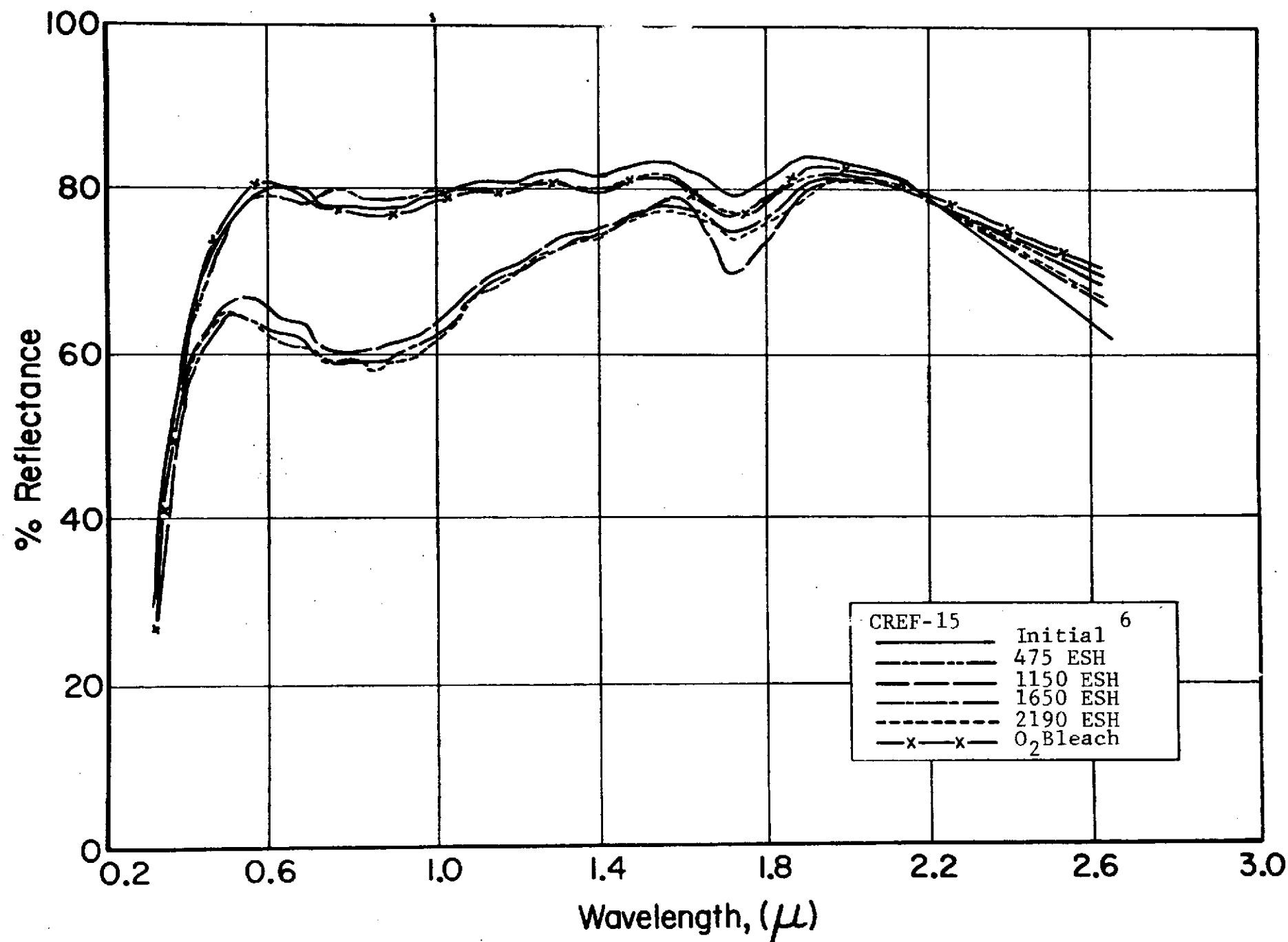
Figure No. 50 REFLECTANCE SPECTRA OF LH-102(6-12-A)/C
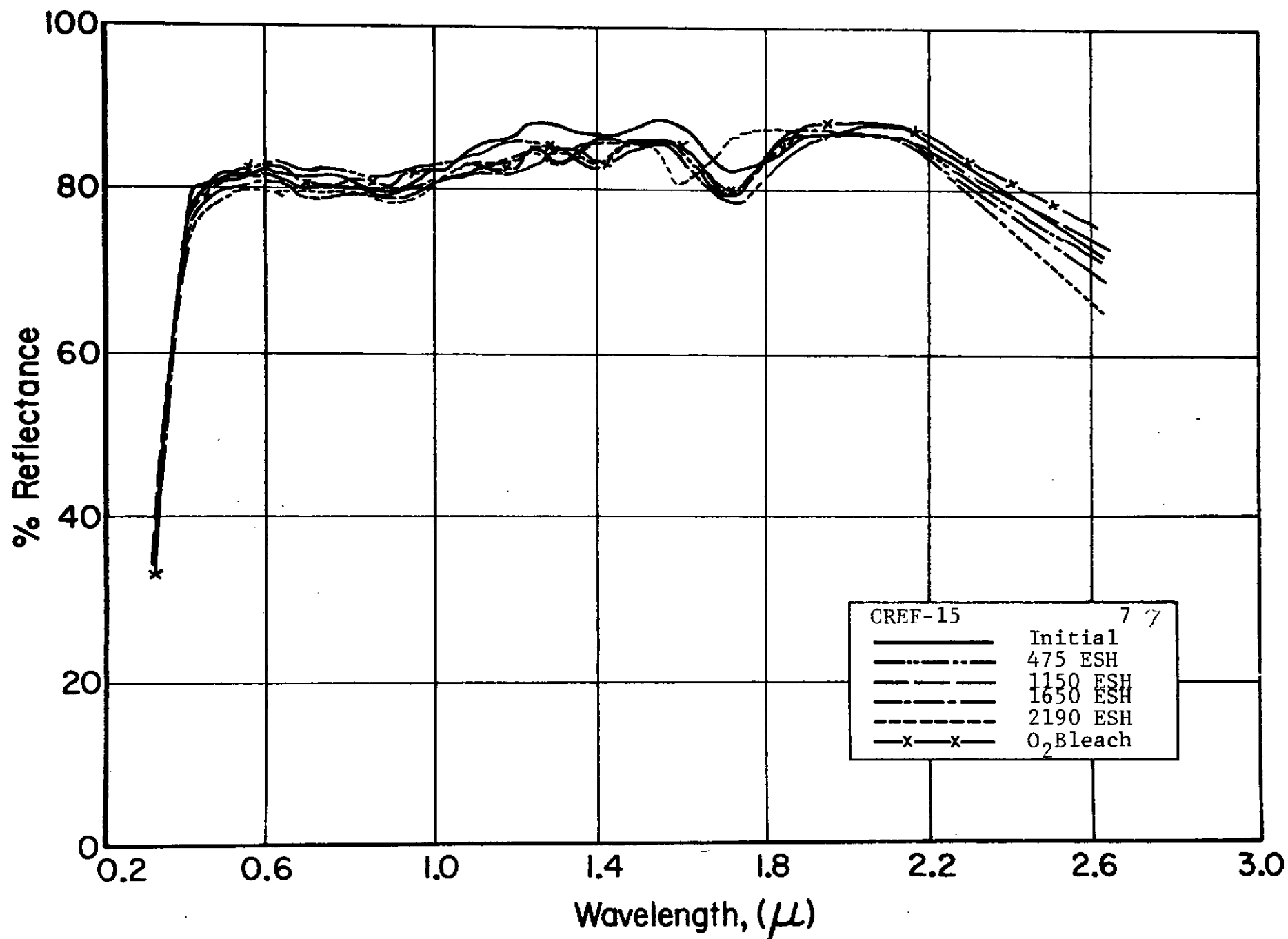
C6233-44

Figure No. 51   REFLECTANCE SPECTRA OF LH-102(6-12-A-10)/G
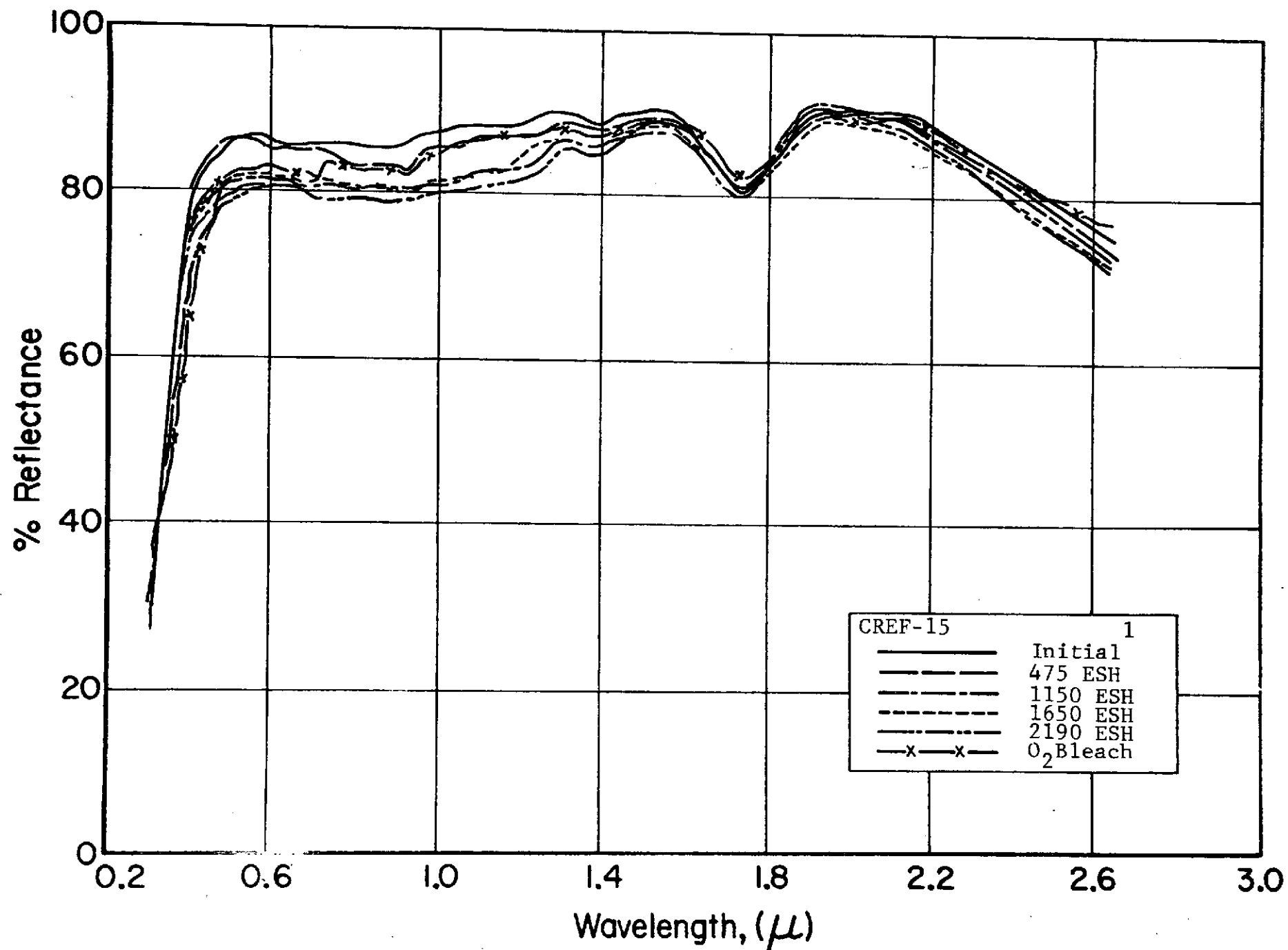
Figure No. 52 REFLECTANCE SPECTRA OF LH-102(6-12):Li$_2$SiO$_3$/G

CREF-15   1
————————————— Initial
— — — — — — — 475 ESH
—·—·—·—·—·—·— 1150 ESH
- - - - - - - - 1650 ESH
—··—··—··—··— 2190 ESH
—x——x——x— O$_2$Bleach

79

C6233-44
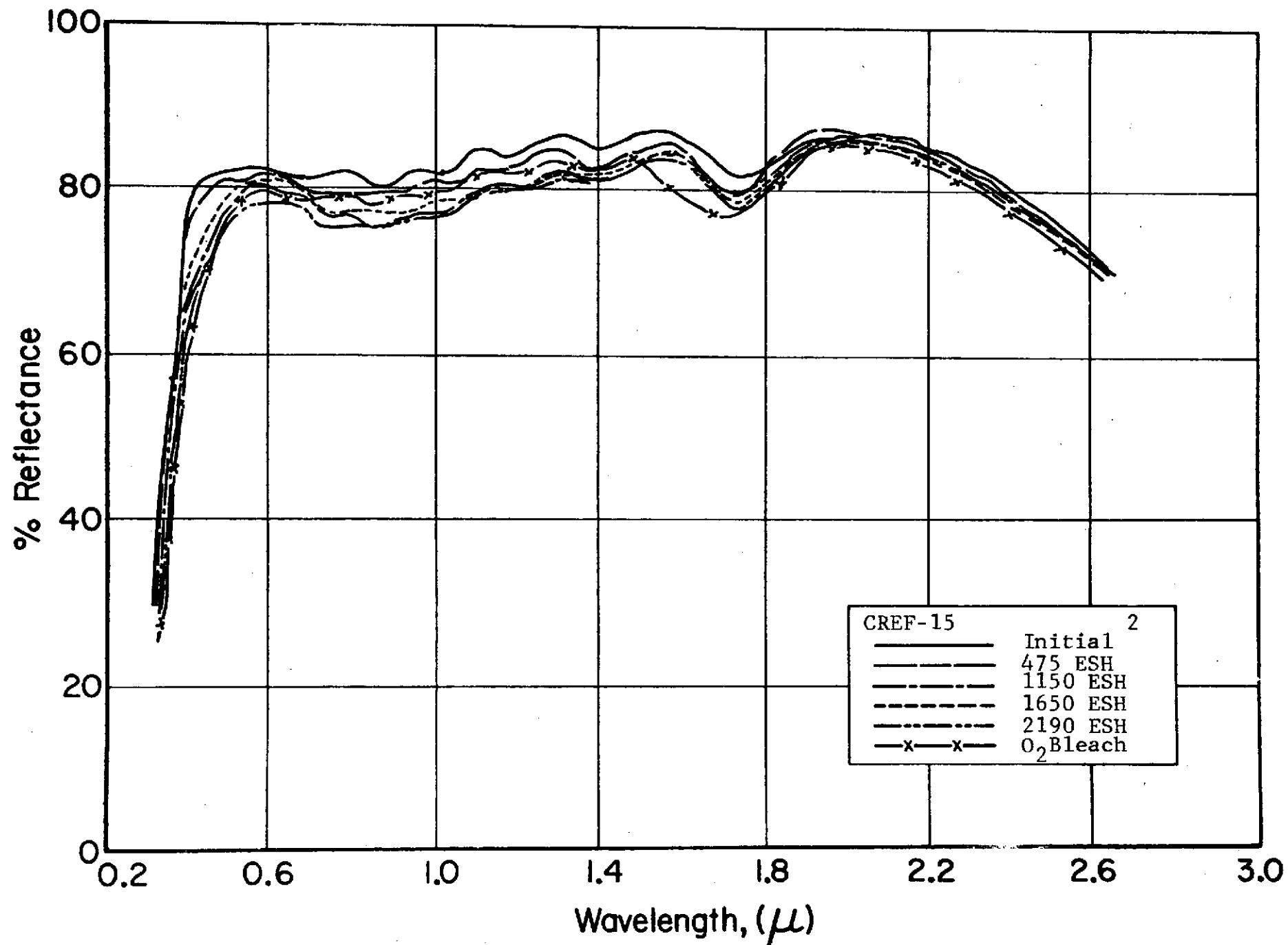
Figure No. 53   REFLECTANCE SPECTRA OF LH-102(6-12-10) Ti_2SiO_3/G
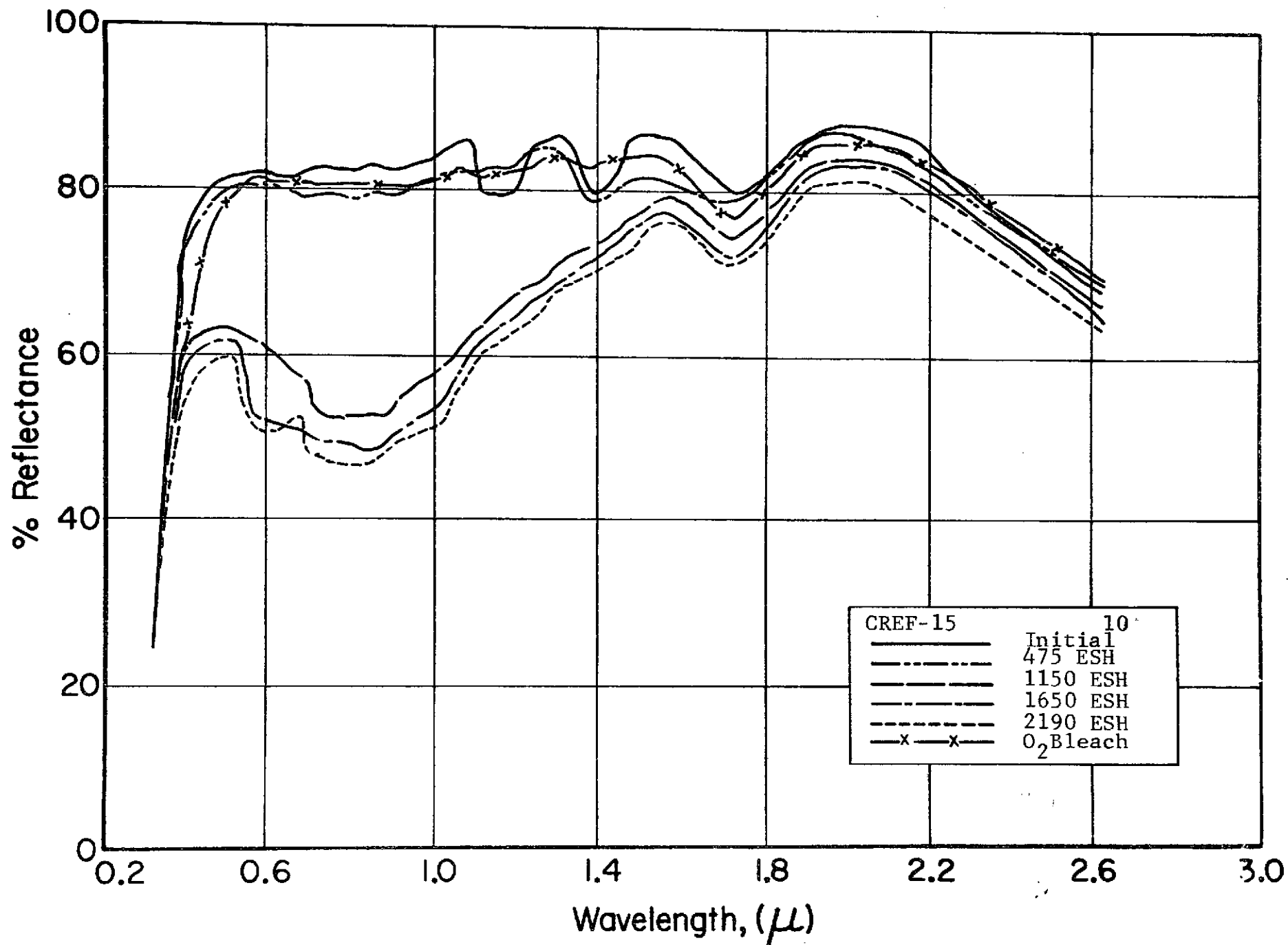
Figure No. 54   REFLECTANCE SPECTRA OF LH-102(6-12-A):Li$_2$SiO$_3$/G

C6233-44
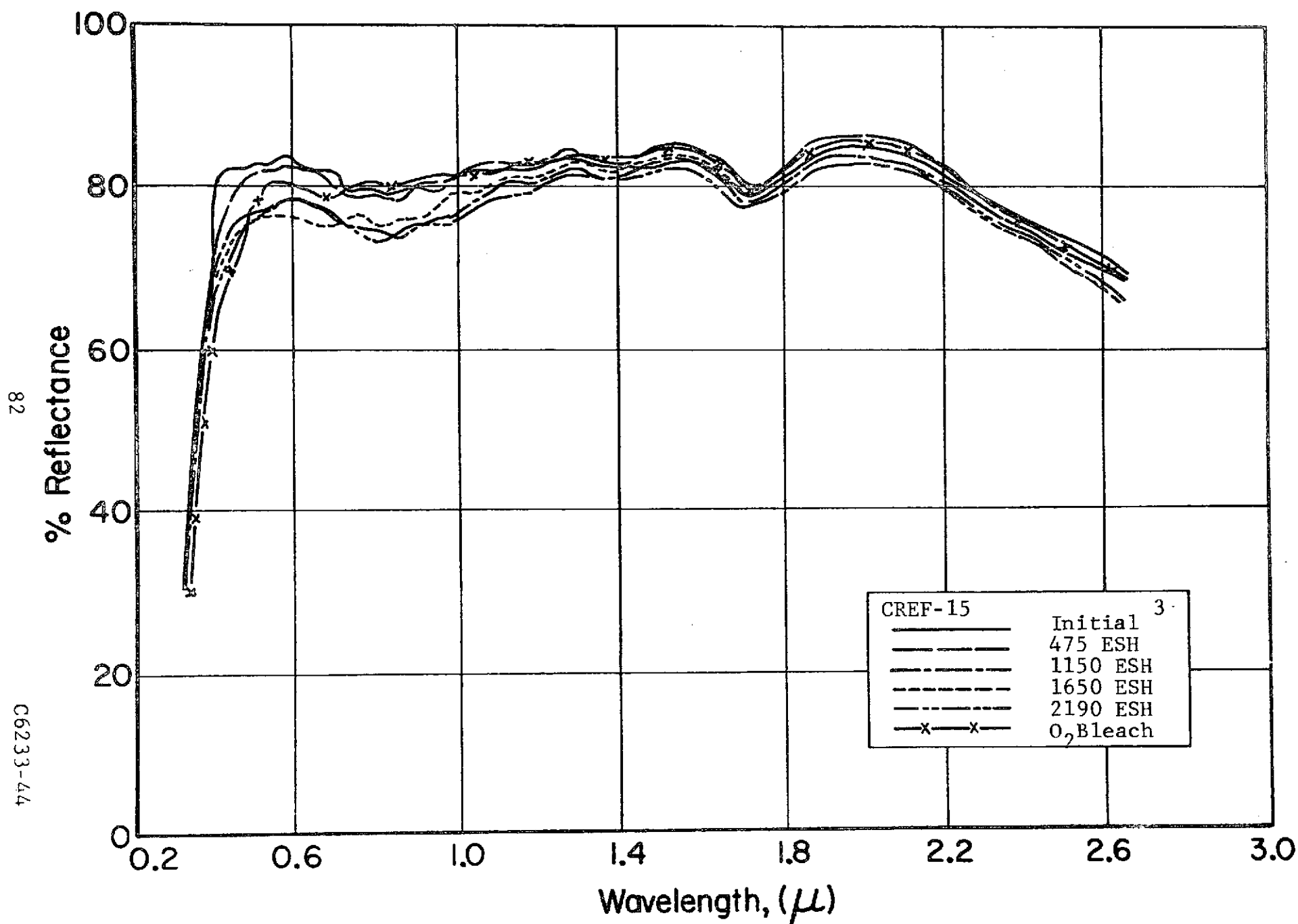
Figure No. 55 REFLECTANCE SPECTRA OF LH-102(6-12-A-10):Li$_2$SiO$_3$/G
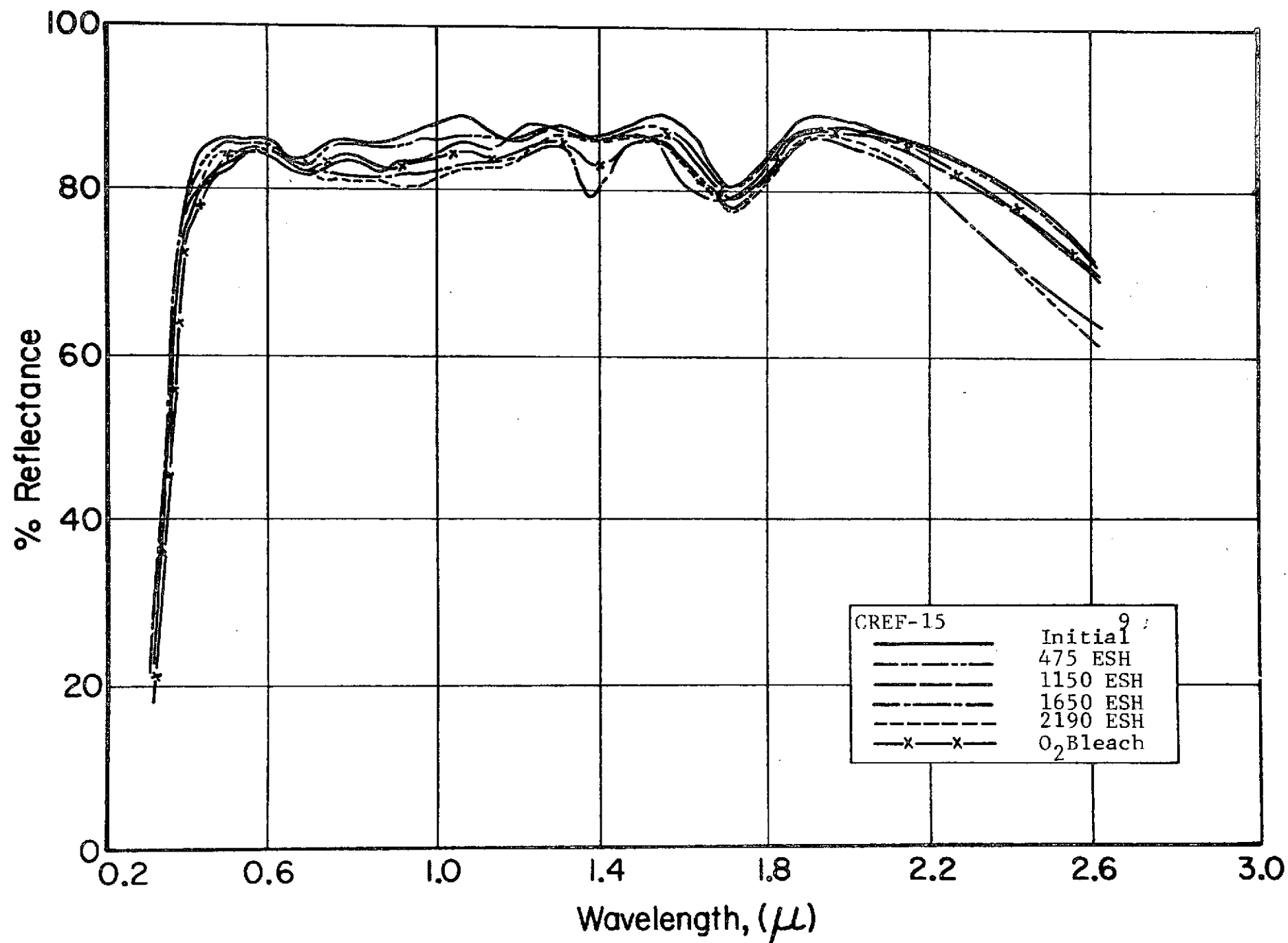
Figure No. 56 REFLECTANCE SPECTRA OF LH-103(6-12)/G

CREF-15

————————	Initial
——————————	475 ESH
— — — —	1150 ESH
—·—·—·—	1650 ESH
– – – –	2190 ESH
—x——x—	O₂ Bleach

83

C6233-44
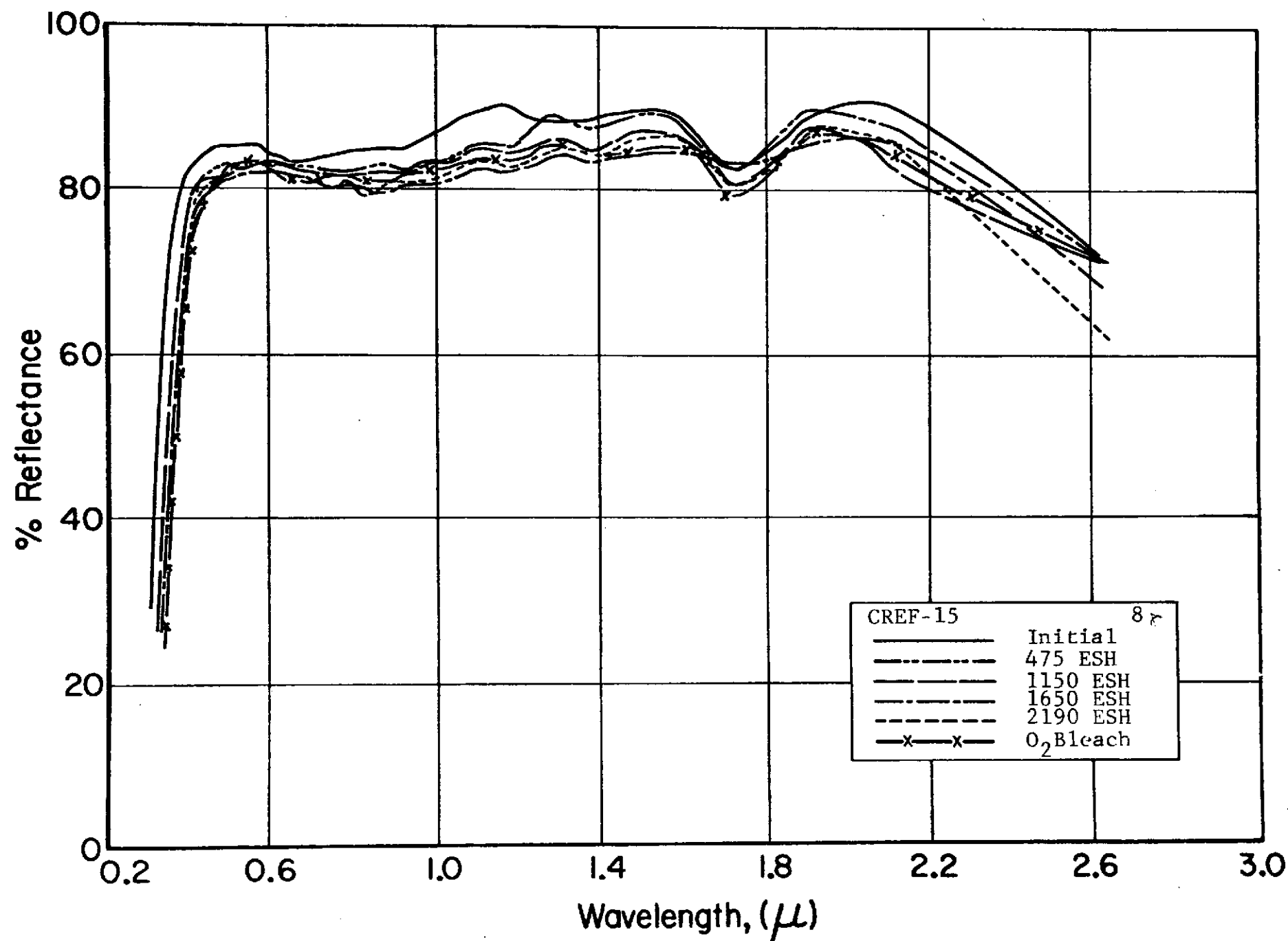
Figure No. 57   REFLECTANCE SPECTRA OF LH-103(6-12):Li$_2$SiO$_3$/G

Table 10

SELECTED IRRADIATION TEST RESULTS

CREF Test No. 15

No.	Sample Description*	$R_k(\%)$	ΔR_{400}**	ΔR_{900}**	Initial α_s	$\Delta\alpha_s$(2190 ESH)
4	LH-102(6-12)	61	.08/.09	.054/.025	.183	.047
5	LH-102(6-12-10)	64	.06/.08	.05/.005	.226	.046
6	LH-102(6-12-A)	55.5	.08/.04	.185/.005	.272	.117
7	LH-102(6-12-A-10)	69	.045/.03	.02/.005	.214	.016
1	LH-102(6-12):Li$_2$SiO$_3$	64.5	.09/.095	.065/.015	.193	.045
2	LH-102(6-12-10):Li$_2$SiO$_3$	68.5	.16/.165	.05/.02	.217	.047
10	LH-102(6-12-A):Li$_2$SiO$_3$	59	.19/.12	.335/.03	.229	.205
3	LH-102(6-12-A-10):Li$_2$SiO$_3$	59.5	.16/.16	.035/.00	.224	.038
9	LH-103(6-12)	23	.05/.05	.04/.025	.219	.027
8	LH-103(6-12):Li$_2$SiO$_3$	38	.04/.05	.025/.01	.209	.042

*All samples are OI-650G paints

**Value of ΔR is given after 2190 ESH and after a subsequent O_2 bleach.

85

C6233-44

effects of Li_2SiO_3 on LH-103(6-12) are to increase R_k and also $\Delta\alpha_s$. The tendency of the encapsulant to increase R_k is also noticeable in the LH-102 series of pigments. The LH-103 series paints have much lower R_k values than do those of the LH-102 series. This apparent anomaly remains to be explained.

The stability of the LH-102(6-12-A-10) paint is excellent. The other paints, with the exception of the "A" treated ones, respond nominally to a 2190 ESH exposure. In the LH-102 series, the Li_2SiO_3 encapsulant greatly increases the degradation at 400nm. The spectra reveal also that the degradation in all cases occurs primarily in the visible region of the spectrum, indicating that the pigment sensitizes the vehicle. The pronounced influence of the Li_2SiO_3 exemplifies this point; the ΔR_{400} values show that the 400nm damage does not recover (bleach) in oxygen. The apparent bleaching of sample No. 10 (fig. 54) results from the recovery in the short wavelength tail of the very large absorption band centered at 900nm. The same effect may also be seen in sample No. 6(Fig. 50).

Summarizing, we believe that the A-10 treatment is effective and helpful, that the -"A" treatment has obviously deleterious effects, and that the -"10" treatment is relatively innocuous. Encapsulation of these pigments in Li_2SiO_3 in general decreases environmental stability and in some instances actually appears to accelerate the degradation of the vehicle. The value of α_s is somewhat higher in these series than in other paints prepared from COP pigments, partly because of a non-optimized particle size and partly because of the low R_k values.

3.6 CREF Test No. 16

3.6.1 Test Conditions

The pressure during this test remained well below 5×10^{-7} Torr. The samples were irradiated at an intensity of three ultraviolet suns. An Hanovia 5kw medium pressure mercury-argon lamp supplied the radiant energy. Two of the samples (nos. 5 and 12) in addition were exposed to a flux of 1.2 KeV proton radiation, estimated to be approximately 10^{15} p/cm^2. Diffuse reflectance measurements over the spectral range from 325nm to 2600nm were performed on each sample before irradiation and after exposure to 335 ESH, 900 ESH, 2750 ESH and 4720 ESH. Oxygen bleaching spectra were not taken.

3.6.2 Materials Descriptions and Test Results

All of the pigments in this test are Zn_2TiO_4 prepared from IITRI batch LH-106 COP material, variously treated. IITRI batches LH-103 (19%), LH-104 (~39%) and LH-105(~42%) were blended to make LH-106. All samples are OI-650G paints cured at 325°F for 16hrs. The descriptions of the pigments involved are given in table 11 along with their relevant test data. The spectra of the paints are shown in figures 58 through 65 inclusive. It should be noted that these paints are the same as described in section 3.2 (IRIF Test No. I-70). The notation in describing these paint systems is consistent with that used in other sections of this document.

3.6.3 Analyses and Discussions

CREF-Test No. 16 has provided data which are directly comparable with the data obtained in IRIF Test No. I-70. Table 12 presents the data which can be compared. Most apparent from table 12 is that degradation in the CREF greatly exceeds that

$\angle^{-}2$

Table 11

CREF-16

IRRADIATION TEST RESULTS

Sample		Solar Absorptance Values					
No.	Description*	Initial	335 ESH	900 ESH	2750 ESH	4720 ESH	$\Delta\alpha_s$**
5	$(6\text{-}12\text{-}A\text{-}10):K_2SiO_3$	.197	.214	.240	.258	.253	.056
6	$(6\text{-}12\text{-}A\text{-}10)$	.182	.225	.236	.236	.246	.064
7	$(6\text{-}12):Li_2SiO_3$	.208	.241	.238	.248	.251	.043
8	$(6\text{-}12\text{-}10):Li_2SiO_3$	.181	.200	.202	.221	.224	.043
9	$(6\text{-}12\text{-}A\text{-}10):Li_2SiO_3$	.217	.232	.241	.242	.245	.028
10	$(6\text{-}12):K_2SiO_3$	.224	.246	.245	.253	.267	.043
11	$(6\text{-}12):K_2SiF_6$	.208	.230	.244	.254	.267	.059
12	$(6\text{-}12\text{-}10):K_2SiF_6$	.226	.247	.251	.267	.266	.040

*All samples are OI650G paints utilizing Zn_2TiO_4 pigments prepared from batch LH-106 and treated as indicated.

**Solar absorptance change after 4720 ESH UV exposure; samples 5 and 12 received a proton exposure of approximately 10^{15} p/cm^2.
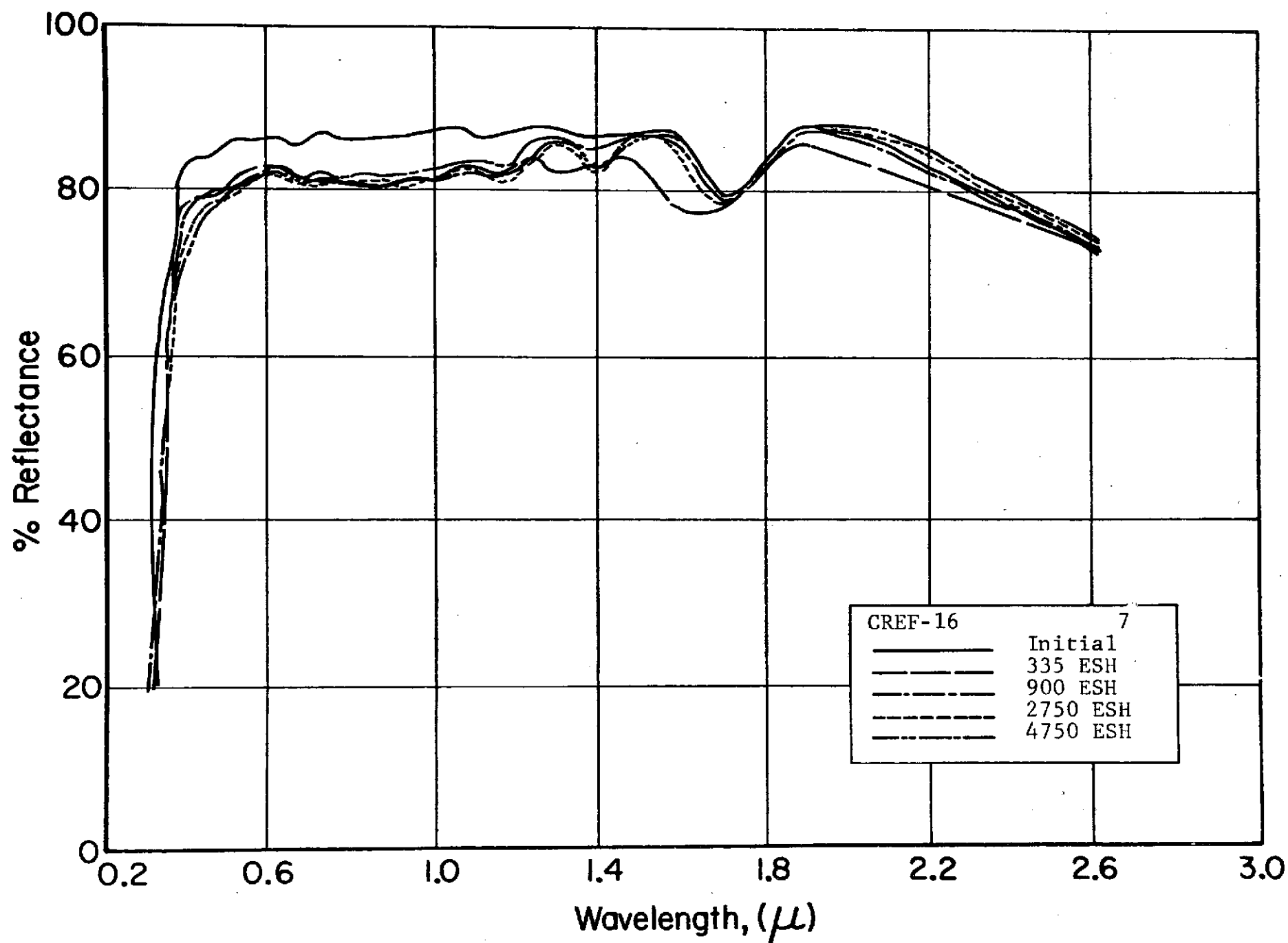
Figure No. 58   REFLECTANCE SPECTRA OF LH-106(6-12):Li$_2$SiO$_3$/G

89

C6233-44

Figure No. 59   REFLECTANCE SPECTRA OF LH-106(6-12):K$_2$SiO$_3$/G

Figure No. 60   REFLECTANCE SPECTRA OF LH-106(6-12):K_2SiF_6/G

The chart legend contains:

CREF-16　　　　　　8?

———————	Initial
———— ————	335 ESH
—·—·—·—	900 ESH
- - - - - - -	2750 ESH
—··—··—··	4750 ESH

Figure No. 61　　REFLECTANCE SPECTRA OF LH-106(6-12-10):Li_2SiO_3/G
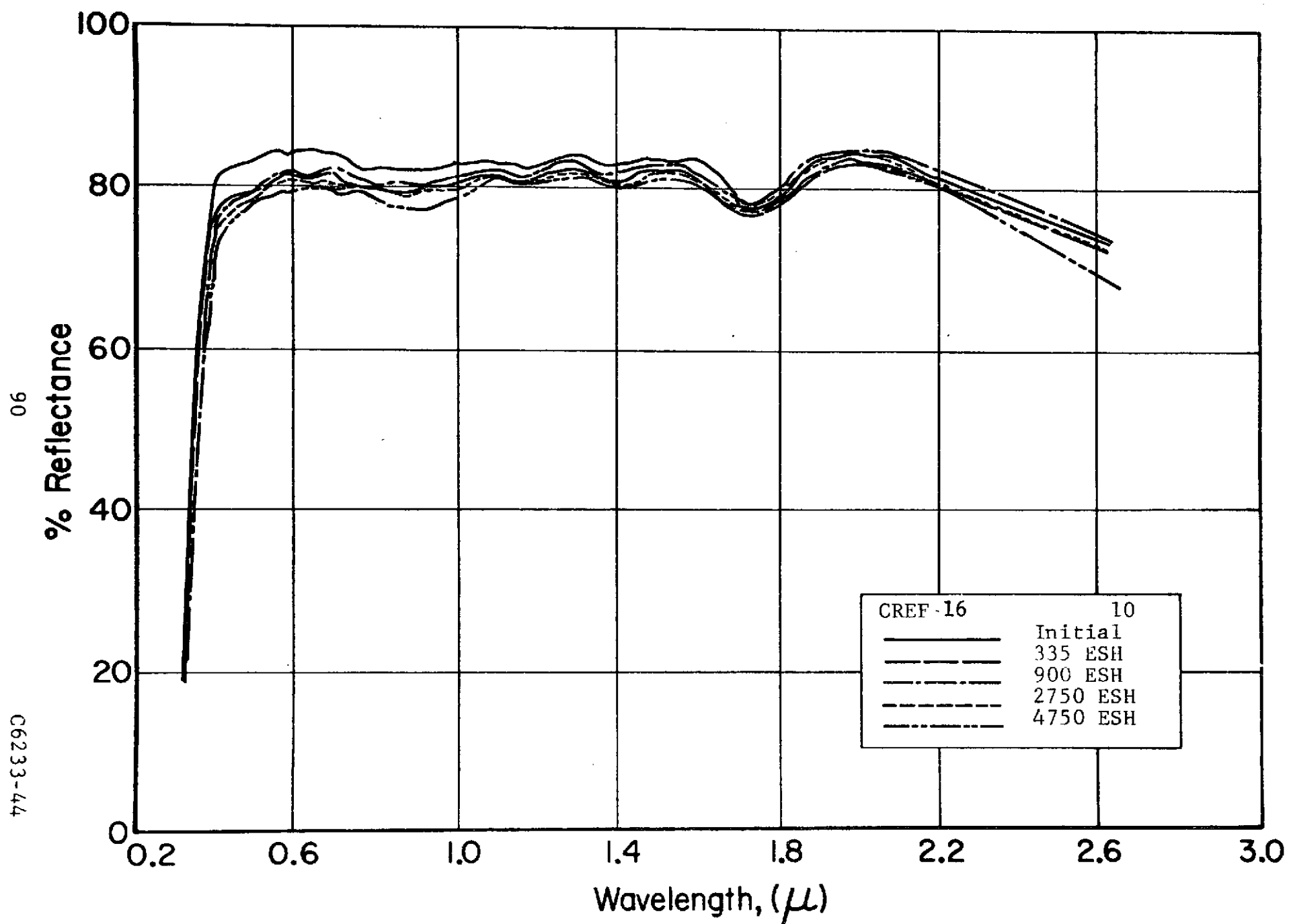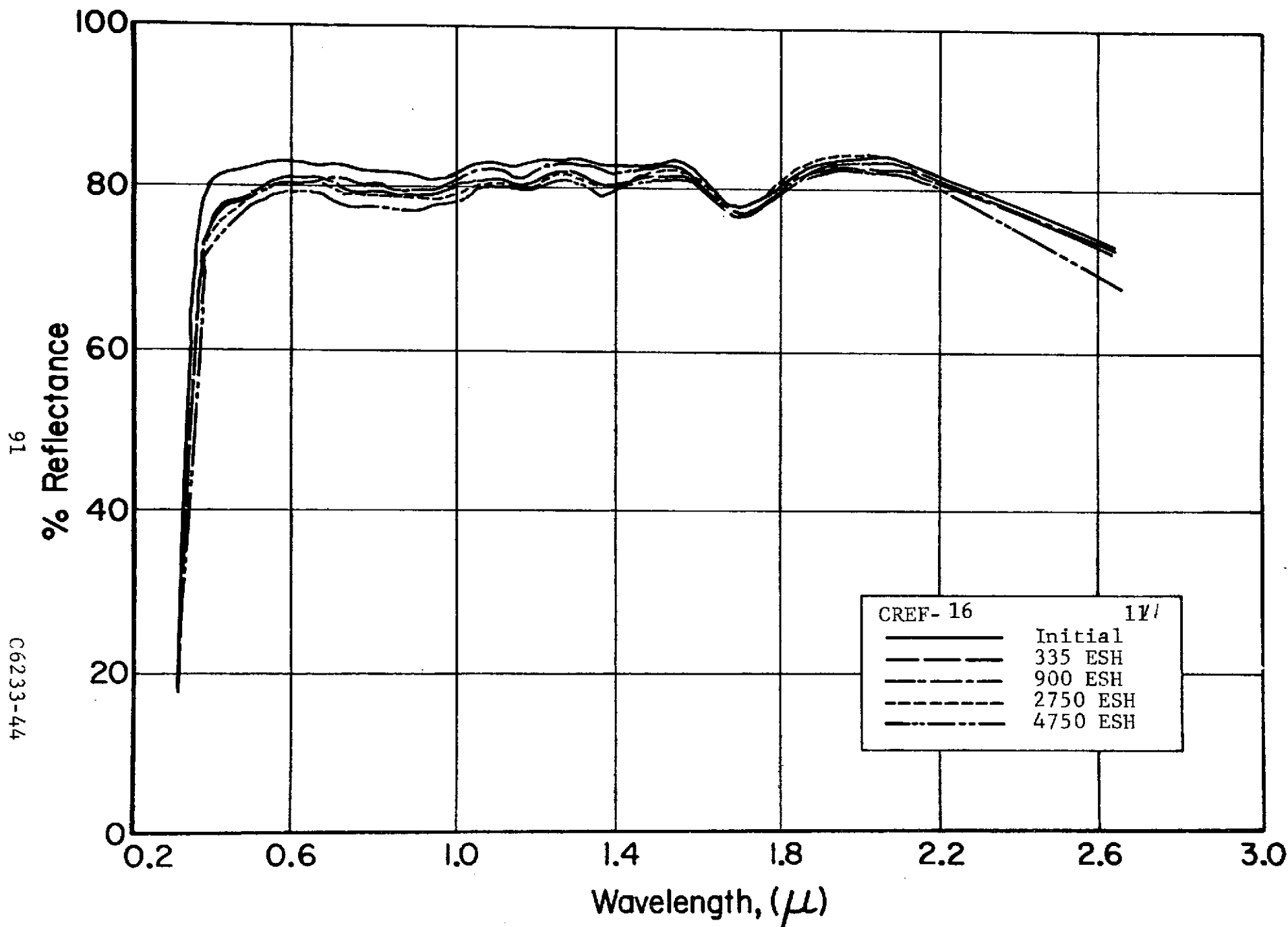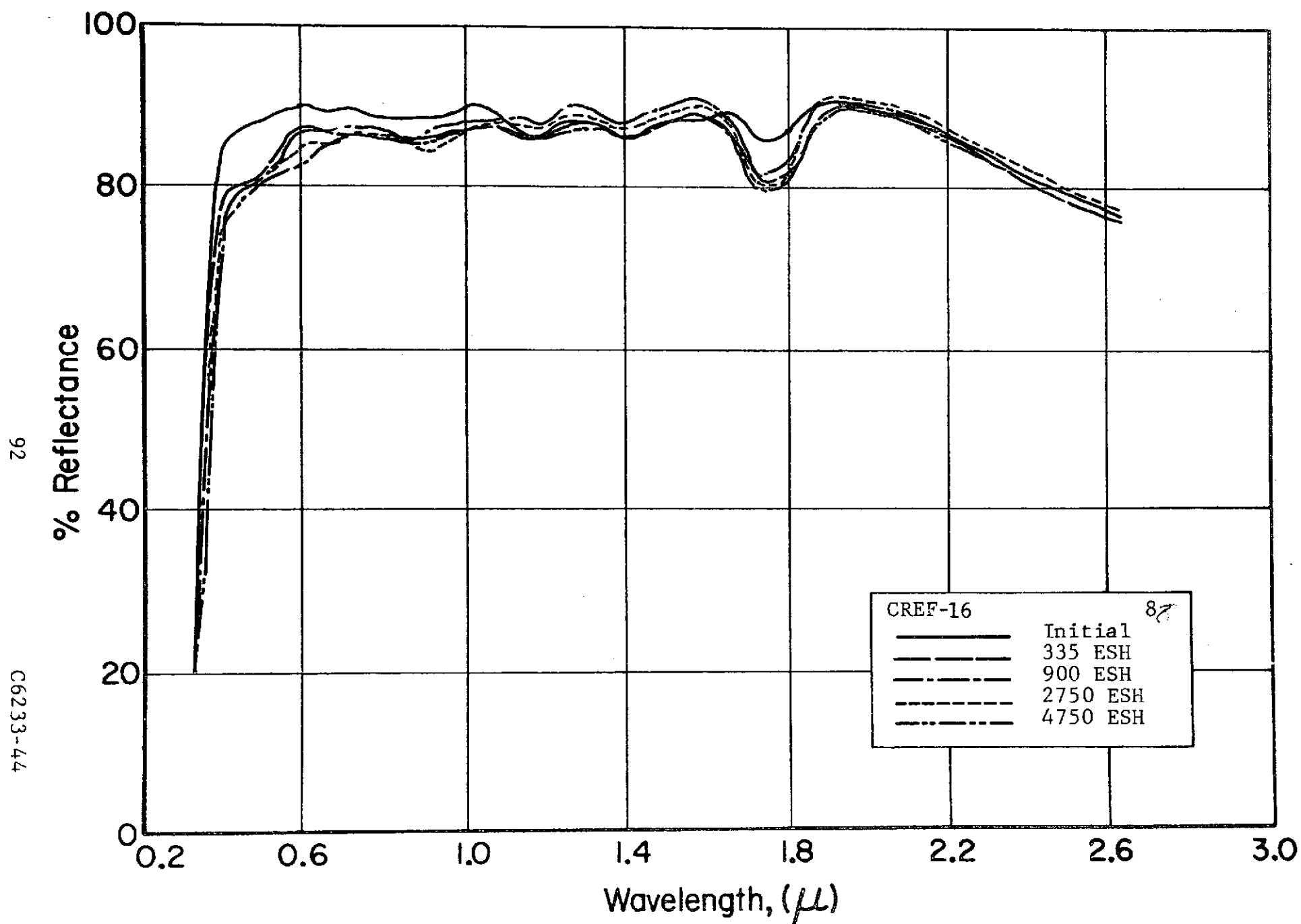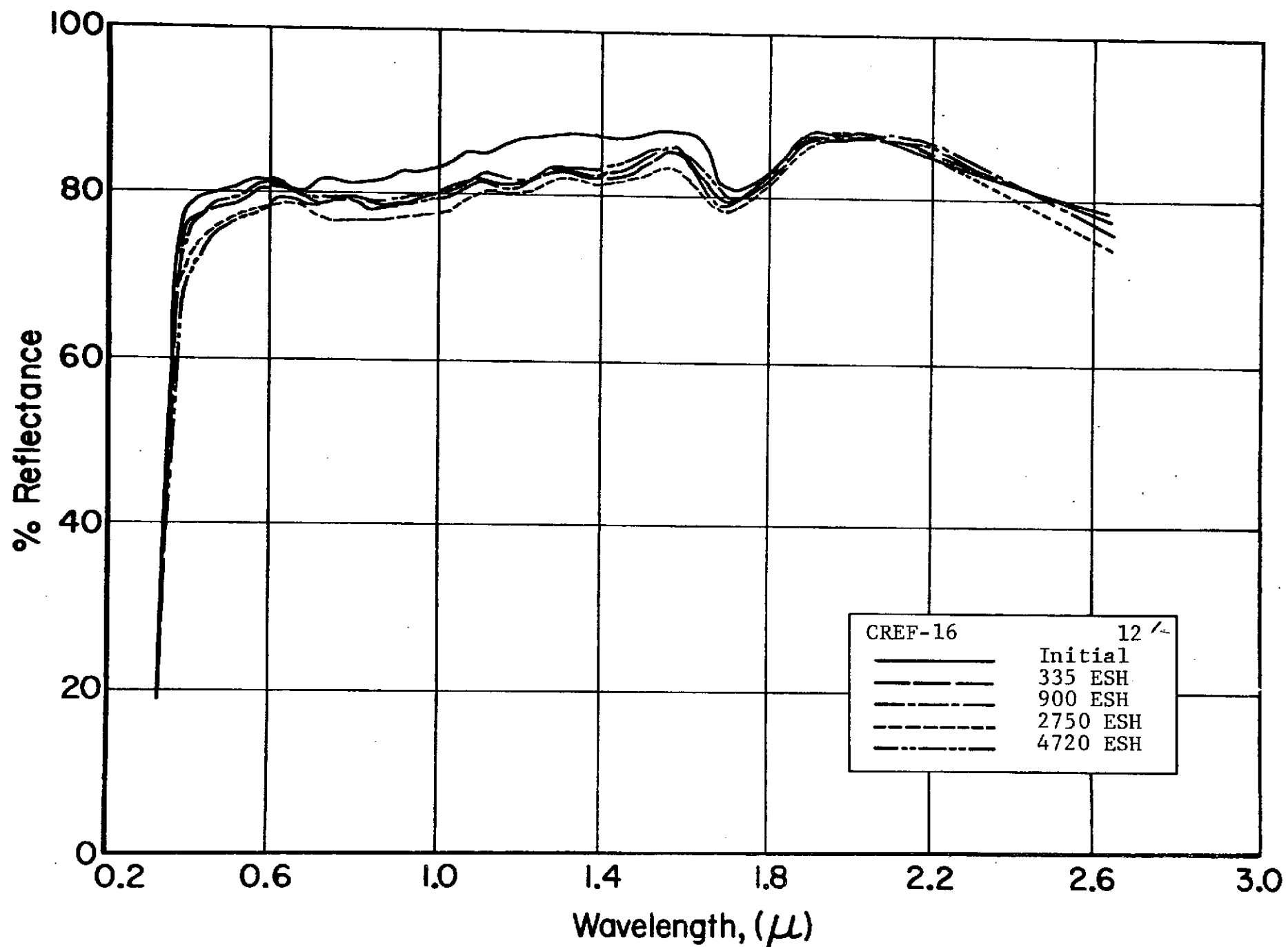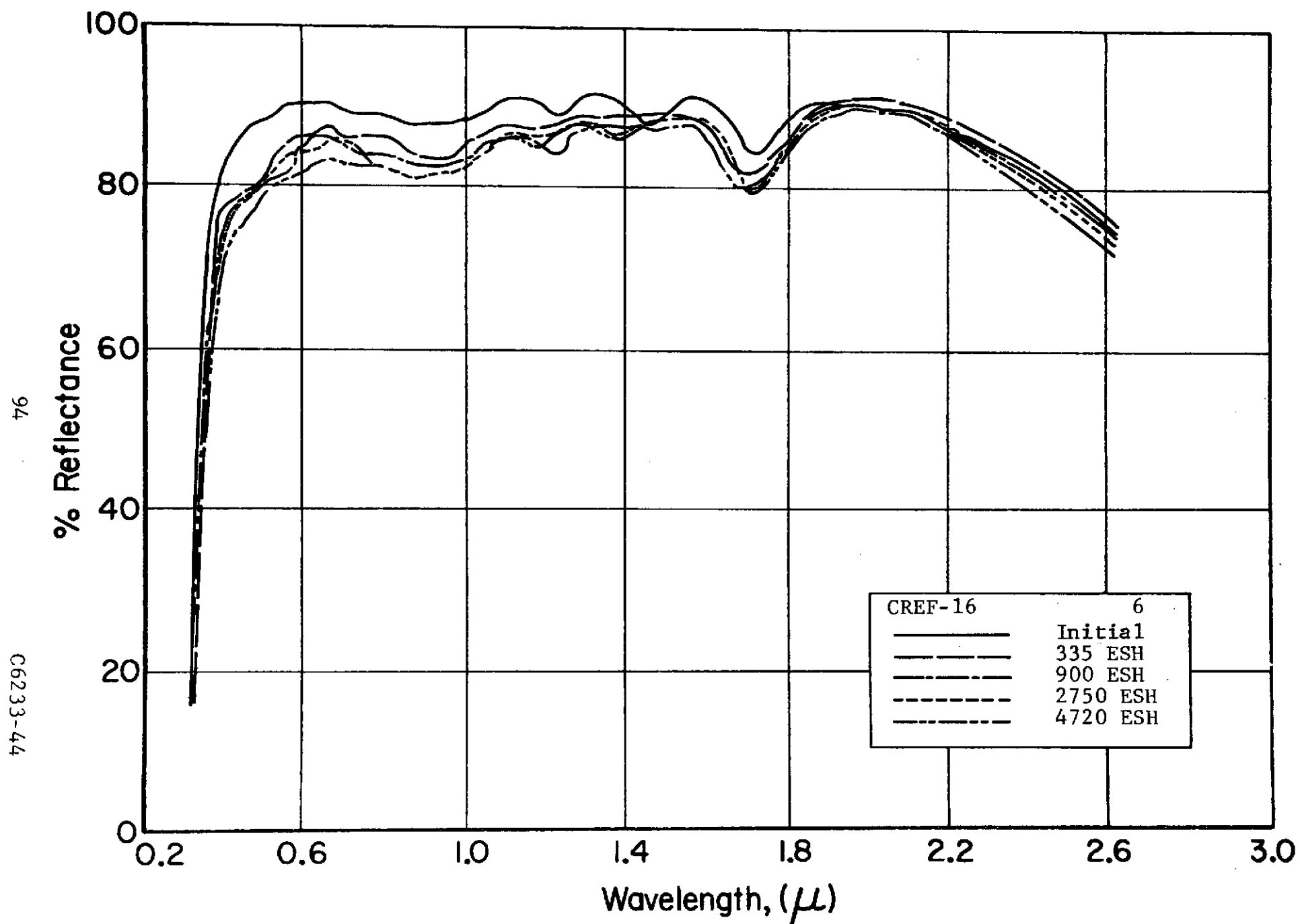
Figure No. 62   REFLECTANCE SPECTRA OF LH-106(6-12-10):K₂SiF₆/G
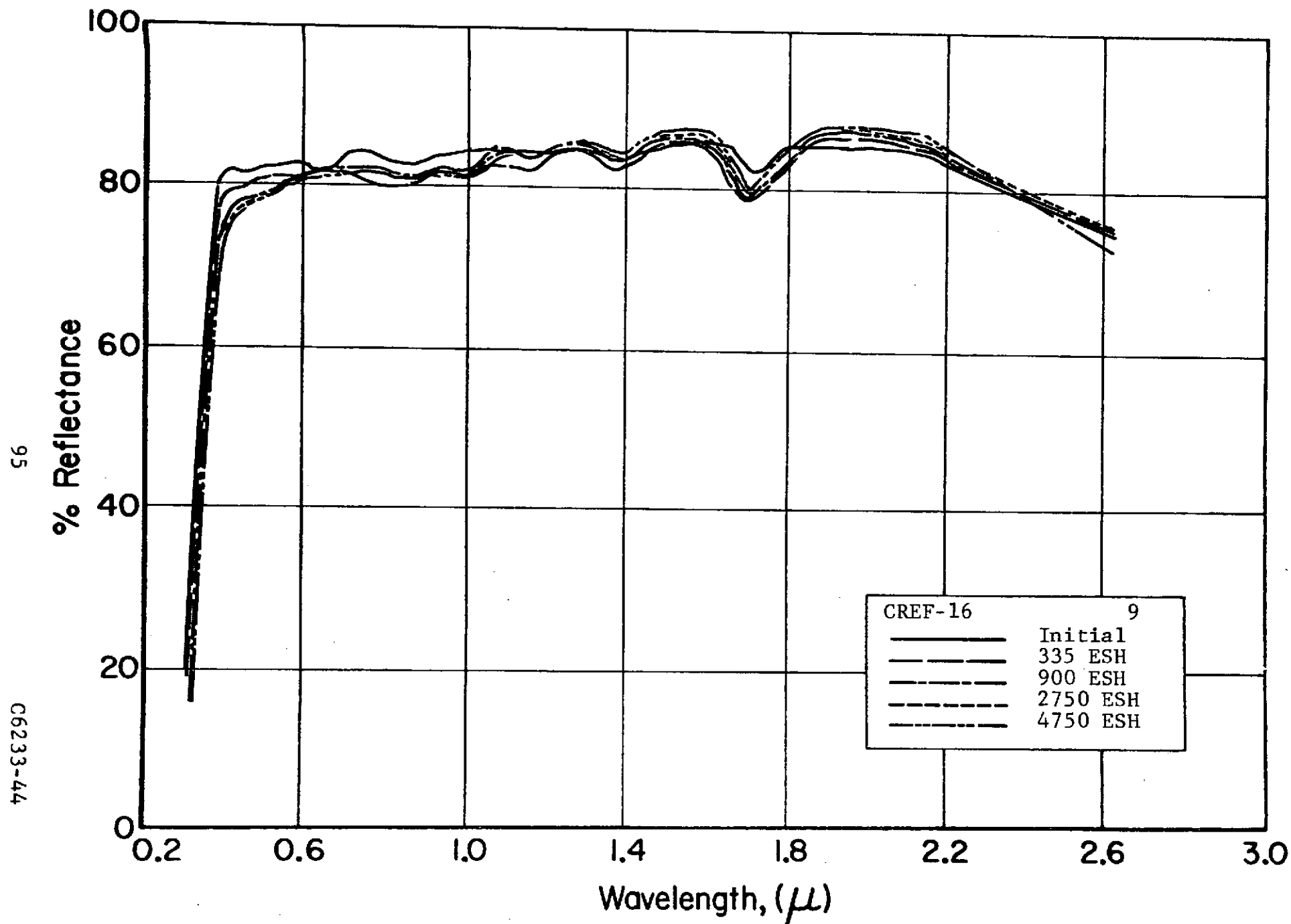
Figure No. 63   REFLECTANCE SPECTRA OF LH-106(6-12-A-10)/G

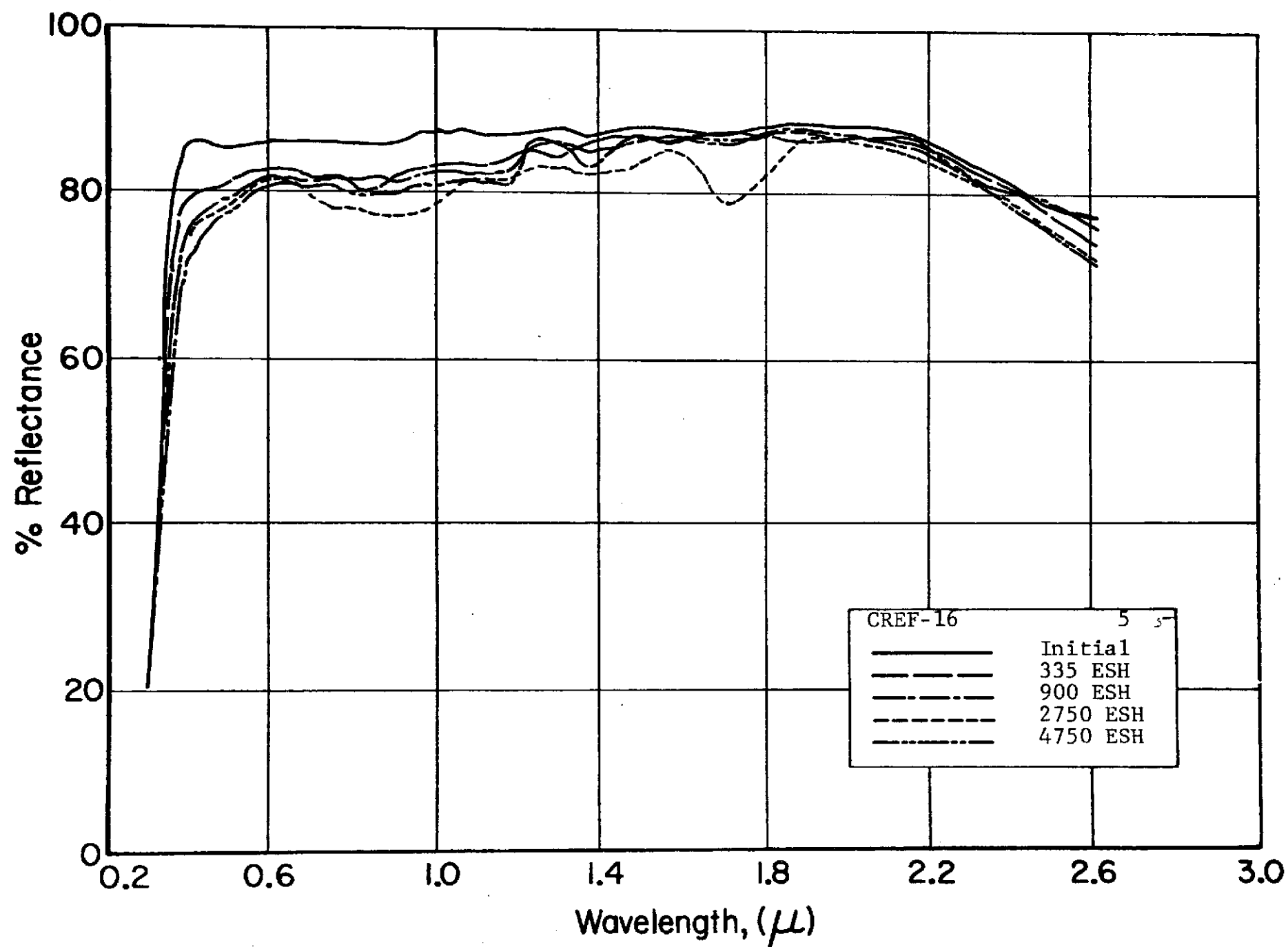Figure No. 64   REFLECTANCE SPECTRA OF LH-106(6-12-A-10):Li$_2$SiO$_3$/G

C6233-44

Figure No. 65   REFLECTANCE SPECTRA OF LH-106(6-12-A-10):K_2SiO_3/G

Table 12

DATA COMPARISON: CREF TEST NO. 16 WITH IRIF-I-70

Sample			R_k		α_s		$\Delta\alpha_s$ Exposure (ESH)			
No. (I-70)	No. (C-16)	Description	I-70	C-16	I-70	C-16	1060(I)*	900(C)*	3130(I)	2750(C)
9	5	(6-12-A-10):K_2SiO_3	76.5	76.5	.210	.197	.010	.043	.015	.051
3	6	(6-12-A-10)	72	72.5	.213	.182	.008	.054	.030	.054
4	7	(6-12):Li_2SiO_3	72	72.5	.203	.208	.008	.030	.021	.040
5	8	(6-12-10):Li_2SiO_3	74	74.0	.194	.181	.015	.021	.018	.040
6	9	(6-12-A-10):Li_2SiO_3	74.5	73.0	.180	.217	.010	.024	.014	.025
7	10	(6-12):K_2SiO_3	73.5	73.0	.232	.225	.010	.020	.012	.029
10	11	(6-12):K_2SiF_6	73.5	73.0	.192	.208	.015	.036	.021	.046
11	12	(6-12-10):K_2SiF_6	73.5	71.5	.215	.226	.015	.025	.016	.041

*Notation used: I = IRIF-I-70

C = CREF Test No. 16

97

C6233-44

in the IRIF. Several possible explanations exist. The difference in solar factor (6X in IRIF vs 3X in CREF) can be significant, particularly if any of the degradation mechanisms are second (or higher) order. It is possible that the CREF test samples Nos. 6 and 11 were also exposed to some proton radiation. Contamination is another possibility since the four other samples in the CREF test were experimental clear films which may, under combined UV and proton radiation, have undergone decomposition and outgassing.

In the case of the CREF samples, the largest increment in α_s occurred in the first 335 ESH. After 4720 ESH the maximum $\Delta\alpha_s$ (.064) was exhibited by the (6-12-A-10) system; the least (.028), by the (6-12-A-10):Li_2SiO_3 system. The exposure corresponds to approximately one-half year of continuous exposure to the sun (at 1 A.U.). All of the paints performed quite well, even though the data differ. It should be noted that the differences between CREF and IRIF test data are of the order of 1-2% in reflectance for samples 7-10; samples 5 and 12 definitely overlap the proton beam, while 6 and 11 may "see" some stray radiation. Thus those samples which display the greatest differences may also have been affected by the combined flux.

3.7 Summary and Conclusions

With minor exceptions the COP pigments and the paints prepared from them demonstrate greater stability than those derived from the "MOX" method. In the series of tests, from IRIF I-70 to CREF-16, it is also evident that encapsulation will be required for most pigments and that K_2SiO_3 represents the best choice of encapsulants. The use of acid-washing clearly must be followed by re-calcination. A recalcination by itself proves to be of no advantage or disadvantage.

The properties of the MOX-A pigments unexpectedly belie the fact that they were prepared from precursors which should lead to very substantial titanium atom excess in the calcined product. The stability of the MOX-A materials, however, is very poor and difficult to associate with preparative conditions. For the other pigments, the effects of various calcination parameters, chemical treatments and other processing parameters in most cases are relatively predictable. The overall results nevertheless point up the inherently good stability of Zn_2TiO_4. The COP method of Zn_2TiO_4 production leads to a better pigment than the MOX method, although the latter holds some definite and worthwhile advantages. With reference to paint stability the basic problem seems to be one of isolating a stable pigment from stable vehicle, thus preventing their mutual interaction. Determining pigment production parameters and conditions that lead to reduced pigment surface activity, and quite probably encapsulation, will solve this problem. A major review has been initiated in order to determine at least semi-systematically the effects of precipitation parameters, calcination conditions, chemical treatments and encapsulants and other process variables on the properties and performance of pigments (and paints) prepared from oxalate precursors. Some of the data from that review including R_k, ΔR_{400}, ΔR_{900} have been used in this document to assist in the analysis of test results.

REFERENCES

1. J.E. Gilligan and Y. Harada, "Development of Space Stable Thermal Control Coatings for Use on Large Space Vehicles". IITRI Report No. C6233-40, (Triannual Report) - July 1974.

2. Courtesy of D.W. Gates, NASA-MSFC

3. G.A. Zerlaut, J.E. Gilligan, and N.A. Ashford, "Investigation of Environmental Effects on Coatings for Thermal Control of Large Space vehicles," IITRI Report No. U6002-97 (Final Report), Oct, 1971.

DISTRIBUTION LIST

Copy No.	Recipient
1-85 + Repro.	National Aeronautics and Space Administration George C. Marshall Space Flight Center Marshall Space Flight Center, Alabama 35812 Attn: ES34/D.W. Gates
86	NASA-Same Address Attn: AP13-I/Fletcher B. Smith
87-91	NASA-Same Address Attn: AS21D
92	NASA-Same Address Attn: AT01
93	NASA-Same Address Attn: EM34/James D. Venus
94	NASA-Same Address Attn: ES33/D.R. Wilkes
95	IIT Research Institute M.J. Klein/Division C Files
96	A.M. Stake/Section Files
97	Patent Office/Main Files
98-99	P. Caputo, Division C
100	F.O. Rogers, Division C
101	S. Bortz, Division D
102	Y. Harada, Division D
103	J.E. Gilligan, Division C
104	J. E. Brzuskiewicz, Division C
105	F. Jarke, Division C
106	C. Giori, Division C